

Kati Rinnekari

HYDROGEL SCREENING FOR 3D VASCULAR MODEL ON MICROFLUIDIC CHIP

Faculty of Medicine and Health
Technology
Master's thesis
April 2024

ABSTRACT

Kati Rinnekari: Hydrogel Screening for 3D Vascular Model on Microfluidic Chip
Master's thesis
Tampere University
Master's Programme in Biotechnology and Biomedical Engineering
April 2024

Hydrogels are biomaterials which consist of crosslinked polymer networks, and they have ability to absorb large amounts of water. In addition, hydrogels allow perfusion and give structural support to the cells. Hydrogels are crucial element for three-dimensional (3D) cell models since they mimic the cells' natural 3D environment, extracellular matrix (ECM). In addition, 3D cell models mimic native tissues better than 2D models and thus are better models for studying human physiology. Vasculature is responsible for transport of oxygen, nutrients and metabolites and is therefore essential for all living tissues in human body. Overall, both hydrogels and vasculature are essential when creating organotypic *in vitro* models such as Organ-on-Chip and even Body-on-Chip applications.

This study focused on analyzing hydrogel size change, including degradation, and shrinking or swelling, by measuring the size of the samples *in vitro* during cultivation, testing protease inhibitors' effects on hydrogel's degradation or size change, and using these hydrogels (\pm inhibitors) to support 3D vascularization on microfluidic chip, that is Vascularization-on-a-Chip. The tested hydrogels included fibrin (human), collagen I (rat tail), VitroCol[®] (human collagen I), TeloCol[®] (bovine Telocollagen I), gelatin-gellan gum (porcine skin, bacterial) and VitroGel[®] (xeno-free). First, human lung fibroblasts (WI-38) were cultured embedded in hydrogels for 10 days. The size change of the hydrogels was measured every day during cultivation period. The area of the samples was measured with tile scan imaging, and the thickness was measured by imaging fluorescent beads embedded in the hydrogels, and volume was calculated based on these measured values. Cell viability and morphology were analyzed with Live/Dead and cytochemical staining. In microfluidic chips, human bone marrow stem/stromal cells (BMSCs), and green fluorescent protein (GFP) tagged human umbilical vein endothelial cells (GFP-HUVECs) were cultured inside a hydrogel for 10 days in dynamic conditions. The cellular reorganization, vascularization and cell morphology were analyzed by imaging signals of GFP and immunocytochemical staining.

Hydrogels in static conditions in a well plate showed varying characteristics in both sample size changes and cell morphology including elongation and spreading of the cells. Functional inhibitors preventing the decrease in size or degradation of the tested hydrogels were discovered during the study. In microfluidic chip experiments with dynamic culture conditions, the inhibitors supported 3D vascularization. Vascular network formed in fibrin hydrogel appeared to be more mature compared to vascular network formed in other hydrogels. In conclusion, a method to analyze hydrogel size change by using fluorescent bead imaging was created, the hydrogel degradation was decreased with inhibitors and fibrin showed to be the most promising hydrogel to support 3D vasculature maintenance on-chip.

Keywords: organ-on-chip, hydrogel stability, extracellular matrix proteins, vascularization

The originality of this thesis has been checked using the Turnitin OriginalityCheck service.

TIIVISTELMÄ

Kati Rinnekari: Hydrogeelien seulonta 3D-verisuonimallia varten mikrofluidistisella alustalla
Diplomityö
Tampereen yliopisto
Bioteknologian ja biolääketieteen tekniikan maisteriohjelma
Huhtikuu 2024

Hydrogeelit ovat biomateriaaleja, jotka koostuvat verkkomaisista polymeerirakenteista ja joilla on kyky absorboida suuri määrä vettä itseensä. Lisäksi hydrogeelit mahdollistavat perfuusion eli nesteen virtaamisen niiden läpi. Hydrogeelit myös antavat soluille niiden tarvitseman tuen ja toimivat niiden kolmiulotteisena (3D) tukirakenteena. Hydrogeelit ovat tärkeitä 3D-solumalleille, koska ne muistuttavat monien ihmiskudosten luonnollista soluväliainetta. Tämän takia hydrogeelejä sisältävät 3D-solumallit myös muistuttavat enemmän luonnollisia kudoksia kuin 2D-mallit ja vastaavat siten paremmin ihmisen fysiologiaa. Verisuonisto vastaa muun muassa hapen, ravinteiden ja aineenvaihduntatuotteiden kuljettamisesta ja on siten elintärkeä osa ihmiskehoa. Tämän takia sekä hydrogeelit että verisuonisto ovat tärkeitä osia kudoksenkaltaisten solumallien kuten kudossirujen (eng. Organ-on-Chip) ja jopa laajempia elimistön kokonaisuuksia jäljittelevien monikudossirujen (eng. Body-on-Chip) kehityksessä.

Tässä diplomityössä hydrogeelien koon muutosta, kutistumista tai hajoamista, analysoitiin mittaamalla näytteen kokoa soluviljelyn aikana. Lisäksi tutkittiin proteaasi-inhibiittoreiden vaikutuksia hydrogeelin koon muutokseen ja verisuonien muodostumiseen käyttämällä hydrogeelejä sekä inhibiittorien kanssa että ilman verisuonimallissa kudossirulla. Tutkittavat hydrogeelit olivat fibrini (ihmisperäinen), kollageeni I (rotan häntä), VitroCol® (ihmisen kollageeni I), TeloCol® (nautaeläimen telokollageeni I), gelatiini-gellaanikumi (sian iho, bakteeri) ja VitroGel® (eläinvapaa). Kuoppalevykokeissa staattisessa ympäristössä ihmisen keuhkojen fibroblasteja (WI-38) viljeltiin hydrogeeleissä kymmenen päivän ajan. Näytteiden koon muutosta mitattiin päivittäin soluviljelyn aikana. Hydrogeelien pinta-ala mitattiin koko kuopasta otettujen kuvien avulla, korkeus mitattiin mikroskoopin ja fluoresoivien partikkelien avulla, ja näiden mittaustulosten avulla näytteiden tilavuus laskettiin. Solujen elinkykyä ja morfologiaa tutkittiin viabiliteettivärjäyksen (eng. Live/Dead staining) ja sytokemiallisen värjäyksen avulla. Kudossirukokeissa ihmisen luuytimen kantasoluja ja vihreällä fluoresoivalla proteiinilla leimattuja ihmisen napanuoran endoteelisoluja viljeltiin hydrogeeleissä kudossirulla kymmenen päivän ajan. Solujen uudelleen organisoitumista, verisuonten muodostusta ja morfologiaa tutkittiin vihreän fluoresoivan proteiinin signaalin ja immunosytokemiallisten värjäyksien avulla.

Kuoppalevyllä hydrogeelien ominaisuudet vaihtelivat niin koon muutoksien kuin solujen levittäytymisen suhteen. Inhibiittorit estivät testattujen hydrogeelien koon pienenemistä soluviljelyn aikana. Kudossirukokeissa suurimmassa osassa hydrogeelejä inhibiittorit eivät haitanneet verisuoniston muodostumista. Fibrinihydrogeeliin muodostunut verisuonitus oli kypsempää verrattuna verisuonitukseen muissa testatuissa hydrogeeleissä. Yhteenvetona voidaan todeta, että tässä diplomityössä hydrogeelin koon muutoksen tutkimiseen kehitettiin uusi menetelmä, hydrogeelien hajoamista tai koon pienenemistä voitiin estää inhibiittoreiden avulla ja fibrini osoittautui kaikista lupaavimmaksi hydrogeeliksi tukemaan 3D-verisuonten muodostusta ja niiden säilymistä kudossirulla.

Avainsanat: kudossiru, hydrogeelin stabiilius, soluväliaineen proteiinit, verisuonten muodostuminen

Tämän julkaisun alkuperäisyys on tarkastettu Turnitin OriginalityCheck –ohjelmalla.

PREFACE

This Master's thesis was done in Adult Stem Cell group and Biomaterials and Tissue Engineering group at the Faculty of Medicine and Health Technology at Tampere University. Firstly, I want to thank my supervisors D.Sc. (Tech) Janne T. Koivisto and PhD Hanna Vuorenpää for all the help, support, and guidance they gave me during the thesis process. I want to also thank the group leaders Prof. Susanna Miettinen and Prof. Minna Kellomäki for the guidance and for giving me the opportunity to do my thesis in their research groups and as part of Centre of Excellence in Body on-Chip Research (CoEBoC). In addition, I want to thank both research groups, Adult Stem Cell group and Biomaterials and Tissue Engineering group, for all the help and advice. Nevertheless, I want to thank the lab technicians Anna-Maija Honkala and Sari Kalliokoski for their help and advice in the lab. I want to thank and acknowledge the Tampere CellTech Laboratories, Biocenter Finland (BF) and Tampere Imaging Facility (TIF) for providing excellent facilities for doing the research.

Lastly, I want to thank my family, friends, and especially my mother and sister to always believing in me during this thesis process as well as through my studies.

Tampere, 24 April 2024

Kati Rinnekari

CONTENTS

1. INTRODUCTION	1
2. THEORETICAL BACKGROUND.....	4
2.1 Hydrogels.....	4
2.1.1 Fibrin.....	6
2.1.2 Collagen	7
2.1.3 Gelatin-gellan gum.....	10
2.2 Hydrogel size change.....	11
2.2.1 Matrix metalloproteinases and their inhibitors	14
2.2.2 Matrix metalloproteinase and vascularization.....	20
2.2.3 Aprotinin	23
2.2.4 Collagenase inhibitor	24
2.3 Cell types.....	24
2.3.1 Human umbilical vein endothelial cells.....	24
2.3.2 Bone marrow-derived stem/stromal cells	25
2.3.3 Fibroblast.....	26
2.4 Vascularization.....	27
2.4.1 Factors affecting angiogenic growth.....	31
2.4.2 Vascularization models <i>in vitro</i>	32
2.5 Organ-on-a-Chip.....	35
2.6 Vascularization-on-a-Chip.....	38
3. OBJECTIVES OF THE THESIS	43
4. MATERIALS AND METHODS	44
4.1 3D cell culturing in a hydrogel on a well plate.....	46
4.1.1 Sample preparation.....	46
4.1.2 Hydrogel size change in different hydrogels on well plate	48
4.1.3 Live/Dead staining	48
4.1.4 Cytochemical staining	49
4.2 3D cell culturing in a hydrogel on-a-chip.....	49
4.2.1 Establishment of 3D vascular network in microfluidic chip using different hydrogels	50
4.2.2 Immunocytochemistry	52
4.2.3 Vascular image analysis and statistical analysis	53
5. RESULTS	54
5.1 3D cell culturing in a hydrogel in static condition on a well plate.....	54
5.1.1 Hydrogel size change in different hydrogels on well plate	54
5.1.2 Viability of cells in static condition on well plate.....	60
5.1.3 Cellular morphology and alignment in static condition on well plate 61	
5.2 3D vascular network formation in dynamic condition on-chip	63
5.2.1 Vessel parameters	66
5.2.2 Vascular network structure in dynamic environment on-chip.....	67
6. DISCUSSION.....	69
6.1 3D Cell culturing in a hydrogel in static condition on well plate.....	69

6.1.1 Hydrogel size change in different hydrogels on well plate	69
6.1.2 Cellular viability, morphology, and alignment in static condition on well plate	73
6.2 3D vascular network formation in dynamic condition on-chip	74
6.3 General sources of error	81
6.4 Future perspectives.....	83
7. CONCLUSIONS.....	84
REFERENCES.....	86
APPENDIX A: EGM-2 MEDIUM COMPOSITION	95
APPENDIX B: FULL TILE SCAN IMAGES OF WELL PLATE	96
APPENDIX C: LIVE/DEAD IMAGES OF WELL PLATE SAMPLES WITH SEPARATE CHANNELS	97
APPENDIX D: CYTOCHEMICALLY STAINED WELL PLATE SAMPLES WITH SEPARATE CHANNELS	102
APPENDIX E: IMMUNOCYTOCHEMICALLY STAINED CHIP SAMPLES WITH SEPARATE CHANNELS	107

LIST OF SYMBOLS AND ABBREVIATIONS

2D	<i>Two dimensional</i>
3D	<i>Three dimensional</i>
α MEM	<i>α-modified Minimum Essential Medium</i>
ASC	<i>Adipose tissue-derived stem/stromal cell</i>
BMSC	<i>Bone marrow-derived stem/stromal cell</i>
BSA	<i>Bovine serum albumin</i>
CDH	<i>Carbodihydrazide</i>
CMF	<i>Collagen microfibers</i>
DAPI	<i>4',6-diamidino-2-phenylindole</i>
dH ₂ O	<i>Distilled water</i>
DMSO	<i>Dimethyl sulfoxide</i>
DPBS	<i>Dulbecco's Phosphate Buffered Saline</i>
EBM-2	<i>Endothelial Basal Medium-2</i>
ECM	<i>Extracellular matrix</i>
EGM-2	<i>Endothelial Growth Medium -2</i>
ESC	<i>Embryonic stem cell</i>
FDA	<i>United States Food and Drug Administration</i>
FGF	<i>Fibroblast growth factor</i>
GelaCDH	<i>Carbodihydrazide modified gelatin</i>
GelaGG	<i>Gelatin-gellan gum</i>
GeMa	<i>Gelatin methacrylate</i>
GG	<i>Gellan gum</i>
GGox	<i>Oxidized gellan gum</i>
HA	<i>Hyaluronic acid</i>
HLF	<i>Human lung fibroblast</i>
HS	<i>Human serum</i>
HUVEC	<i>Human umbilical vein endothelial cell</i>
iPSC	<i>Induced pluripotent stem cell</i>
LED	<i>Light-emitting diode</i>
MIX	<i>Mixture of aprotinin and Collagenase Inhibitor I (1:1)</i>
LOX	<i>Lysyl oxidase</i>
MMP	<i>Matrix metalloproteinase</i>
mRNA	<i>Messenger RNA</i>
MSC	<i>Mesenchymal stem cell</i>
MT-MMP	<i>Membrane type matrix metalloproteinase</i>
N/A	<i>Not applicable</i>
NaOH	<i>Sodium hydroxide</i>
OOAC	<i>Organ-on-a-Chip</i>
P/S	<i>Penicillin and Streptomycin</i>
P4H	<i>Prolyl 4-hydroxylase</i>
PCL	<i>Polycaprolactone</i>
PDGF	<i>Platelet derived growth factors</i>
PDMS	<i>Poly-dimethylsiloxane</i>
PEG	<i>Poly(ethylene glycol)</i>
PFA	<i>Paraformaldehyde</i>
PGA	<i>Poly(glycolic acid)</i>
PLA	<i>Poly(lactic acid)</i>
PLGA	<i>Poly(lactic-co-glycolic acid)</i>
POMaC	<i>poly(octamethylene maleate (anhydride) citrate)</i>
PSC	<i>Pluripotent stem cell</i>
RNA	<i>Ribonucleic acid</i>
RT	<i>Room temperature</i>

<i>RT-qPCR</i>	<i>Reverse transcription-quantitative polymerase chain reaction</i>
<i>S1P</i>	<i>Sphingosine-1-phosphate</i>
<i>siRNA</i>	<i>Small interference RNA</i>
<i>TAYS</i>	<i>Tampere University Hospital</i>
<i>TIMP</i>	<i>Tissue inhibitor of metalloproteinases</i>
<i>VEGF</i>	<i>Vascular endothelial growth factor</i>
<i>v/v-%</i>	<i>Volume/volume-%</i>
<i>vSMC</i>	<i>Vascular smooth muscle cell</i>

1. INTRODUCTION

Already in 1993, Langer and Vacanti defined tissue engineering as “an interdisciplinary field that applies the principles of engineering and the life sciences toward the development of biological substitutes that restore, maintain, or improve tissue function” [1]. The three main strategies in tissue engineering includes using isolated cells or cell substitutes, tissue-inducing substances like signal molecules, and cells placed on or within matrices like biomaterials [1]. In 2018, biomaterial or biomedical material was redefined as “a material designed to take a form that can direct, through interactions with living systems, the course of any therapeutic or diagnostic procedure” [2].

Hydrogels are biomaterials with a porous, crosslinked three-dimensional (3D) polymer network that can absorb large amount of water. The hydrogels also have ability to give support to the cells, guide them as well as direct the formation of desired tissue by giving mechanical and chemical stimuli. In addition, hydrogels are suitable scaffold materials because their structure resembles the natural extracellular matrix (ECM) of multiple human tissues. [3] Cells cultured in 2D compared to 3D environment have also shown to have different cell-matrix contacts, cell migration, cell morphology, gene expression, and signaling cascades [4]. Therefore, 3D cell models mimic native tissues better than 2D models and thus are better models for studying human physiology.

One problem when using hydrogels as 3D scaffolds in cell culturing is their uncontrolled decrease in size. This problem has been observed especially in case of natural or protein-based ECM hydrogels. Decrease in size of the hydrogel can be due to hydrogel degradation or shrinking depending on the cause of size change. This decrease in size of the hydrogel during cell cultivation is a known problem in many *in vitro* disease models and in advanced organotypic applications such as Organ-on-a-Chips (OOAC). Degradation or shrinking of supporting hydrogel leads to loss of the 3D structure, collapse of cell culture or condensed structure and limits the length of cell experiments, thus hindering the full potential of modern tissue engineering seeking more information about mechanisms behind tissue actions in healthy and diseased tissues.

This degradation problem mainly appears with hydrogels composed of proteins with natural origin because they mimic the natural ECM therefore being the most suitable and

widely used options for cell cultures. The hydrogel degradation problem has not yet been solved despite many efforts to find case-by-case application-specific hydrogel concentration that does not shrink and provides 3D support for the cells. This can be a solution in traditional cell culture applications with single or few cell types but when moving towards multiorgan systems, mimicking tissue or even organ functions, such as Body-on-Chip applications, these specific hydrogels often lack the support for all used cell types. Therefore, there is a need to find a solution to prevent the degradation of ECM-like hydrogels during culturing period especially when aiming for *in vivo*-like tissue replication and long-term culture. Furthermore, with better disease models, testing of, for example, drug safety and efficacy, becomes faster and cheaper, and, in the future, they can even be used in personalized medicine. In addition to preventing degradation or size change of hydrogels, it is also important to be able to measure, control, and study the size change of the used hydrogel.

In vivo, cells and especially fibroblasts produce different proteases, including matrix metalloproteinases (MMPs), which degrade matrix by cleaving the peptide bonds of ECM [5]. The MMPs are a family of enzymes which can degrade ECM components such as collagen fibers [6,7]. Therefore, MMPs regulate the integrity and composition of ECM *in vivo* [8]. *In vivo*, there is a complex regulation cycle which regulates the enzymatic activity of MMPs including MMP inhibitors which help maintaining the mechanical properties of the ECM. [5] MMPs can, for example, be inhibited with tissue inhibitors of metalloproteinases (TIMP) *in vivo* but there are also synthetic MMP inhibitors created. TIMPs are a family of proteins secreted by many cells. The TIMPs are able to selectively target individual MMPs by adding a preserved anchor into the active side of the target MMP. [6]

Human body is maintained and supported through two major circulatory systems, cardiovascular system, and lymphatic system. The cardiovascular system consists of heart and blood vessels which include arteries, veins, and capillaries. The cardiovascular or vascular system plays an important role in delivering nutrients and oxygen to the cells and removing metabolites and carbon dioxide from the cells. [9] Blood vessels are networking through the human body in approximately 100 000 km thus making vascular endothelium the largest endocrine organ [10]. MMPs are needed also in formation of new blood vessels [11,12].

The vascularization is essential for almost all tissues and therefore it is also important for organotypic *in vitro* models such as OOACs where it enables transport of nutrients and oxygen to the cells and tissues while it also gives mechanical support for the tissue

and supports target cell functionality and maturation beside the circulatory functions. Generation of vascular network in different tissue models is important to increase the physiological relevance and resemblance of human tissue functions. [13,14]

This thesis consists of a literature review and an experimental part. Firstly, the literature review covers the theoretical background behind the study. That part focuses on hydrogels, OOAC applications and vascularization and combining these. In addition, the part includes background information about the cells, biomaterials and inhibitors used in this study. The experimental part starts by presenting the aims of the experimental part of the thesis. The aim was to find or create better method to analyze size change of the samples during cultivation, find a solution to prevent the degradation or size change of the hydrogel during cultivation without disturbing the cells' natural actions and functions, and find better hydrogel options for 3D vascularization model on microfluidic chip. This includes increasing the longevity of the hydrogels while supporting the cells' viability, elongation, proliferation, and vascular formation.

After the aims are presented, the materials and methods used in this study are explained. The experimental work consists of two main parts: cell culture within hydrogels in static conditions on well plate and in more dynamic conditions on microfluidic chips. The well plate experiments include studying the degradation or size change of the chosen hydrogels via measuring size changes of the hydrogels during cultivation as well as testing two inhibitors and their combination's effects on to the cultured cells and hydrogels. The well plate experiments were included to the study because the size changes of the samples are easier to observe and measure in well plate environment compared to microfluidic chip. In addition, the well plate experiments acted as preliminary studies based on which the hydrogels and inhibitor combinations were chosen for chip experiments.

In the second part of the experimental study, the hydrogels and inhibitors chosen based on the first part, were used in microfluidic chip in Vascularization-on-a-Chip application where the aim was to find intact and long-lasting or durable hydrogel options that supports 3D vascular network formation. Finally, the obtained results of the study are presented and discussed. Lastly, the main findings and future perspectives of the thesis are concluded.

2. THEORETICAL BACKGROUND

2.1 Hydrogels

Biomaterials are natural or synthetic materials used in interaction with living cells or organisms. Biomaterials can provide a 3D microenvironment which promotes cell attachments, growth, and development of tissues. Natural biomaterials usually mimic better the native environment of the cells, thus having enhancing effect on cell culture. However, the natural biomaterials' mechanical properties are usually not properly supporting tissue dynamics and maturation. [15] Another major problem when using natural polymers as biomaterials are batch-to-batch variation. In addition, there is a risk of transferring diseases or infectious agents when using animal-based materials. Furthermore, there is risk of immune response or even rejection. Synthetic biomaterials, on the other hand, usually have better mechanical properties, are controllable, and tunable. In addition, they are non-immunogenic, so they cause fewer immune reactions. Furthermore, they have better storage life without batch-to-batch variation but they lack cell attachment sites. [15] Therefore, finding suitable biomaterial which would have cell attachment sites as well as appropriate mechanical properties is important to be able to create better cell models.

Hydrogels are biomaterials composed of hydrophilic and crosslinked polymer chain networks. The origin of the polymers can either be natural or synthetic. Polymer chains form crosslinks which can be either chemical bonds or physical interactions. These crosslinks affect in the integrity of the structure of the hydrogel. [3]

Hydrogels have porous 3D structure (Figure 1) which allows it to absorb large amounts of water into them. In addition, hydrogels have ability to organize cells as well as direct the formation of desired tissue by giving different stimuli like mechanical and chemical stimuli. Hydrogels are also good scaffold materials because their structure resembles the ECM of multiple human tissues. Furthermore, hydrogels can be processed under mild conditions and delivered in a minimally invasive manner. [3]

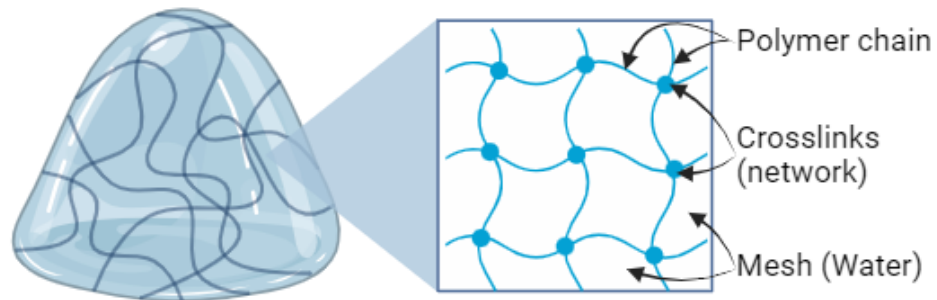


Figure 1. Hydrogel structure. Created in BioRender.com, Modified from [16]

Hydrogels, used as a scaffold which encapsulates cells, have certain requirements. Firstly, the cells should not be damaged during gelation of the hydrogel, and the hydrogel must be nontoxic to the cells. The hydrogel should allow the diffusion of oxygen, carbon dioxide, nutrients, and metabolites through the hydrogel to and from the cells and surrounding tissue environment. In addition to all this, the hydrogel should have suitable mechanical and biological properties for the cells. [3] This means that the hydrogel should be able to withstand the forces caused by the cells as well as allow the cellular functions like proliferation and differentiation.

A 3D hydrogel provides environment for the cells that mimics the cells' natural environment better compared to traditional, planar monolayer culture (2D). This is due to cell interactions with ECM and with other cells which play an important role in maintaining the tissue functions *in vivo*. The complex chemical and mechanical signals of cell interactions enable maintaining the cell function. Therefore, the better these natural conditions can be mimicked, the better cells can maintain their functions and differentiated stage when cultured *in vitro*. [17] In addition, in 2D cell cultures the cells have very different environment in different sides: on the bottom they have really hard surface ahead of them while on the other side they face liquid environment. This kind of living environment is rare in natural human body and therefore do not mimic the basic environment of the body. This is why, creating 3D culture environment is important when aiming models with *in vivo*-like tissue replication.

Natural hydrogels like collagen and fibrin are widely used scaffold materials because they have certain advantages. For instance, the mechanical properties of the collagen are easy to adjust by gelation at different temperatures or pH or by altering protein concentration [18,19]. Fibrin, on the other hand, has ideal strain stiffening properties for the formation of vascular network composed of endothelial cells [18]. By combining these

two hydrogels, collagen and fibrin, better scaffold material for vascular model could be formed.

In the experimental part of the thesis, the used hydrogels are fibrin, collagen I with different origins, inhouse-made gelatin-gellan gum (gelaGG), and one commercial ECM-based material (VitroGel®). Next, focus more deeply to a few hydrogels used in this thesis and which are commonly used in the tissue engineering and OOAC applications.

2.1.1 Fibrin

Fibrin and its preform fibrinogen are essential for haemostasis, a process to prevent and stop bleeding. In addition to having key role in wound healing, they have also major role in other biological functions like inflammation and angiogenesis. Fibrinogen is normally present in human blood plasma as a soluble macromolecule. Fibrinogen forms insoluble gel, fibrin, when in contact with serine protease thrombin (Figure 2). Thrombin, on the other hand, is activated via cascade which is triggered, for example, by vessel wall injury, activated blood cells or a foreign surface. [20]



Figure 2. Thrombin cleave fibrinogen forming fibrin. Created in BioRender.com

Fibrinogen is mainly produced by the liver. The production of fibrinogen is upregulated in response to an injury or inflammation and the regulation is mediated by interleukin-6 and other proinflammatory mediators. The fibrinogen is composed of three pairs of polypeptide chains: $A\alpha$, $B\beta$, and γ . The chains are held together by disulphide bonds. The thrombin cleaves N-terminal ends of the $A\alpha$ and $B\beta$ chains but γ is left intact. The α -helical coiled-coil is composed of three right-handed α -helices which form a left-handed supercoil. However, each of the coiled-coils of fibrinogen has a fourth helix in the bundle which is rare compared to other triple helices. [20]

Fibrin hydrogel has a suitable biological and physical characteristic including porosity, deformability, elasticity, and biodegradability [20,21]. Fibrin has inherent biological activity due to its integrin and growth factor binding sites [22]. Therefore, fibrin hydrogel is widely used hydrogel in tissue engineering applications. This is also because it supports cell adhesion, proliferation, stem cell differentiation as well as angiogenesis. [23] In addition, the fibrin has an ability to support the formation of a homogenous blood capillary network [24]. However, it has relatively fast resorption rate which may reduce the applicability [22]. In addition, fibrin has poor mechanical properties, and the scaffold

usually degrades or shrunk fast. Proteases, such as plasmin and MMPs, degrade fibrin hydrogels. [21,23]

Problems related to fibrin degradation have been tried to solve by refining the polymerization parameters, adding protease inhibitors like aprotinin, using photochemical crosslinking, or by combining the fibrin with other materials [21,23,25]. Fibrin has been combined with both natural and synthetic polymers including alginate, collagen, hyaluronic acid (HA), polylactic acid (PLA), poly(lactic-co-glycolic acid) (PLGA) and polycaprolactone (PCL) [23,26]. Combining collagen and fibrin hydrogels have shown to provide extra stiffness, and durability to the material combination. In addition, fibrin can be covalently crosslinked by the plasma transglutaminase, Factor IIIa. The crosslinking changes the polymerization to be irreversible and therefore make the forming hydrogel more stable, mechanically stronger and also resistant to fibrinolysis. [20] Furthermore, the gel shrinkage can be prevented by incorporating a fixing agent like poly-L-lysine into the fibrin hydrogel during cultivation period. The stability of fibrin can also be improved by optimizing pH, and the concentrations of fibrinogen and calcium ion (Ca^{2+}). [21] Both serine protease inhibitor, aprotinin, and MMP inhibitor, galardin, have shown to prevent the degradation of fibrin and when used together they even enhanced the accumulation of ECM [21,27].

Fibrin was chosen to be used in this study because it has shown to be the golden standard in vascularization assays as shown in the previous study [28] made in our research group.

2.1.2 Collagen

Collagen is a natural polymer. It is the most abundant protein in mammalian tissues, and it is also the main component of natural ECM. Collagen plays an important structural role in the ECM, but it also plays major roles in cellular and molecular interactions in the ECM. Thus it defines the forms and shapes of different tissues. [29,30] Because of all this, collagen mimics well the natural ECM of multiple tissues and is therefore widely used in tissue engineering.

There are multiple different types of collagens, but collagen type I is the most abundant one in the human body, especially in the connective tissue. Figure 3 presents the structure of collagen fibers. The collagen is composed of three polypeptide chains, left handed α chains, which form three-stranded right-handed helical structure. [3,31,32] The α chains are composed of repeating peptide triplets: glycine-X-Y where X and Y are

usually proline and hydroxyproline but they can also be any amino acid [20,31]. The glycine plays an important role in the structure of collagen because the structure is so tight that there is no space for bigger amino acid than glycine. In addition, hydroxyproline, which is post-translationally modified proline, is important for collagen since it increases the thermal stability of collagen. Furthermore, it appears to have essential role in self-association and in certain receptor interactions. [29] The strands are held together via hydrogen bonds which are formed between every third glycine and amino acid in X position [3,20,31]. In addition, the collagen fibrils are stabilized with covalent intermolecular crosslinks which are initiated due to activity of enzyme lysyl oxidase (LOX) [20].

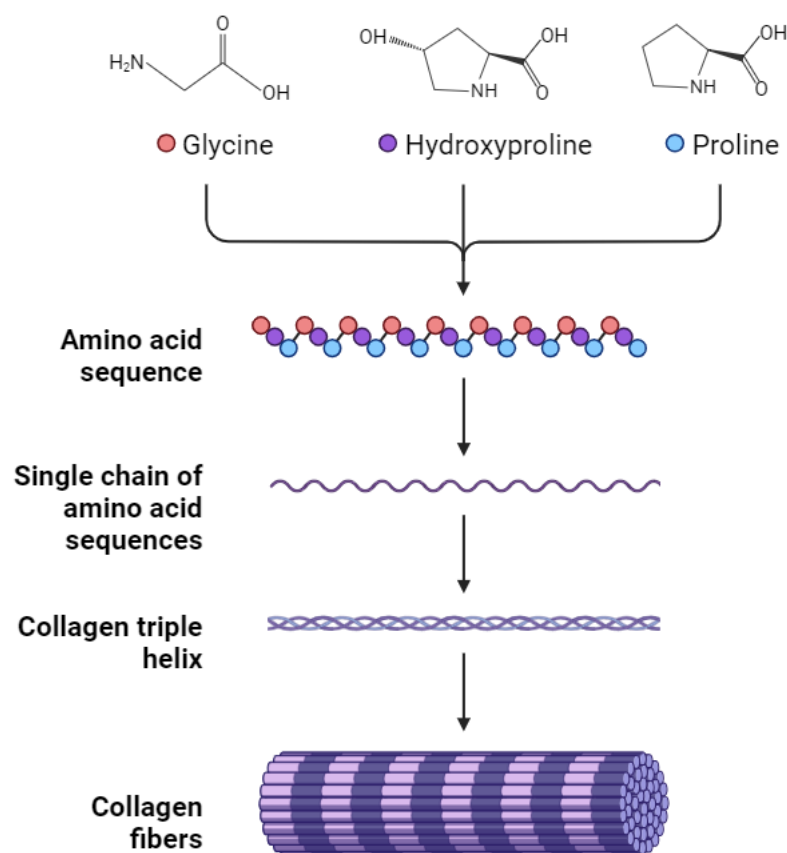


Figure 3. Structure of collagen. Created in BioRender.com, Modified from [33]

Collagen can either be homotrimer, when all three chains are identical, or heterotrimer, when the chains are different. Collagen type I, for example, is a heterodimer consisting of two $\alpha 1(I)$ and one $\alpha 2(I)$ chains. Collagen type I is the main protein in bone, skin and tendon but it is also the main structural component of blood vessels together with collagen type III. [20]

Collagen is widely used in biomedical engineering applications, like in tissue engineering, due to its structural and physical properties. These properties include mechanical

strength, hydration, integrity, and resistance to most common enzymes. In addition, the physiological interactions between collagen and cells or other ECM components give a lot of opportunities for the applications. [20] Collagen is naturally degraded by metalloproteases such as collagenase and serine proteases [3,20]. All MMPs cleave the collagen molecules from the same site which is about $\frac{3}{4}$ away from the N-terminus (end of polypeptide with free amine group $-\text{NH}_2$) [20]. The properties of the collagen can be modified by using different crosslinkers, either chemical or physical, or by blending it with other polymers. Collagen have been blended with HA, PLA, poly(glycolic acid) (PGA), and PLGA. [3]

There are many kinds of sources of commercial collagen. Usually, collagen is obtained from an animal source like from bovine hide, porcine or rat tail. Nowadays, there are also another option for the source, recombinant collagen. The recombinant collagen is purer, without immunogenicity, and there is also possibility to manipulate the amino acid sequence of the collagen which is a major advantage. However, recombinant materials do not have all the features that native collagen has because they lack some of the post-translational modifications like hydroxylation and glycosylation of lysine and LOX-mediated crosslinking. These modifications affect the stability of the collagen so without the modifications, the collagen is less stable. Other limitations of recombinant collagen is high cost compared to animal-derived collagen and its availability is also limited. [20,29]

Nowadays, recombinant collagen has been produced by bacteria, plants, and yeast from which the plant systems have shown the best outcome. [29] In addition to those, recombinant collagen can be produced with bioreactor based eucaryotic production system, mammalian cell culture, insect cell culture, and transgenic production systems. Recombinant human collagen usually lacks post-translational modifications which makes the collagen unstable. This stability problem concerns other production systems except production of recombinant collagen with mammalian cell cultures because the collagens produced in mammalian cell cultures do not lack post-translational modifications. The stability problem has been solved by co-expressing recombinant collagen I with human prolyl 4-hydroxylase (P4H). [34]

VitroCol[®], one of the materials used in this study, is based on human collagen I which is naturally secreted by human neonatal fibroblast. The fibroblasts are cultured in optimal

conditions where they secrete ECM which is then processed and purified to be used as human collagen in research. [35]

Other sources of collagen used in this study are rat tail collagen I, and type I bovine Telocollagen, TeloCol[®] [36]. Telocollagen is extracted by using acids while Atelocollagens are extracted enzymatically. When the collagen is extracted enzymatically, the enzyme cleaves the telopeptide portions from the ends of the collagen molecule while when the collagen is extracted by using acid, these telopeptides remains intact. Telocollagen gellates faster and creates stronger gels compared to Atelocollagen. [37,38] Rat tail collagen I and VitroCol[®] are both Atelocollagens.

Collagen I with different origins were chosen to be used in this study due to its *in vivo*-like properties, and its localization close to vascular network in the human body. In addition, it is abundant protein in the human body and widely used in tissue engineering applications.

2.1.3 Gelatin-gellan gum

Gelatin-gellan gum or gelaGG is an inhouse-made biomaterial composed of modified gelatin and gellan gum (GG). Gelatin is derived from collagen, the abundant ECM protein. Gelatin can form hydrogel by itself via reversible physical crosslinking which is temperature dependent. However, the gelation temperature is under physiological requirements (+ 37 °C) which means that the gelatin hydrogel cannot be used in cell culture applications alone. GG, on the other hand, is a bacterial polysaccharide which can form hydrogels via ionic crosslinking with adjustable mechanical properties. As a downside, the GG is bioinert material, so it does not provide cell attachment sites. However, bioactive functionalization of GG have shown to maintain its mechanical stability while also improving cell response. [39–41]

To be able to form crosslinks between gelatin and GG, they must be modified. Hydrazide groups are introduced to the carboxylic group in gelatin backbone via carbodihydrazide (CDH). Carbodihydrazide modified gelatin (gelaCDH) can form crosslinks with aldehyde groups which are formed in GG's structure via periodate oxidation modification. The oxidized GG (GGox) and gelaCDH form hydrazone bonds as a chemical crosslinking to form hydrogel under physiological conditions. [39–41]

This modified biomaterial is developed in-house and therefore it is quite novel and rarely used. However, Koivisto et al. (2019) succeeded to create beating human induced pluripotent stem cell (iPSC) derived cardiomyocytes inside 3D gelaGG hydrogel [39]. In

addition, gelaGG was used with human umbilical vein endothelial cells (HUVECs) and human adipose tissue-derived stem/stomal cells (ASCs) to create vascular network with promising results [40].

GelaGG was used in this study because it is an in-house made material which full potential have not yet been discovered and due to previous experience in our research group and promising results obtained from the vascular study [40]. In addition, it has not been used on microfluidic chip before so one goal is to investigate whether it could be used in such applications.

2.2 Hydrogel size change

One of the problems when creating 3D vascularization models is that the hydrogel's size decreases during cultivation. The hydrogels have shown to have ability to shrink or degrade during culturing period which decreases the support that they provide for the cells. This usually leads to problems the further the cultivation continues as the hydrogel degradation leads to loss of the 3D structure, collapse of cell culture and limits the length of experiments, thus hindering the full potential of modern tissue engineering. Cells and culture medium have shown to play a role in the shrinkage of the hydrogels during cultivation.

A couple of studies have noticed the shrinkage of the hydrogels during cultivation [24,42,43]. For example, Liu et al. (2020) reported that the collagen microfibers (CMF-20) with 20 μm diameter prevented the shrinkage of the hydrogel, caused by the cells, in z-axis [24]. They measured the thickness of the samples from histological images [24]. Furthermore, Isosaari (2021, 2023) observed shrinking of the hydrogel in her bachelor's thesis and in her article [42,43]. She suggested that the medium affects to the shrinking of the hydrogel, but it was not clear whether the shrinking was caused by the medium itself or the fact that the medium changes the cell behavior. The shrinking of the hydrogels were observed under a phase contrast microscope but not quantified. [42,43]

There are multiple factors that can affect to size change, such as degradation, shrinkage or swelling of the hydrogel. These factors include temperature, pH, swelling due to solvent, gas-foaming, use of nanoparticles, and variation in crosslinking ratio [44]. Temperature is probably the easiest factor to monitor when modifying hydrogels. Thermoresponsive hydrogels have shown volume shrinkage in cell culture [44,45]. It has also been noted that higher concentration of gelatin methacrylate (GelMA) blocks the

shrinkage of thermoresponsive hydrogels. [45] However, the size change of hydrogel during cultivation can be caused by the actions of the cells.

Cells can also have an impact of the materials or hydrogels' properties or characteristics they have been seeded in. For example, Boucard et al. (2022) proved that especially fibroblasts, both primary and immortalized, from different origins can degrade alginate, gelatin, and fibrin-based hydrogels and biomaterials [46]. That degradation can be prevented by using serine protease inhibitors, like aprotinin, because the degradation happens through the secretion of MMPs and urokinase which are two types of serine proteases. Using aprotinin resulted stable fibrin hydrogel for at least 48 h. [46] Therefore, the degradation of fibrin can be prevented by choosing suitable cell types or by using serine protease inhibitors.

Studying the shrinking of the hydrogel is still uncommon and not many studies can be found to investigate the shrinking or degradation of the hydrogel. Usually, the swelling of the hydrogels is studied especially when creating new hydrogels because they can absorb water in them. The size change can be studied by casting the samples into mold, like modified or cut syringes, from which the samples can be taken out to make the measurements. The samples are usually weighed and their diameter is measured, for example, by hand with vernier calipers. [47] This method has problems since the measurement might have a lot of error, and the samples can be damaged when removing them from the mold and when handling them during measurements, and thus the same samples are not usually used in multiple timepoints which can add even bigger error to the results. Therefore, there are not so many methods to study the degradation or size change of the samples and thus better methods are needed.

One example of these methods includes Boucard et al. (2022) where they studied the gel degradation by measuring white light diffusion through manually deposited hydrogel cast in culture inserts. There were light-emitting diode (LED) light source (4000 K) and a digital microscope which was used to collect the images. They compared the obtained light diffusion results to values obtained from controls. In controls, hydrogel right after casting and pure culture medium without hydrogel were used to mark 0 % and 100 % degradation. [46] Figure 4 shows the experimental setup used in Boucard et al. (2022) study [46]. This method gives information about the degradation of the hydrogel but do not give any information about the size change of the samples.

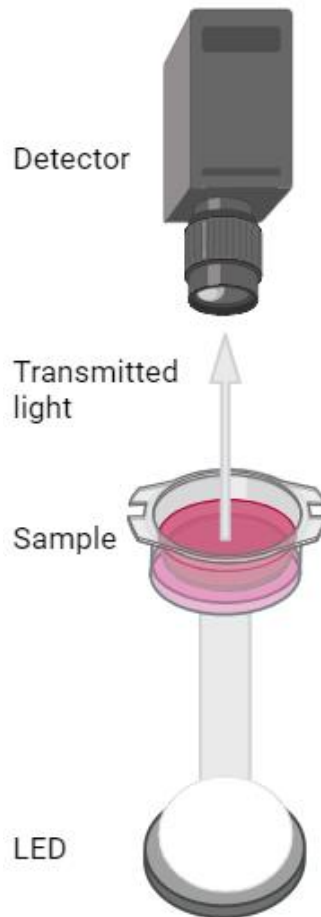


Figure 4. *Experimental setup for studying the degradation of samples. Created in BioRender.com, Modified from [46]*

Other method for investigating hydrogel shrinkage is to measure the change of the diameter of the hydrogel. For example, rod-shaped thermoresponsive hydrogels' diameter was observed with a microscope and the diameter was analyzed with Fiji/ImageJ software. These results have then been compared to results obtained after shrinking and as a results the shrinking can be analyzed. [48] This method gives information about the shrinking in 2D but do not give any information how the thickness of the samples changes so the shrinking in 3D is still unknown.

Furthermore, the shrinking of the cell sheet has also been studied with a shrinking assay where the shrinking of the cell sheet area was measured by using Fiji/ImageJ software [49]. The cell sheet was first detached from the culturing well plate and then the diameter of the cell sheet was measured. That measured value was then compared to the diameter of the whole well which was indicated to be the full size in the beginning. [49,50] The thickness of the harvested cell sheet was observed by measuring the height of the cell from different parts of cell sheet [51]. This kind of method could also be used to study the shrinking of the area of the hydrogel. However, the hydrogel samples cannot be

detached from the well plate without damaging them so other methods must be found to study the thickness of the samples.

2.2.1 Matrix metalloproteinases and their inhibitors

Matrix metalloproteinases or MMPs are enzymes which have the ability to degrade complex substances of ECM [6,7,52]. The MMP family contains 23 or 24 different zinc-dependent endopeptidases depending on the reference [6,8,53]. The activity of MMPs can be regulated at four levels in normal physiological conditions. These levels are transcription, activation of precursor zymogens, interaction with specific components of ECM, and inhibition by tissue inhibitor of metalloproteinases (TIMPs). [54] The most of the MMPs are secreted as zymogens and they can be activated by removing the interaction between zinc and cysteine [6,8,53]. The MMP zymogens are activated by other active MMPs or proteases extracellularly [8,52]. Also oxidants, plasmin, thiol-modifying agents, low pH, and warm temperature can activate the MMPs [52].

The MMPs regulate the integrity and composition of ECM and by doing so they play a role in ECM molecule signaling and also influence some processes including proliferation, migration, differentiation and apoptosis of the cells [8]. In addition, MMPs can adjust biological processes during pathophysiological events. These events include angiogenesis, arthritis, cancer, cardiovascular diseases, cell migration, coagulation, inflammation, pulmonary, skeletal formation, vascular remodeling and wound healing. [52,54] Due to importance of MMPs, they are strictly regulated at multiple levels including transcriptional and translational level, by activation of the zymogen forms, by the extracellular or endogenous inhibitors, by subcellular or extracellular localization and internalization by endocytosis. [8,52] The MMPs' role is often estimated by measuring their messenger RNA (mRNA) expression, protein levels, and proteolytic activity using gel zymography [52].

The activity of MMPs can be inhibited with TIMPs which are the family of proteins secreted by various cells [7]. The protein family contains four mammalian TIMPs from which TIMP-1 and -3 are glycoproteins while TIMP-2 and -4 do not contain carbohydrates [8]. The TIMPs are able to selectively target individual MMPs by adding a preserved anchor into the active side of the target MMP and chelate the catalytic zinc ion. [7] In addition to TIMPs, some other biological molecules can inhibit MMPs. These molecules include the serpine family member, monoclonal antibodies, small interference ribonucleic

acid (siRNA), alpha2-macrogobulin, and secreted form of beta-amyloid precursor protein [8,52].

The ECM's structure is not static and therefore MMPs and TIMPs participate in taking care of the homeostasis of the ECM. Overexpression of MMPs or insufficient function of TIMPs leads to dysregulated tissue remodeling and therefore causes variety of diseases including Alzheimer's disease, rheumatoid arthritis, and tumors. In addition to tissue-remodeling functions, MMPs also have a role in regulating many non-matrix targets including cell surface receptors, cell-cell adhesion molecules, cytokines, clotting factors, chemokines and other proteinases [6].

The overexpression of TIMPs have shown to inhibit the proliferation of both normal and tumor cells. In addition, the use of TIMPs have shown to inhibit the angiogenesis. However, the TIMPs have also shown to promote the cell growth and proliferation. [53] Therefore, it is important to find the golden mean where the inhibition will not disturb the cells natural functions.

The MMP family can degrade all the main components of ECM. However, specific MMPs show characteristics preferences for different ECM molecules as well as non-matrix molecules. According to these preferences, the MMPs can be subdivided into collagenases including MMP-1, -8 and -13, gelatinases including MMP-2 and -9, stromelysins including MMP-3, -10, and -11, matrilysins including MMP-7 and -26, membrane type MMPs (MT-MMP) including MMP-14 to -17, -24 and -25, and others including MMP-12, -20 and -27. The collagenases are specialized to degrade fibrillar collagens including types I, II, III, and VII, while gelatinases mostly degrade denatured collagen and collagen IV, but it can also degrade collagen types I, V, and X, and laminin 5. Stromelysins, on the other hand, can degrade collagen types IV, V, IX, and X, as well as fibronectin, laminin, elastin, gelatin, and proteoglycan core proteins. In addition to these secreted MMPs, there is also MMPs anchored into the cell membrane. These MT-MMPs are able to degrade native-type I collagen, fibronectin, laminin, fibrin, gelatin, and cartilage proteoglycan core protein. [8,53] This classification method is commonly used but it carries a few limitations because the divination is not complete. For example, MMP-1 is named as collagenase, but it can also degrade tenascin and aggrecan. On the other hand, MMP-2 is named as gelatinase, but it can also cleave fibronectin, aggrecan and substrates that are not part of the ECM. [6] Table 4 summarizes different MMPs, their classification, and what they cleave.

Table 1. Different matrix metalloproteases. [8, 12]

MMP	OTHER NAME	GROUP	COLLAGEN SUBSTRATES	NON-COLLAGENOUS ECM SUBSTRATES	NON-ECM SUBSTRATES	DISTRIBUTION
MMP-1	Collagenase I	Collagenases	Collagen types I, II, III, VII, VIII, X and gelatin	Aggrecan, casein, serpins, versican, perlecan, proteoglycan link protein and tenascin-C	α 1-antitrypsin/ α 1-antichymotrypsin, IL-1 β , latent TNF- α , MCP-1, -2, -3, -4, IGFBP-2, -3, SDF-1, VEGF	Endothelium, SMCs, fibroblasts, platelets, macrophages, varicose veins (interstitial/fibroblast collagenase)
MMP-2	Gelatinase-A, Type IV Collagenase	Gelatinases	Collagen types I, IV, V, VII, X, XI, XIV and gelatin	Aggrecan, elastin, fibronectin, laminin, perlecan, proteoglycan link protein and versican	IL-1 β , Pro-IL-1 β , SDF-1, MCP-3, IGFBP3, latent TGF- β , latent TNF- α . FGFR1, pleiotrophin, CTGF	Endothelium, VSM, adventitia, platelets, leukocytes, aortic aneurysm, varicose veins
MMP-3	Stromelysin-1	Stromelysins	Collagen types II, IV, IX, X and gelatin	Aggrecan, casein, elastin, fibronectin, laminin, perlecan, proteoglycan, proteoglycan link protein and versican	α 1-antitrypsin/ α 1-antichymotrypsin, IL-1 β , Pro-IL-1 β , MCP-1, -2, -3, -4, SDF-1, IGFBP-1, -3, latent TGF- β , latent TNF- α , Pro-HB-EGF, osteopontin, VEGF	Endothelium, intima, VSM, platelets, coronary artery disease, hypertension, varicose veins, synovial fibroblasts, tumor invasion
MMP-7	Matrilysin-1	Matrilysins	Collagen types I, II, III, V, VI and X	Aggrecan, casein, elastin, entactin, laminin and proteoglycan link protein	α 1-antitrypsin, Pro-HB-EGF, Latent TNF- α , syndecan-1, osteopontin, cellular membrane bound FasL, VEGF	Endothelium, intima, VSM, uterus, varicose veins (PUMP)
MMP-8	Collagenase II	Collagenases	Collagen types I, II, III, V, VII, VIII, X and gelatin	Aggrecan and laminin	α 1-antitrypsin, CXCL5, IL-8	Macrophages, neutrophils (PMNL or neutrophil collagenase)
MMP-9	Gelatinase-B, Type IV Collagenase	Gelatinases	Collagen types V, VI, VII, X and XIV	Fibronectin, laminin, proteoglycan link protein and versican	α 1-antitrypsin, IL-1 β , Pro-IL-1 β , CXCL5, IL-8, SDF-1, latent TGF- β , latent TNF- α , IL-2R α , IGFBP-1, VEGF	Endothelium, VSM, adventitia, microvessels, macrophages, aortic aneurysm, varicose veins
MMP-10	Stromelysin-2	Stromelysins	Collagen types II, IV, V and gelatin	Fibronectin and laminin	Casein, proMMP-1, -8 and -10	Atherosclerosis, uterus, preeclampsia, arthritis, carcinoma cells
MMP-11	Stromelysin-3	Stromelysins	None known	Aggrecan, fibronectin, laminin	α 1-antitrypsin, α 1-proteinase inhibitor, IGFBP-1	Brain, uterus, angiogenesis

MMP-12	Metalloelastase	Other MMPs	Collagen type IV, and gelatin	Elastin, laminin	fibronectin,	Latent TNF- α , plasminogen	Casein,	SMCs, fibroblasts, macrophages, great saphenous vein
MMP-13	Collagenase III	Collagenases	Collagen types I, II, III, IV, V, IX, X, XI and gelatin	Aggrecan, laminin, perlecan and tenascin	fibronectin, perlecan and	α 1-antichymotrypsin, latent TGF- β , latent TNF- α , MCP-3, SDF-1	SMCs, macrophages, varicose veins, preeclampsia, breast cancer	
MMP-14	MT1-MMP	Membrane-Type	Collagen types I, II, III and gelatin	Aggrecan, dermatan sulfate proteoglycan, elastin, fibrin, fibronectin, laminin, perlecan, tenascin and vitronectin		MCP-3, SDF-1, α v β 3 integrin, CD44, proMMP-2 and -13, pro-TNF- α , α 1-proteinase inhibitor, tissue transglutaminase	VSM, fibroblasts, platelets, brain, uterus, angiogenesis	
MMP-15	MT2-MMP	Membrane-Type	Collagen types I, II, III and gelatin	Aggrecan, laminin, tenascin and vitronectin	fibronectin, perlecan,	ProMMP-2 and -13, tissue transglutaminase	Fibroblasts, leukocytes, preeclampsia	
MMP-16	MT3-MMP	Membrane-Type	Collagen types I, III and gelatin	Aggrecan, fibronectin, perlecan and vitronectin	casein, laminin,	VEGF, casein, proMMP-2 and -13	Leukocytes, angiogenesis	
MMP-17	MT4-MMP	Membrane-Type	Gelatin	Fibrin and fibronectin		TNF- α	Brain, breast cancer	
MMP-18	Collagenase IV	Collagenases	Collagen types I, II, III, and gelatin			α 1-antitrypsin	Xenopus (amphibian, Xenopus collagenase) heart, lung, colon	
MMP-19	RASI-1	Other MMPs	Collagen types I, IV and gelatin	Aggrecan, fibronectin, laminin, and tenascin	casein,	VEGF	Liver	
MMP-20	Enamelysin	Other MMPs	Collagen type V	Aggrecan, amelogenin and cartilage oligomeric protein			Tooth enamel	
MMP-21	Xenopus-MMP	Other MMPs				α 1-antitrypsin	Fibroblasts, macrophages, placenta	
MMP-22	Chicken-MMP	Other MMPs	Gelatin				Chicken fibroblasts	
MMP-23	CA-MMP	Other MMPs	Gelatin	Chondroitin sulfate, dermatan sulfate and fibronectin			Ovary, testis, prostate Other (type II) MT-MMP	

MMP-24	MT5-MMP	Membrane-Type	Gelatin	Fibrin and fibronectin, chondroitin sulfate, dermatin sulfate, N-cadherin	ProMMP-2 and -13	Leukocytes, lung, pancreas, kidney, brain, astrocytoma, glioblastoma
MMP-25	MT6-MMP	Membrane-Type	Collagen type IV and gelatin	Casein, fibrinogen, and fibronectin	proMMP-2, α 1-proteinase inhibitor	Leukocytes (Leukolysin), anaplastic astrocytomas, glioblastomas
MMP-26	Matrilysin-2, Endometase	Matrilysins	Collagen type IV and gelatin	Casein, fibrinogen, fibronectin, vitronectin	α 1-antitrypsin, β 1-proteinase inhibitor, proMMP-2	Breast cancer, endometrial tumors
MMP-27	Human MMP-22 homolog	Other MMPs				Heart, leukocytes, macrophages, kidney, endometrium, menstruation, bone, osteoarthritis, breast cancer
MMP-28	Epilysin	Other MMPs			Casein	Skin, keratinocytes

CA-MMP: cysteine array MMP, CTGF: connective tissue growth factor, CXCL5: C-X-C motif chemokine ligand 5, EGF: epidermal growth factor, ECM: extracellular matrix, FGFR: fibroblast growth factor receptor, IGFBP: Insulin-like growth factor-binding protein, IL-1: interleukin 1, IL-8: interleukin 8, IL-2R: interleukin 2 receptor, MCP: monocyte chemoattractant protein, MMP: matrix metalloproteinase, MT-MMP: membrane type MMP, pro-HB-EGF: pro-heparin-binding epidermal growth factor-like growth factor, RAS1-1: rheumatoid arthritis synovium inflamed-1, SDF: stromal cell-derived factor, TGF: tumor growth factor, TNF: tumor necrosis factor, VEGF: vascular endothelial growth factor.

Other way of classifying MMPs is based on their domain organization. In this classifying method, the MMPs are divided into archetypal MMPs, matrilysins, gelatinases and furin-activable MMPs. Almost all MMPs share the same domain structures. These structures include signal peptide which mediates MMP secretion, pro-peptide which protects the Zn^{2+} binding site through interaction with a cysteine residue keeping the MMPs in the pro-forms until the cleavage of the pro-peptide domain, catalytic domain which contains Zn^{2+} and is responsible of substrate hydrolysis, and lastly hemopexin domain which is linked to catalytic domain through a flexible hinge, and which takes care of substrate recognition and dimerization. In addition to these common structures, there are features which are characteristics only for a few MMPs. For example, MMP-7 and -26 lack the hinge region and the hemopexin domain, MMP-2 and -9's catalytic site contain three fibronectin type II motifs which are collagen binding domains, furin-activable MMPs have a furin cleavage motif between the pro-peptide and catalytic domain, membrane type MMPs have a transmembrane domain or glycoposphatidylinositol anchor on their C-terminus, and MMP-23 lacks the signal peptide, the cysteine-switch motif and the hemopexin domain. [6,8]

Many cell types and especially fibroblasts and leukocytes produce different proteases, including MMPs, which cause the degradation of matrix by cleaving the peptide bonds of ECM [5,12]. In addition, lymphocytes, granulocytes and activated macrophages produce MMPs [55]. For that reason, protease inhibitors are needed to prevent the degradation of ECM matrix. *In vivo*, there is a complex regulation cycle which regulates the enzymatic activity of MMPs. This regulation cycle includes MMP inhibitors which help maintaining the mechanical properties of the ECM. [5]

The development of MMP inhibitors can be divided into four generations where the inhibitors varied from small molecules or peptides to antibodies and even protein-engineered inhibitors. The first generation includes hydroxamate-based inhibitors, the second generation non-hydroxamate-based inhibitors, the third generation catalytic domain and non-zinc binding inhibitors, and lastly the fourth generation allosteric and exosite inhibitors. Nowadays new techniques have been used to develop new MMP inhibitors. These techniques include antibody based inhibitors and protein-engineered inhibitors. [6,8]

MMP inhibitors are studied to be used especially in cancer treatments to prevent the tumor vascularization. However, most of the developed inhibitors had some kind of side effects during different stages of trials. Nevertheless, collagenase inhibitor, doxycycline

hyclate, which is a tetracycline analogue, is the only MMP inhibitor that United States Food and Drug Administration (FDA) have approved to be used for any human diseases. [8,52] In addition, few broad inhibitors for MMPs have also been created. Marimastat is an example of broad MMP inhibitors. It has been used, for example, in Boucard et al. (2022) and Zhang et al. (2022) studies to prevent the degradation of hydrogels [46,56].

MMPs are really conserved molecules which makes the creation of specific MMP inhibitors difficult. Natural inhibitors, TIMPS, usually inhibit multiple MMPs and therefore are not so specific. Synthetic MMP inhibitors have also poor selectivity and affect many biological events causing side effects. [12] Therefore, new synthetic MMP inhibitors with more selective specificity are highly needed.

The use of inhibitors can affect the properties of the matrix. For example, Hafner et al. (2020) showed that the elasticity of the ECM increased when protease inhibitor cocktail was used [5]. More studies are still needed to confirm which kind of changes the use of inhibitors do to a hydrogel.

Aprotinin is a serine protease inhibitor and therefore it is not a MMP inhibitor. However, it has been showed that aprotinin is able to inhibit the activation of MMPs by inhibiting plasminogen and plasmin which do not only increase the secretion of MMPs but also induce the cleavage needed to activate MMPs [57]. As a matter of fact, serine protease, plasmin, has been considered to be the most significant activator of MMPs *in vivo* [8]. Due to this fact, the aprotinin can also be used *in vitro* to inhibit the activation of MMPs. The use of aprotinin *in vitro* will not probably inhibit MMPs activity totally but it could be used to slow down the degradation of ECM. At the moment, aprotinin is widely used with fibrin hydrogels preventing their degradation but it could be used with other hydrogels as well.

2.2.2 Matrix metalloproteinase and vascularization

MMP-1, -2, -3, -7, -8, -9, -12, -13, MT1-MMP and MT3-MMP are expressed in several vascular cells and tissues. MMP-2 and -9 are, for example, located in different layers of the venous wall of rat's inferior vena cava. In the venous wall, the MMP-2 and -9 probably interact with different molecules and signaling pathways of endothelial cells, vascular smooth muscle cells (vSMC), and ECM. MMP-1, -2, -3, and -7 have also shown to be distributed in endothelial cells and vSMC. [12]

MMPs regulate vSMCs growth and proliferation via various mechanisms. These mechanisms include proteolytic cleavage of growth factors making them available to the

cells that are not in physical contact, degradation of ECM allowing cells to migrate across the tissues, and regulated receptor cleavage terminating the migratory signaling and cell migration. MMPs can induce the release of growth factors by cleaving the proteins and matrix molecules binding them. In addition, the use of synthetic MMP inhibitors have shown to inhibit vSMC proliferation *in vitro*. However, MMP-1 have shown to increase vSMC migration and MMP-9 may also be involved in it. The vSMC migration requires basement membrane distribution, the MMPs degrade the basement membrane and thus enable ECM-integrin interactions. [12]

In angiogenesis, the endothelial cells migrate to the surrounding tissue and to be able to do so, it involves degradation of the vascular basement membrane and ECM remodeling caused by MMPs. In addition, MMPs enhance the angiogenesis, for example, by detaching pericytes from the vessels, cleaving endothelial cell-cell adhesions, and releasing ECM-bound angiogenic factors. Furthermore, angiogenic factors can induce the MMP expression in endothelial and stromal cells while MMPs can enhance the availability of angiogenic factors released from degrading ECM. Therefore, HUVECs which are treated with vascular endothelial growth factor (VEGF), upregulate more the expression of MMP-1, -3, -7, -8, -9, -10, -13, and -19. [11,12,52] Angiogenic factors can induce MMP expression in endothelial and stromal cells but MMPs can also enhance the availability of angiogenic factors [11,12].

MMPs can also negatively influence the angiogenesis. This can be done via generation of endogenous angiogenesis inhibitors by cleaving proteolytically certain collagen chains and plasminogen and by modulating the cell receptor signaling by cleaving the ligand binding domains of the receptors. For example, MMP-7, -9, and -12 may block angiogenesis by converting plasminogen to angiostatin which is an angiogenesis inhibitor. In addition, MMP-14 cleaves endoglin, a TGF- β co-receptor, and therefore inhibits its angiogenic effect. Furthermore, downregulation of MMP-2 and -9 decreases the tumor angiogenesis [11,12]. Figure 5 presents the effects of MMP-2 and MMP-9 to the angiogenesis.

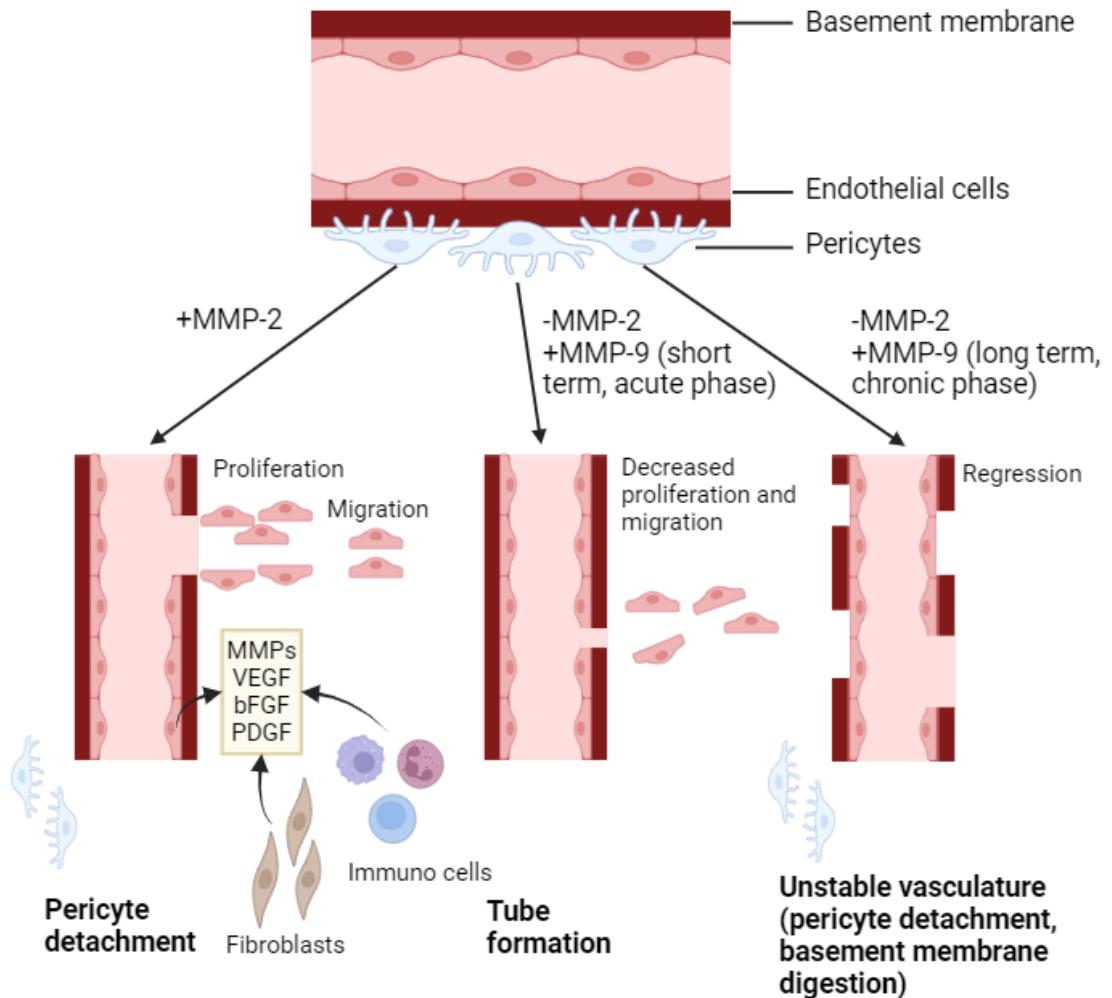


Figure 5. Role of MMP-2 and MMP-9 on angiogenesis. MMP-2 regulates proliferation of endothelial cells and tube formation while MMP-9 momentarily supports only the tube formation. However, prolonged expression of MMP-9 leads to pericyte detachment and vascular regression. MMP: Matrix metalloproteinase, VEGF: vascular endothelial growth factor, bFGF: basic fibroblast growth factor, PDGF: platelet-derived growth factor, Created in BioRender.com, Modified from [58,59]

When studying vascularization *in vitro*, it is important that the used inhibitor will not disturb the vascular network formation. Zhang et al. (2022) tested different inhibitors with vascularization model on a perfused microfluidic chip [56]. They found out that aprotinin, plasminogen activator inhibitor-1 (PAI), NSC 405020 (selective inhibitor of MMP-14), and Anti-MMP-1 neutralizing antibody did not have any effect on vascular network formation [56]. This means that inhibition of plasmin, plasminogen, MMP-1 or collagenase I, or MMP-14, does not affect the formation of vascular networks. However, they found out that MMP-2 is an essential for vasculogenesis and when MMP-2 is inhibited, the formed vessels were narrower, they were not perfusable, and they had more branches. In addition, the vessel coverage was reduced. Furthermore, with higher concentrations of

the MMP-2 inhibitor, no vessels were formed. [56] According to this study, the inhibitors used in this thesis should not disturb the vascularization.

Endogenous TIMPs have also shown anti-angiogenic activities. TIMP-2 inhibits the proliferation of endothelial cells, TIMP-3 inhibits cell migration and proliferation of endothelial cells and TIMP-4 inhibits endothelial cell tube formation. [11] These anti-angiogenic activities are useful when preventing tumor angiogenesis *in vivo*, but they might be problematic when used in vascular models *in vitro* where the inhibitors are used to prevent the degradation of the ECM and not to prevent the angiogenesis and vascularization.

Aprotinin and Collagenase Inhibitor are used in this study so next focus more on these two inhibitors.

2.2.3 Aprotinin

Aprotinin is a bovine pancreatic trypsin inhibitor isolated from bovine lung tissue and it is a hydrophilic polypeptide [22,60]. In addition, it is a small monomeric serine protease inhibitor which can be, in addition to wild type or animal origin aprotinin, engineered or recombinant aprotinin [22]. Aprotinin, also known as bovine antitrypsin, represents a large protein family of antienzymes which inhibit serine proteases. Serine is the crucial amino acid of active protein-cleaving site of serine proteases due to being the cleaver. Aprotinin inhibits the activity of serine proteases by selectively attaching to the vital serine. [61] In addition, it has shown to successfully inhibit the activation of multiple proteases such as plasmin, trypsin, chymotrypsin, and kallikrein proteases [22]. Furthermore, aprotinin can inhibit the activity of elastase, activated protein C, Factor Xa and Xa, and thrombin [60].

Aprotinin has especially been used to inhibit the degradation of fibrin because the fibrin is degraded via proteases, like plasmin and MMPs [22,23]. The main problem when using aprotinin in inhibiting the degradation of fibrin is that it diffuses rapidly out of the fibrin matrices, and therefore, it does not give prolonged protection from degradation. Longer protection can be obtained when using engineered aprotinin which have been covalently bound to fibrin during the gel formation. The use of engineered aprotinin also reduce the needed dosage of inhibitor. [22] Aprotinin is used in this study to prevent the degradation of fibrin hydrogels and its effects on the degradation of other hydrogels are also studied.

2.2.4 Collagenase inhibitor

Collagenase Inhibitor I inhibits the activity of collagenase enzyme which cleaves collagen type I peptides. Odake et al. (1990) synthesized different series of tripeptidyl analogues which had hydroxamic acid residue in the C-terminus and they tested the inhibitory properties of these molecules against vertebrate collagenase [62]. They found out two peptides, Z-Pro-Leu-Ala-NHOH and Z-Pro-D-Leu-D-Ala-NHOH, which showed to have good inhibitory activity against vertebrate collagenase (IC_{50} 10^{-6} M) [62]. One of these two peptides, called Collagenase Inhibitor I, is used in this study to prevent the degradation of collagen hydrogels but its effects are also studied with other hydrogels as well because MMPs degrade other ECM materials too.

In addition to Collagenase Inhibitor I, there is also other collagenase inhibitors available. Trocade™ is an example of MMP inhibitor which selectively inhibits the activity of collagenase family, including MMP-1, -8, and -13, more likely than gelatinases including MMP-2, -3, and -9. The Trocade™ have also good solubility and it has potential to be used as inhibitor in cartilage collagen metabolism of arthritis models both *in vitro* and *in vivo*. [63]

As mentioned before, doxycycline hyclate is the only collagenase inhibitor that FDA has approved to be used for any human diseases [8,64]. Doxycycline as other tetracyclines have the ability to inhibit MMPs while they also have antimicrobial activities. Doxycycline can inhibit MMPs, for example, by inhibiting the catalytic activity, suppressing MMP gene expression, and preventing the proteolytic and oxidative activation of MMPs. In clinical, doxycycline hyclate has been used with low dosages to treat periodontitis because it loses its antibiotic or antibacterial activities when used with low dosage. [64]

2.3 Cell types

Next, cell types used in this thesis' experiments are presented. These cell types include fibroblasts used in well plate experiments and HUVECs (human umbilical vein endothelial cells) and bone marrow stem/stromal cells (BMSCs) used in Vascularization-on-a-Chip experiments.

2.3.1 Human umbilical vein endothelial cells

Human umbilical vein endothelial cells or HUVECs are endothelial cells isolated from umbilical vein of the human. As a matter of fact, the umbilical cord has become one of the most important sources of endothelial cells used in vascular applications. In addition,

the HUVECs are widely used in different models *in vitro*. [65] They are widely used source of primary endothelial cells especially in vasculature and angiogenesis studies *in vitro* because they are relatively easy to isolate, and the cords are easily available due to being biological waste after child birth [66]. In addition, HUVEC can be used as primary cells or as a part of immortalized fused cell lines [9].

HUVECs express many endothelial markers as well as signaling molecules which are associated with regulation of vascular homeostasis. HUVECs can also respond to several physiological and pathophysiological stimuli including high glucose concentration and shear stress. Furthermore, HUVECs can be co-cultured with other cell types in a 3D environment which enables the formation of advanced research and vascularization models. Therefore, the HUVECs have been used in vascularization of various engineered tissues. In addition, the HUVECs have shown to be the most commonly used endothelial cell type to be used in research on biomaterials. [66]

HUVECs have shown to have a good ability to form vascular networks *in vitro*. However, their proliferation is limited when they are missing pro-angiogenic factors. [18,67] Furthermore, stem cells like embryonic stem cells (ESCs) and iPSCs could be a useful alternative for HUVECs, at least in the future.

Despite all mentioned properties, HUVECs have a few cons. Firstly, HUVECs have tissue-specific phenotype, and immunogenic properties. In addition, it is impossible to use HUVECs in autotransplantation in patients due to the source of the cells being umbilical cord which is disposed soon after birth and therefore the HUVECs are not available later for autotransplantation. [66]

HUVECs were chosen to be used in this study due to their properties and because they seem to be the golden standard in the field of vascular modeling. The HUVECs used in this study are commercial, obtained from Cellworks.

2.3.2 Bone marrow-derived stem/stromal cells

Bone marrow-derived stem/stromal cells or BMSCs are mesenchymal stem/stromal cells (MSC) isolated from bone marrow. Therefore, the BMSCs are multipotent stem cells which can differentiate into mesodermal cell lineages like adipocytes, chondroblasts, fibroblasts, osteoblasts, and skeletal myoblasts. [68]

Mesenchymal stem cells have a major role in tissue regeneration due to their abilities to self-renewal and differentiation into multiple tissue types. The BMSCs are widely used in

both experimental and clinical studies. [69,70] BMSCs have huge therapeutic potential because they can be harvested from the patients themselves which reduces the ethical and immunological problems. Therefore, BMSCs are easy to obtain and expand. [68]

The BMSCs produce and secrete growth factors and cytokines which influence the formation and function of stromal microenvironment. In addition, BMSCs are involved in inflammatory processes. [68] The BMSCs have ability to move from bone marrow to the injured site of the body by using peripheral circulation [70]. Therefore, they take part in tissue repair and regeneration.

BMSC were chosen to be used in this study due to their properties, their natural location in the human body being close to vascular network and due to previous study [28] done in our research group. The BMSCs used in this study are obtained from TAYS as a leftover material from surgeries.

2.3.3 Fibroblast

Fibroblasts, or fibroblast-like cells, are standardized cell type used in cell culture and tissue biology [71,72]. This is due to their ability to produce and organize ECM and to communicate with other cells [72,73]. Fibroblasts have characteristic spindle-like shape [74]. In addition, fibroblasts, like other stromal cells, interact with ECM proteins on all sides of the cells as they lack the apical-basal polarity of epithelial cells [73]. Fibroblasts are active cells producing collagen and all ECM components including structural proteins, adhesion proteins, and space filling ground substances composed of glycosaminoglycans and proteoglycans [75,76]. In addition, the primary fibroblasts have a limited lifespan but human fibroblasts usually have longer lifespan in culture compared to mouse fibroblasts [75].

Fibroblasts are main cell type of connective tissue appearing practically in every organ of the body [72,73]. Fibroblasts form diverse and pervasive cell population. Their main function is to establish, maintain, and modify stroma of connective tissue. Due to fibroblasts being so heterogenic cell population, they have wide range of different functions. Based on the location, the fibroblasts have different cellular orientation and ECM organization. [72]

Fibroblast play an integrative role in sites of wounds and inflammation through their interactions with immunocompetent cells and regulation of neuropeptides. Fibroblasts in various tissues express CD40 antigen which is part of the communication between stromal cells and T cells. Therefore, the fibroblasts are participating in inflammatory

responses and act as guards interacting with immunocompetent cells like dendritic cells. [72] Fibroblasts are known to activate in response to tissue damage as they play a role in wound healing. Activation of fibroblasts can be observed from increased motility, ECM deposition, and proliferation. The activated fibroblasts are more proliferative and contractile myofibroblasts which have similar characteristics as smooth muscle cells. [73,77] Furthermore, fibroblasts have been associated with different diseases varying from cancer to fibrosis [73].

It has been reported that proliferation and grow rate of fibroblasts in collagen hydrogel are slower compared to fibroblasts seeded on plastic. This was most probably due to cells arresting in G0/1 phase of cell cycle. Fibroblast naturally contract hydrogels. There are two different conditions: relaxed, where hydrogel is free to contract, and mechanically loaded, where hydrogel is anchored and when cell try to contract, they form tensions. The cells embedded in these two different conditions have also different morphology. In relaxed hydrogels, the fibroblasts are nonproliferative and have dendritic morphology while in loaded hydrogels, the fibroblasts are proliferative and form bipolar extensions. [73]

Fibroblasts are widely used in initial tests for biocompatibility and cytotoxicity when developing novel 3D biomaterials. Fibroblasts are used in the initial tests because there is various well-established and robust immortal cell lines available. [73] Therefore, the fibroblasts are used in this study. In addition, fibroblasts were chosen to be used in this study because they can be used as mural cells in vascularization and because they have been shown to secrete MMPs degrading ECM. The chosen cell line is human lung fibroblasts, WI-38. The WI-38 cell line is the first human diploid cell line to be used in human vaccine development. The cell line is isolated from normal female embryonic lung tissue after 3 months of gestation. Their lifetime is up to 50 passages. [78] The WI-38 cell line is one of the oldest and most widely available cell line in the world [79].

2.4 Vascularization

Vasculature is a network system in the body. It is formed from blood vessels which are networking through human body in approximately 100 000 km thus making vascular endothelium the largest endocrine organ [10]. The blood vessels are coated with endothelial cells. The endothelial cells act as a barrier that selects as well as controls the movement of substances from bloodstream to tissue and vice versa [80]. Blood vessels can be divided into arteries, veins and capillaries based on the structure and function of the vessel (Figure 6). The arteries are elastic and rounded with muscles. They carry the

high-pressure blood away from heart. Veins, on the other hand, have thin walls and they have venous valves which prevent the blood to flow into wrong direction. Veins carry the low-pressure blood towards heart. Lastly, the capillaries are located between arteries and veins, and they consist of only from the innermost layer of the artery and vein, which is called tunica intima. The tunica intima consists of basement membrane and endothelium [9]. The capillaries are the site of vasculature where the exchange of multiple substances happen through thin endothelial layer.

The basic structure of these vessels is the same, first, there is a single layer of endothelial cells which is covered with basement membrane and then there is the mural cells which are either vSMCs or pericytes. [9] Endothelium, layer of endothelial cells, is an important component of blood vessels because endothelial cells form monolayer around the vessel that act as barrier. In addition, endothelium regulates vasodilation or vessel distension, and vessel formation. This endothelial layer is surrounded with smooth muscle cells and ECM in larger vessels. The ECM around vessels mostly contain collagen and elastin. [18] The mural cells support the migration of endothelial cells in angiogenesis via MMP secretion. They also regulate the permeability of the endothelium, contribute to the formation of basement membrane and contractility of the vessels. [81] The vSMCs plays major role in maintaining the pressure, tone, and stability of the vessels and therefore they are found in arteries which carry high-pressure blood. Pericytes, on the other hand, are responsible for the barrier and transport properties of blood vessels. In addition, they have shown to have contractile properties which is why they are found mostly in veins and capillaries. [9] In this study, pericytes are used together with endothelial cells to support the formation of microvascular network on chip.

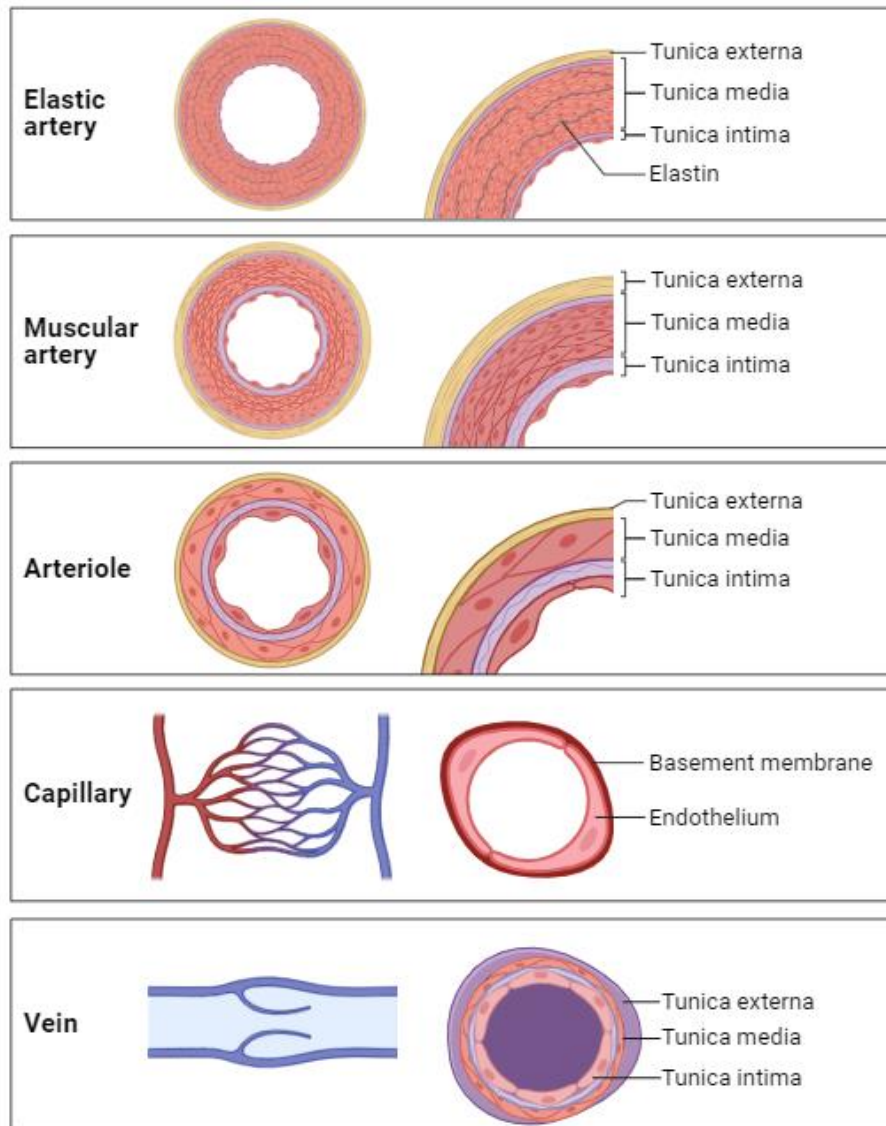


Figure 6. Structures of different blood vessels: arteries, capillary, and vein. Created in BioRender.com

Vascular networks are essential for almost every human tissue. The vascular system and blood vessels carry and circulate blood through the body while the blood delivers nutrients and oxygen for the cells and collects carbon dioxide (CO₂), waste products and metabolites from the cells in all tissues. Furthermore, the vasculature has a role in immune system since they carry leucocytes and other immune cells in the bloodstream [82]. In addition, the vascular system maintains tissue homeostasis and regeneration by regulating the transport of different substances and also by providing angiocrine signaling. [28] It also has a role in the development, growth, and repair of tissues because it carries molecules and substances that are needed in those processes. Therefore, generation of vascularization and vascular system models *in vitro* are important also for the generation of multi-Organ-on-a-Chip applications.

Vasculature in mammals is highly dynamic and tissue specific. It remodels constantly throughout the life and the balance is maintained by strict regulatory system via biochemical and mechanical cues. However, pathological remodeling can cause changes in vascular cell phenotype, proliferation, or motility. It can also affect degradation or modification of the ECM and abnormal deposition of ECM. [83]

Vascularization or vascular network formation can happen via two different ways: vasculogenesis and angiogenesis (Figure 7). Vasculogenesis is a process where angioblasts differentiate into endothelial cells and form early capillary-like networks. Vasculogenesis happen during early embryogenesis, but it also occurs during adulthood when the endothelial cells come from bone marrow. Angiogenesis, on the other hand, is a process where new blood vessels are formed through expansion and sprouting of blood vessels from the existing ones. All in all, vessels can be formed through growth, proliferation, alignment, tube formation, and anastomose with surrounding vessels. [18] Figure 7 shows the difference between vasculogenesis and angiogenesis.

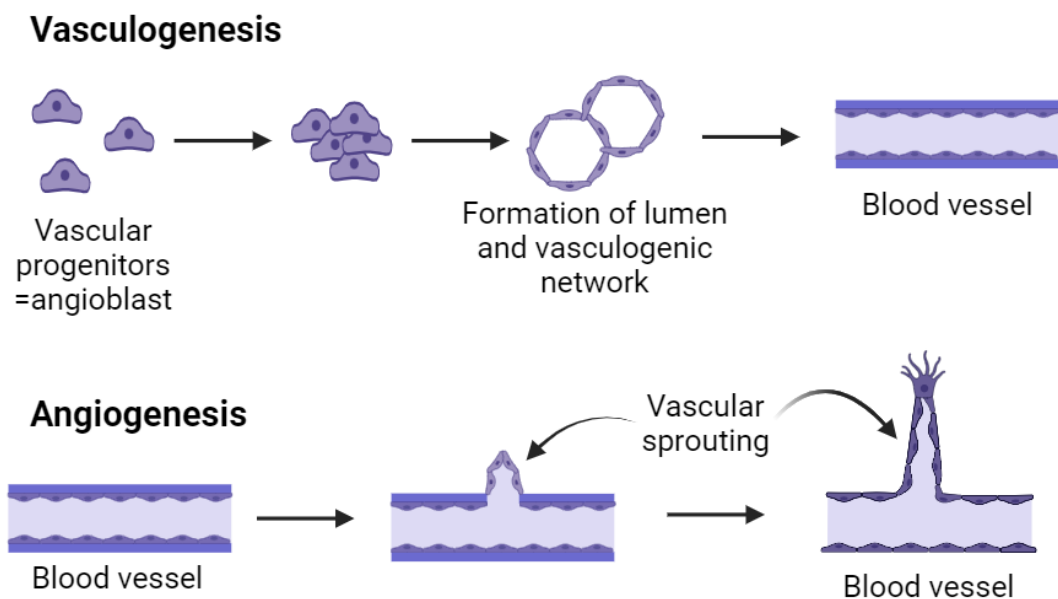


Figure 7. Difference between vasculogenesis and angiogenesis. Created in BioRender.com, Modified from [84]

Angiogenic sprouting of blood vessels is essential for tissue remodeling, regeneration and in solid tumor growth because it enables the delivery of nutrients and gas exchange [85]. During angiogenesis, the endothelial cells degrade the ECM by secreting MMPs to make room for new vessel sprouts. In addition to degradation of surrounding matrix, invasion, proliferation, morphogenic reorganization and vessel stabilization are parts of angiogenesis [86–89].

2.4.1 Factors affecting angiogenic growth

Angiogenic growth depends on many soluble biochemical cues which induce the migratory and phenotypic state of endothelial cells. This influence comes via autocrine, endocrine, and paracrine feedback. [87] These biochemical cues include multiple signaling molecules, adhesion proteins, growth factors and inhibitors which regulate the formation and growth of new vessel sprouts. One of these regulating molecules is VEGF which is released by fibroblasts, monocytes, macrophages, and lymphocytes. The VEGF act as mitogen of endothelial cells and therefore it induces angiogenesis. [18] Other growth factors affecting angiogenesis are angiopoietins, fibroblast growth factors (FGF), platelet derived growth factors (PDGF). Furthermore, chemokines, MMPs, and signaling lipids like sphingosine-1-phosphate (S1P) are part of biochemical cues affecting angiogenesis. [87] In addition to regulating molecules, pressure and basal-to-apical flow can trigger the angiogenesis [89].

The VEGF controls vessel morphogenesis, and stimulates migration and proliferation of endothelial cells, as well as degradation of matrix. In addition, VEGF has shown to guide sprouts toward hypoxic regions, meaning the areas that lack oxygen. Whereas interstitial flow directs the sprouts towards other vessels, against the direction of interstitial flow meaning that it directs the sprouts towards vessels having higher microvascular pressure compared to their own. [86] Furthermore, VEGF-gradient has shown to direct the angiogenesis towards higher concentration of VEGF [90].

Farahat et al. (2012) tested the effects of S1P used with VEGF to the angiogenesis [87]. The used microfluidic culture device had gel channel in the middle and two media channels in both sides of the gel channel. Collagen I was used in the gel channel and human dermal microvascular endothelial cells (HMVECs) were seeded into the one media channel where they formed a monolayer. The idea of the research was to study the angiogenesis through collagen I. As a result, they found out that the presence of S1P with VEGF gradient amplified the influenced angiogenic responses. The use of S1P with VEGF gradient also resulted angiogenic sprouts which aspect ratio was higher compared to model with background levels of VEGF. However, the total migratory activity in the model with VEGF gradient was decreased. [87]

Fluid shear stress sends signals that mediate transcription of endothelial cells, membrane fluidity, conformational changes of VEGF receptors, tubule formation, intraluminal morphology, barrier function, and vessel homeostasis. All this is possible due to fluid force stress maintaining vessel lumens and controlling proliferation of

endothelial cells. Furthermore, fluid shear stress can induce major changes in the morphology of endothelial cells and affect to the endothelial phenotype. [86] In addition, applying mechanical stimulation have also shown to be favorable to engineered vascular structures [91].

Song and Munn (2011) tested the effects of fluid force stress to the sprouting endothelial cells [86]. They used microfluidic cell culture device with collagen I in the middle channel and HUVECs in two other channels located both sides of gel channel. They tested positive and negative VEGF gradients as well as interstitial fluid forces. As a result, they found out that interstitial fluid flow directs endothelial morphogenesis and sprout formation. In addition, they showed that positive VEGF gradients introduced sprouting. [86] All in all, they proved that both VEGF gradient and interstitial flow direct the sprouting and vessel expansion.

Matrix density moderates VEGF-induced sprout polarization as well as lumen formation. This is because matrices with higher densities have shown to result shorter, thicker, and slower-growing sprouts. In addition, the sprouts have shown to polarize more likely towards higher VEGF concentrations including more cells. They also demonstrated formation of more stabled sprouts compared to matrices with lower densities. [4]

The hydrogels properties effect on the formation of microvascular networks and they also have an impact on the ability to mimic *in vivo*-like processes like degradation, sprouting and neovascularization of *in vitro* vascular networks. For example, stiffer hydrogels produce vascular network which morphology mimics better *in vivo* morphology. They can also generate lumens which diameter is smaller and they can limit endothelial cell migration. [18,92] Furthermore, Shamloo and Heilshorn (2010) showed that the matrix density affected the sprouting morphogenesis [4]. The endothelial cells formed stable sprouts in intermediate collagen I matrix densities (1.2-1.9 mg/mg), while lower densities (0.3-0.7 mg/ml) resulted uncoordinated endothelial cell migration. In higher matrix densities (2.7 mg/ml), the cells formed clusters and did not elongate. All in all, endothelial cells in higher density matrices resulted shorter, thicker, and slower-growing sprouts. They also suggested that the matrix density affects the sprouting by regulating the balance between migration and proliferation rates of endothelial cells. [4]

2.4.2 Vascularization models *in vitro*

The *in vitro* vascularization models available at the moment are mimicking the *in vivo* vasculogenesis and angiogenesis processes. This mimicking is based on using the

natural ability of endothelial cells to self-organize into vessel-like structures as well as to create new vessels from pre-existing ones. [93–97] However, mimicking vascularization is still one of the key challenges in tissue engineering. The main challenge is to achieve dense, highly perfusable, mature and organized microvascular networks which also represents the vascular network of native tissues [98].

This maturation problem has been tried to solve with multiple techniques. One of these techniques is 3D bioprinting where bioink, like alginate, is 3D-bioprinted inside a prepolymer which is then polymerized and bioink is removed which then leads the formation of vascularized structure inside a hydrogel [99]. Cast or patterning of hydrogels to form vascular networks are also widely used methods in both macro- and microscale vasculature models. In that method, hydrogels are casted into a hollow structures and endothelial cells are then seeded into those hollow structures to form vessels. The most used endothelial cells in these kinds of models are HUVECs. Collagen I and fibrin are usually used as scaffold materials while gelatin, sodium alginate and synthetic poly(ethylene glycol) (PEG) have been used as sacrificial materials which are removed from the scaffold before adding the cells. [18] Another method to form vascular network is 3D spheroid based. The 3D spheroid formed from endothelial cells allows cell-cell interactions and is sensitive to angiogenic stimulation. [81] All in all, there is two main techniques to form vascularized models *in vitro*: engineered scaffolds and naturally formed. In engineered scaffolds, the vessel structure is already engineered inside the scaffold while in naturally formed models, the cells make room for the vessel structures and therefore the model is cell-based. [18] Figure 8 shows a few of these methods used to create vascular models *in vitro*. In this study, the naturally formed vascularization is used to form vascular network.

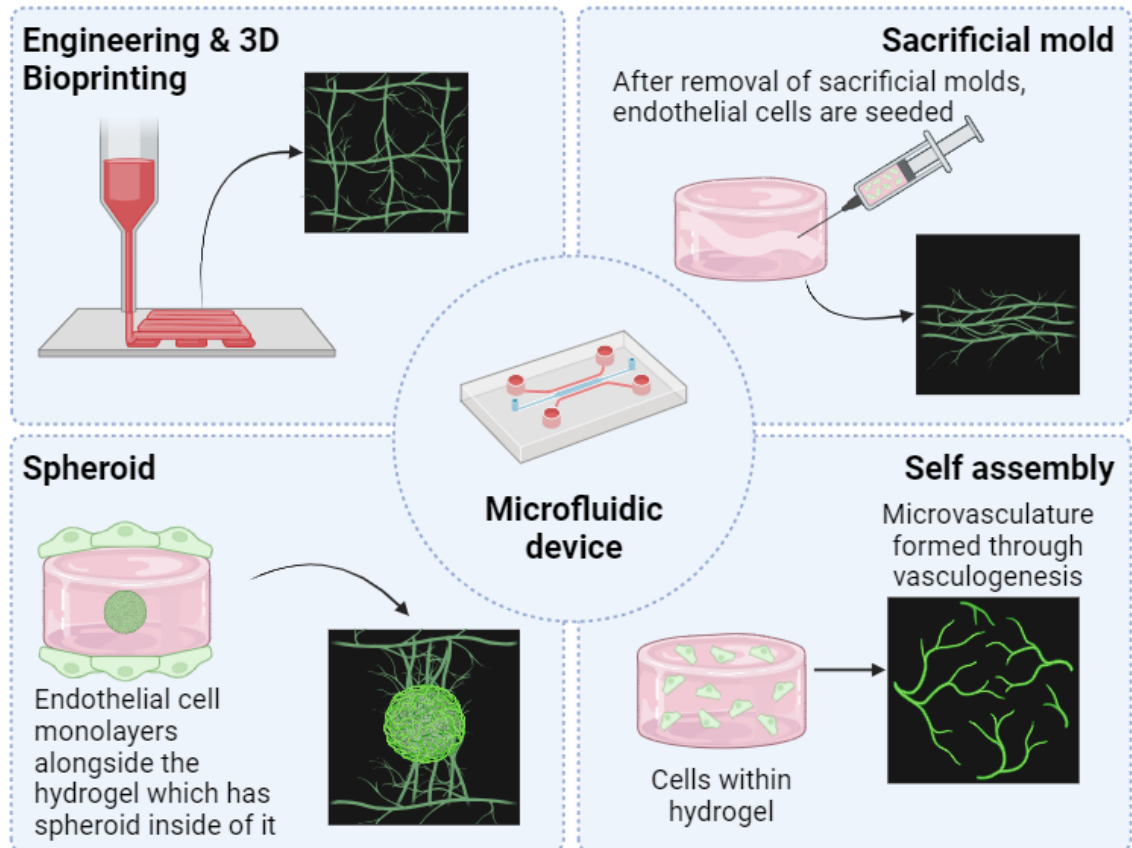


Figure 8. Schematic graph of different methods to model vascularization in vitro. Created in BioRender.com, Modified from [13,14]

The scaffold material used in vascularization models should support physiologically relevant cellular arrangements and be able to mimic tissue behaviors. In addition to that, the scaffold material should support long-term cell culture, allow the diffusion of nutrients and solutes involved in intercellular communications, and permit ECM remodeling. [83] Natural hydrogels are widely used in tissue engineering applications due to their ability to mimic natural ECM. This is because they consist of proteins that are part of natural ECM and therefore, they provide biocompatibility and bioactivity. However, they usually lack mechanical properties, they are difficult to control, and they have batch-to-batch variation. Therefore, synthetic hydrogels are an alternative for natural hydrogels. Synthetic hydrogels properties can be controlled and adjusted, for example, by tuning their mechanical properties and chemical composition to making it suitable for specific application. However, the synthetic hydrogels usually lack cell attachment sites and are thus bioinert, but this problem can be solved by adding sites for cellular interactions, for example, by adding natural pro-angiogenic agents or mixing it with natural hydrogel to enhance the bioactivity. [81,83]

Main limitations of vasculature models include a lack of appropriate stromal cells and the use of poly-dimethylsiloxane (PDMS) in the channels. This is because the PDMS does

not allow vasodilation and because it also absorbs small and hydrophobic molecules. In addition, the microvessels formed *in vitro* models are modeling bigger arterioles because the vessels tend to be larger compared to *in vivo* microvessels and capillaries. [18] These limitations should be solved before to be able to create better functioning vasculature models which would mimic better *in vivo* vascular system.

The use of stromal cells in microfluidic vascular system has not only shown to stabilize the model but also organize endothelial cells into more mature and smaller networks that mimic better *in vivo* vascular system. Especially fibroblasts direct the formation of network by synthesizing and maintaining the ECM as well as by secreting angiogenic growth factors and proteins. [18] The stromal cells used in this study are human BMSCs.

Vascular endothelial cells are often used in tissue engineering to create vascular networks. This is because vascular endothelial cells have inherent angiogenic behaviors which are important in vascular formation *in vitro*. Examples of vascular endothelial cells are human primary aortic endothelial cells (HAEC) and human primary dermal microvascular endothelial cells (HDMVEC) which both have limited expansion potential, and the isolation requires invasive surgeries. Other problems related to these cell types are loss of functionality, variability between donors, and tissue specificity. Therefore, pluripotent stem cells (PSCs) including ESCs and iPSCs, would be potential cell sources for vascular tissue engineering applications. [81]

2.5 Organ-on-a-Chip

Organ-on-a-Chip or OOAC is a microfluidic cell culture device (Figure 9). It contains perfused chambers which contains living cells. [100] The OOAC is a biomimetic system that can mimic the environment of physiological organ. This mimicking is based on the ability to regulate the key parameters which include cell patterning [101], concentration gradients [102], shear forces [103], tissue-boundaries [104], and tissue-organ interactions [17]. Furthermore, the OOAC's ability to recapitulate multicellular architectures, physicochemical microenvironments, tissue-tissue interfaces, and vascular perfusion of the body gives huge advantage compared to conventional 2D and 3D culture systems. This advantage is due to the OOAC being capable to culture cells which functionality is not possible to be achieved with conventional and stable 2D and 3D cell culture systems. [100]

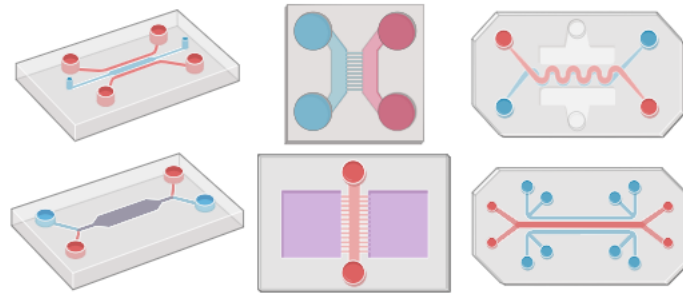


Figure 9. Schematic images of different microfluidic devices. Created in BioRender.com

The OOAC allows perfusion of medium going through the sample. This perfusion mimics better the native conditions with blood flow resulting more mature cell models. The fluid flow can improve the nutrition supply and cellular crosstalk while also providing physical stimuli to the cells. There are multiple methods how to create the fluid flow but the most used methods include gravitational flow based, and different pump based methods. [105] In this study, gravitational flow based perfusion is used in the microfluidic chip.

The main goal of OOAC is to be able to mimic the *in vivo* conditions of human organs by stimulating the physiological environment [100]. However, the ultimate goal of OOAC is to be able to integrate multiple organs in chip, and therefore creating multi-organ-on-a-chip models and even human-on-a-chip models [106]. The OOAC combines multiple disciplines including cell biology, engineering, and biomaterial technology and therefore it is one of the emerging technologies [107,108].

The OOAC is based on microfluidics by using small microchannels which size vary between tens to hundreds of microns. Sometimes this application is also known as Lab-on-a-chip. Even though the channel is small, it still has relatively large area and high mass transfer. These properties are favorable when using the microchannels in microfluidic applications because they allow control of chemical and physical properties as well as control of volumes, fast mixing speed, low reagent use, and rapid responses. [109–111] Microfluidics can integrate sample preparation, reactions, separation, detection and basic operating units like cell culture, sorting and cell lysis [112]. All these properties make OOAC a good application for studying cell behavior and toxicity *in vitro*. In addition, the OOAC application has a great potential to be used to study biomarker identification, disease etiology, drug discovery and development, molecular mechanisms, organ physiology, tissue development as well as toxicity testing [100].

The OOAC devices are often fabricated from PDMS because it has many suitable properties for cell culture device. These properties include high optical clarity, gas permeability and biocompatibility. The optical properties are important for the application

because it allows real-time and high-resolution optical imaging of the cell culture. In addition, the PDMS is easy to use. [100,113,114] The PDMS is a good material for chips also because it allows fabrication of structures with different dimensions such as structures which are only a few nanometers in size [115,116]. All these properties of the device allow powerful characterization of cellular functions. On the other hand, the PDMS has poor chemical resistance and therefore it can absorb small organic compounds like hydrophobic molecules including drugs. Furthermore, its high gas permeability may disturb some cell culture applications. [100,113] Other possible problems that may come up when using devices made of PDMS are toxicity, if material is not fully cured, and insufficient cell adhesion which can be solved by using extended post producing and pretreating it with adhesion molecules [117]. Other possible materials for the device are silicon, plastic, glass, silk, and other polymers like polyurethane. These materials can be fabricated by using various methods which include micro molding, injection molding, soft lithography, and other microscale manufacturing approaches. [100]

Microfluidic cell culturing is relatively new application. The advantages and disadvantages or challenges of microfluidic cell culture are summarized in the Table 2.

Table 2. *Advantages and disadvantages of microfluidic cell culture. [17,100–104,108,117]*

ADVANTAGES	DISADVANTAGES/CHALLENGES
A low number of cells and reagents	Complex operational control and chip design
Ability to incorporate analytical biosensors into the culture platform	Non-standard cell culture protocols
Ability to recapitulate multicellular architectures, physicochemical microenvironments, tissue-tissue interfaces, and vascular perfusion of the body	Novel culture surface
Able to regulate the key parameters, including cell patterning, concentration gradients, shear force, tissue-boundaries, and tissue-organ interactions	PDMS absorbs hydrophobic molecules
Allow characterization of transcription factors and gene expression	PDMS is hydrophobic → needs surface treatment or coating to allow cellular attachment
Automation	PDMS is permeable to gases and water vapor → drying problems and problems with pH
Controlled co-culture	Small volumes → difficult analytical chemistry
Experimental flexibility and control	
Flexibility of device design	
Low costs of experiments due to small volumes used	
Precise control over experimental conditions	
Real-time, on-chip analysis	
Reduced contamination risk	

PDMS: poly-dimethylsiloxane

OOAC is widely used cell culture platform with multiple possibilities. It has, for example, been used to create cancer [17], liver [118,119], neuro [42] models and models to study, for example, biocompatibility [15] and trans endothelial migration [93]. Table 2

summarizes some of the cells and materials that have been used in OOAC applications focusing on vascularization.

Organ-on-a-chip models have potential to reduce and replace animal tests and they are also a step closer to personalized medicine when combined with iPSCs. In this study, commercial AIM Biotech's idenTx 3 Chip is used. The commercial chip was chosen to this study because it has been used in previous studies [28,43] done in our research group and because it is easy to use.

2.6 Vascularization-on-a-Chip

As said before, flow is an important factor in vascular formation and function. Therefore, the microfluidic chip supports the vessel formation by providing the fluid flow through the sample. This makes the microfluidic chip an excellent cell culturing platform for vascular applications and thus Vascularization-on-a-Chip was created.

As mentioned before, vascularization is essential for almost every tissue in the human body. Therefore, it is important to develop better vascularization models and combine it with other tissue models to be able to create more *in vivo*-like tissue models that mimic better the natural conditions of human body. These better models would help studying the human body's functions while also making drug screening and development faster and cheaper. Lastly these better models are leading towards personalized medicine in the future.

Multiple Vascularization-on-a-Chip models have been created. Table 2 summarizes some of these different Vascularization-on-a-Chip models. Next some of these models are covered more detailed.

Table 3. *Examples of Vascularization-on-a-Chip models.*

CELLS	MATERIALS	INFORMATION	YEAR	REF
HMVEC	Collagen I	Novel microfluidic device for studying capillary morphogenesis	2008	[120]
HMVEC, HMVEC cocultured with MTLn3/U87MG or with 10T 1/2	Collagen I	Novel microfluidic platform for studying capillary growth and endothelial cell migration	2008	[92]
HMVEC	Collagen I with fibronectin	Studying sprouting morphogenesis with different matrix densities, Different concentrations of collagen I was tested, Microcarrier beads were used	2010	[4]
HUVEC	Matrigel	Investigating the effects of pro-angiogenic factors on the proliferation, migration, and tube-like structure formation	2011	[67]
HUVECs	Collagen I	Studying the effects of fluid force stress to the sprouting of endothelial cells	2011	[86]
HMVECs	Collagen I	Evaluating the combined effects of vascular endothelial growth factor (VEGF) and the signaling lipid sphingosine-1-phosphate (S1P)	2012	[87]
HUVECs, HBVPCs or HUASMCs	Collagen I	Investigating angiogenic remodeling, interactions between endothelial cells and perivascular cells and interactions between blood components and endothelium with flow	2012	[121]
HUVECs, HLFs, Human promyelocytic leukemia cells, HL-60	Fibrin + Collagen I +aprotinin	Creation of functional and perfusable 3D microvascular networks on a chip mimicking <i>in vivo</i> -like vascularization	2013	[122]
HUVECs	Collagen I	Creating microfluidic angiogenesis model for studying anti-angiogenic therapeutic drugs	2015	[123]
HUVECs, HLFs	hydroxyapatite + fibrin	Creation of bone angiogenesis model in microfluidic device	2015	[95]
HUVECs, hMSCs, primary rat hepatocytes, hESCs derived hepatocytes, neonatal eat cardiomyocyte, hESC-derived cardiomyocytes	poly(octamethylene maleate (anhydride) citrate) (POMaC), Matrigel, Collagen/Matrigel mixture	Creation of built-in vascularization by molding scaffold with vascular lumens. Vascular model can be combined with cardiac or hepatic tissues.	2016	[124, 125]

HUVECs, BMSCs, hNDFs	gelatin +fibrin crosslinked with thrombin and transglutaminase (Moo Glue)	Bioprinting was used to create thick vascularized tissue on a chip	2016	[126]
HUVEC with HLFs spheroids	Fibrin +aprotinin +collagen	Creating a cellular spheroid with perfusable vascular network	2017	[127]
HUVECs, HBMECs, hPC-PL, NHA, HLF	Fibrin +aprotinin	Creation of Blood-Brain-Barrier (BBB) on-a-Chip	2019	[128]
BMSCs and ASCs co-cultured with HUVECs	Fibrin +aprotinin	Testing the difference between BMSCs, and ASCs used with HUVECs	2022	[28]
HUVECs, HAVSMC, HDF	Collagen I (rat tail)	Creation of three-layered model of vascular wall to study mechanical stimulation and vessel wall maturation	2022	[91]
HUVECs, Human primary pericytes, HCA2, N/TERT	Fibrin (bovine) for vascularization, collagen I (rat tail) and collagen I/Matrigel mixture for dermal	Creation of Microvascularized Human Skin-on-a-Chip tissue model	2022	[129]
HUVECs, HLF and cancer patient-derived fibroblasts	Fibrin	Creating more vascularized tumor spheroids by adding fibroblasts into the tumor spheroid	2023	[130]
HUVECs, HAoECs, HPMECs	Fibrin +aprotinin	Creation of continuously perfusable and customizable vasculature on chip platform.	2023	[131]
HUVECs, BMSCs, or ASCs, iPSC-derived neurons	Collagen I -Fibrin mixture +aprotinin	Creation of neurovascular multiculture prolonging the cultivation period	2023	[43]

10T 1/2: Mouse smooth muscle precursor cells, ASC: Adipose tissue-derived stem/stromal cell, BBB: Blood-Brain-Barrier, BMSC: Bone marrow mesenchymal stem cell, HAoEC: human aortic endothelial cell, HAVSMC: Human aortic vascular smooth muscle cells, HBMEC: Primary human brain microvascular endothelial cells, HBVPC: human brain vascular pericytes, HCA2: immortalized human dermal fibroblast cell line, HDF: Neonatal human dermal fibroblasts, hESC: human embryonic stem cell, HL-60: Human promyelocytic leukemia cell, HLF: human lung fibroblast, hMSC: human mesenchymal stem cell, HMVEC: Human dermal microvascular endothelial cell, hNDF: human neonatal dermal fibroblast, hPC-PL: Primary human pericytes from placenta, HPMEC: human pulmonary microvascular endothelial cell, HUASMC: human umbilical arterial smooth muscle cell, HUVEC: human umbilical vein endothelial cell, MTLn3/U87MG: rat mammary adenocarcinoma cells/ human glioblastoma cell line, NHA: Primary normal human astrocyte, N/TERT: human keratinocyte cell line, POMaC: poly(octamethylene maleate (anhydride) citrate), REF: reference, S1P: sphingosine-1-phosphate, VEGF: vascular endothelial growth factor

According to Table 2, the commonly used cell types in Vascularization-on-a-Chip models are HMVECs and HUVECs [28,67,86,87,92,93,120]. HUVECs are widely used cell type when modeling blood vessels *in vitro* because their availability is high, and they can be from primary cells or as a part of immortalized fused cell lines [9]. These endothelial cells are often cultured together with human lung fibroblasts (HLF) as shown in Table 1. These cell types are usually cultured with collagen I [86,87,91,92,120–124,127,129] or fibrin [28,95,122,126–131] hydrogel in vascularization models. Due to fibrin's and collagen I's location in the body they are widely used hydrogels in angiogenic applications. In addition, Matrigel has shown good angiogenic properties and is therefore been designated to be the standard ECM to be used in endothelial cell tube forming assays. [81] However, Matrigel is derived from mouse tumor and can induce endothelial cells with different origins to form capillary-like structures [132].

Zhang et. al. (2016 & 2018) created an AngioChip which is an example of Vascularization-on-a-Chip where the scaffold for vascular network is created by molding a poly(octamethylene maleate (anhydride) citrate) (POMaC) polymer material into a wanted structure with tunnels for vessels [124,125]. After the scaffold is formed, its surfaces are coated with gelatin to enhance the cell attachment. Then the HUVECs are seeded inside these tunnels, vessel lumens, while pericytes or human MSCs mixed with Matrigel or Collagen/Matrigel mixture are seeded outside these tunnel or vessel-like structures. Hepatic or cardiac tissue can be applied to AngioChip by adding hepatocytes or cardiomyocytes outside the vessel-like structures together with hMSCs. [124,125]

Kolesky et. al. (2016) used bioprinting to create vascularized tissue. They used sequential co-printing of multiple inks [126]. The cell-laden ink contained BMSCs, and human neonatal dermal fibroblast (hNDF) cells embedded in gelatin-fibrin matrix which was crosslinked with transglutaminase after printing. The HUVECs are seeded into the bioprinted vascular lumens. [126] These studies where vascularization is made via mold casting or 3D bioprinting revealed the potential of these engineered methods to be used to create vascularized tissues rather than forming vascularization naturally.

Natural vascular formation based on self-assembly of endothelial cells and supporting stromal cells is used in this study and the culturing method is based on the studies done in our research group [28,43]. In the study done by Mykuliak and Yrjänäinen et. al. (2022), the difference in vascularization and vascular formation between BMSCs and ASCs were observed [28]. They cocultured both cell types with HUVECs in fibrin hydrogel in perfusable microfluidic chip. As a result, both MSCs supported the vascular

formation but BMSCs induced the formation of more mature and fully perfusable vessels with larger vessel area compared to the vessels formed with ASCs. [28] According to this study, the BMSCs were chosen to be used in this study.

A few steps forwards multi-Organ-on-a-Chip or Body-on-a-Chip applications have been taken by applying vascularization with some other cell or tissue types. Vascularization has, for example, been applied to full-thickness human skin-on-a-chip application [129], bone tissue [95], neurovascular-on-a-chip [43] and Blood-Brain-Barrier (BBB) [128] among others.

The 3D neurovascular network done by Isosaari et. al. (2023), combined the vascular model created by Mykuliak and Yrjänäinen et. al. (2022) to the neuro-model [28,42,43]. This neurovascular model showed that the neuronal network supported the formation of vascular network. In addition to that, the neuronal network enabled the extended cultivation time of the vascular model. Furthermore, they discovered that the BMSCs seemed to boost the extension of neurovascular model. [43] This model is important for the future development of Body-on-a-Chip applications where both vascularization and innervation play an essential role making the models more *in vivo*-like.

3. OBJECTIVES OF THE THESIS

Objectives of the thesis include finding better solutions to analyze size change of the hydrogels, finding solution to prevent the decrease in size of the hydrogel and finding hydrogels that support 3D vascularization in microfluidic environment with fluidic flow. In more details, the objectives are as follows:

1. Create a method for studying the size changes of the hydrogel samples during cultivation by measuring the thicknesses and areas of the samples during cultivation. Hypothesis: The hydrogel size change can be measured by using fluorescent beads and microscope.
2. Find a solution to prevent the decrease in size of hydrogel during cultivation by using aprotinin, Collagenase Inhibitor I and/or mixture of these inhibitors with hydrogels and in vascularization model. Hypothesis: The hydrogel degradation can be prevented by using inhibitors and the use of inhibitors will not disturb the cell viability, elongation, or the vascular network formation in a chip.
3. Test different hydrogels and inhibitor combinations in 3D vascularization model in microfluidic chip to find out inhibitors' effects on vascularization and hydrogel size change. Compare the formed vasculature to the current golden standard, fibrin, to find better options for the Vasculature-on-a-Chip application. Hypothesis: Different inhibitors affect the vascularization and hydrogel size change in different ways in different hydrogels. Some of the tested materials support vascularization more robustly compared to fibrin.

4. MATERIALS AND METHODS

This study consists of two main parts. Firstly, the hydrogels' size change is studied on 96-well plate with fibroblasts. Secondly, the hydrogels are tested in vascularization model on a commercial microfluidic chip. Figure 10 illustrates the setup of these two different experiments.

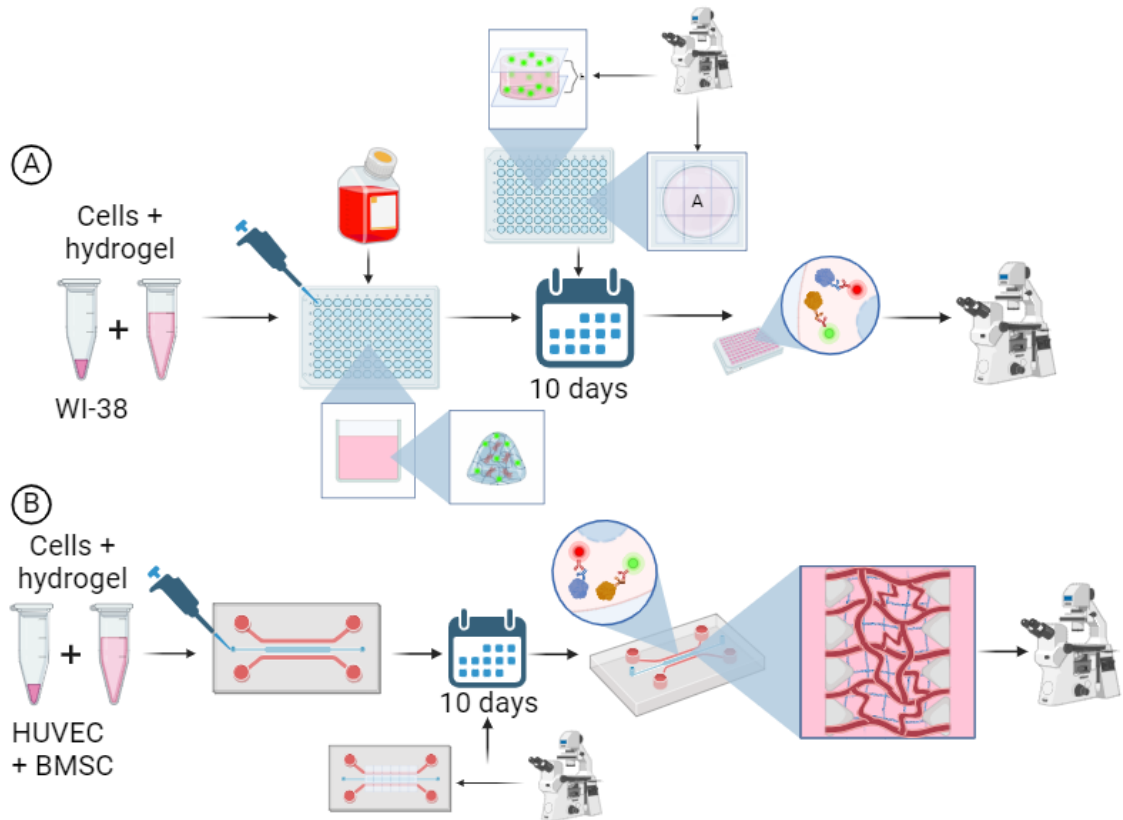


Figure 10. (A) Descriptive image of the setup of well plate experiment. (B) Descriptive image of the setup of the chip experiment. WI-38: human lung fibroblasts, HUVEC: human umbilical vein endothelial cell, BMSC: bone marrow stem/stromal cells. Created in BioRender.com

Materials, cells, and inhibitors used in this study are collected in Table 4.

Table 4. *Used materials and conditions in different experiments.*

Material	Well plate experiment with WI-38 (α MEM medium)				Chip experiment with HUVECs and BMSCs (EGM-2 medium)			
	No in-hibitor	Apro-tinin	Collagenase Inhibitor I	MIX	No in-hibitor	Apro-tinin	Collagenase Inhibitor I	MIX
Fibrin (human)		x	x	x		x		x
Collagen I (rat tail)	x	x	x	x	x		x	
VitroCol[®] (human collagen I)	x	x	x	x	x		x	
TeloCol[®] (bovine Telocollagen I)	x							
GelaGG (porcine skin, bacterial)	x	x	x	x	x			x
VitroGel[®] (xeno-free)					x			x

α MEM: α -modified Minimum Essential Medium, BMSC: bone marrow-derived stem/stromal cells, EGM-2: Endothelial Cell Growth Medium-2, GelaGG: gelatin-gellan gum, HUVEC: human umbilical vein endothelial cells, WI-38: human lung fibroblasts

Fibrin was used in this study because it is the golden standard in vascular models at the moment. Collagen I (rat tail) was chosen due to collagen type I being an abundant protein in the human body and because it is widely used in tissue engineering. VitroCol[®], another commercial version of collagen I, was chosen as an alternative to rat tail collagen due to its human origin. TeloCol[®] was chosen because it is Telocollagen which should be more stable compared to Atelocollagen, in addition to being collagen I. GelaGG was chosen to be used in this study because it is an in-house made material which potential is not fully revealed yet. Lastly, the VitroGel[®] was chosen because it is a xeno-free option and because it has shown good results in static culture conditions. TeloCol[®] was used only in well plate experiments and VitroGel[®] only in chip experiments.

The WI-38 cell line was chosen to be used in this study due to ISO 10993-5:2009 standard (Biological evaluation of medical devices. Part 5: Tests for *In Vitro* Cytotoxicity) [133] and because it is widely used cell line in biomaterial screening. The HUVECs were chosen to be used, because their availability is high, they have shown to have ability for capillary morphology, and because they are the most widely used endothelial cell type in tissue engineering with biomaterials [40,134]. The BMSCs were chosen to be used in this experiment since they showed better vascular formation ability in previous study done in our research group [28].

4.1 3D cell culturing in a hydrogel on a well plate

4.1.1 Sample preparation

Human fibroblasts, WI-38 (European Culture Collections, Public Health England, United Kingdom [135]), are used in this part of the study. They are cultured in α -modified Minimum Essential Medium (α MEM; Gibco™, Thermo Fisher Scientific, United States of America) supplemented with 5 volume/volume-% (v/v-%) of human serum (HS; Serana Europe GmbH, Germany) and 1 v/v-% of penicillin (100 U/ml)-streptomycin (100 μ g/ml) (P/S; EuroClone, Italy and Lonza, Switzerland). The WI-38 used in this experiment were passages from 14 to 23.

The WI-38 cells were mixed with hydrogels and samples were pipetted on 96-well plate (Nunc Microwell 96-well, Nuclon Delta-treated, flat bottom microplate, Thermo Fisher Scientific, United States of America). The cell concentration in the samples were 1×10^6 cells/ml and the sample size were 100 μ l. The used hydrogels were fibrin (fibrinogen and thrombin: Sigma-Aldrich, United States of America), rat tail collagen I (Gibco™, Thermo Fisher Scientific, United States of America), TeloCol® (Advanced BioMatrix, BICO, United States of America), VitroCol® (Advanced BioMatrix, BICO, United States of America), and gelatin-gellan gum (gelaGG; in-house made [39]). Three parallel samples and one control sample without cells were made from each material. In addition, three parallel samples were made for inhibitory tests for each inhibitor condition and two parallel samples for day 2 Live/Dead staining from each material and each condition were also made.

For samples containing fibrin hydrogel, the cells were spun down with centrifuge (200 G, 5 min) and then the cell pellet was resuspended in 2 IU/ml human thrombin in 5 % HS + 1 % P/S in α MEM. Then 10 μ l 0.001 v/v-% fluorescent microbeads (2 μ l, yellow-green, FluoSphere Carboxylate-modified Microspheres, 2 % solids, Invitrogen by Thermo Fisher Scientific, United States of America) in culture medium per sample was added into the solution. The solution was then mixed with sterile filtered 5 mg/ml human fibrinogen in Dulbecco's Phosphate Buffered Saline (DPBS; EuroClone, Italy and Lonza, Switzerland) at 1:1 volume ratio. The final mixture (2.5 mg/ml) was then pipetted into 96-well plate, 100 μ l per sample.

For samples containing rat tail collagen I hydrogel, the cell pellet was resuspended with 10 μ l 0.001 v/v-% fluorescent microbeads in culture medium per sample. The solution was then mixed with collagen solution containing rat tail collagen I (3 mg/ml), distilled

water (dH₂O), 1 M sodium hydroxide (NaOH), and 10x DPBS with phenol red pH indicator dye. The final mixture (2 mg/ml) was then pipetted into 96-well plate, 100 µl per sample. Samples containing human Collagen I, VitroCol[®], were made in the same way, but the solution contained VitroCol[®] (3.2 mg/ml), 10X DPBS with phenol red pH indicator dye, dH₂O, and 1 M NaOH.

For samples containing TeloCol[®], the cell pellet was mixed with 10 µl 0.001 % fluorescent microbeads in culture medium per sample and the cell-bead-suspension was then mixed with solution containing TeloCol[®] (6 mg/ml), DPBS and Neutralization solution for TeloCol[®]-6 (Advanced BioMatrix, BICO, United States of America). The final mixture (2 mg/ml) was then pipetted into 96-well plate, 100 µl per sample.

Samples containing gelaGG were made in the same way, but the solution contained 1:1 volume ratio of gelaCDH (60 mg/ml, CDH modified gelatin, Rousselot X-Pure 10P STD, lot#F9203, Acid extracted porcine skin gelatin) and GGox (40 mg/ml, oxidized gellan gum, *Sphingomonas elodea*). GelaCDH and GGox, which form gelaGG, are produced in-house according to previously produced protocol [39]. GelaCDH and GGox components were dissolved into αMEM in hot water bath at + 37 °C with magnetic stirrer for almost an hour. After that the gelaCDH was dissolved completely and it was sterile filtered (Whatman puradisc 30/0.2 CA S MLL 0.2 µm, United Kingdom) and the temperature of hot water bath was increased into + 60 °C for a while to allow GGox to dissolve completely after which the GGox was also sterile filtered.

In addition, control sample without cells were made in the same way as other samples but the cells were replaced with 10 µl 0.001 % fluorescent microbeads in culture medium. One control sample was made from each material. After plating all samples, the well plate was placed inside the incubator for 30 minutes to allow the gelation of the hydrogels.

After gelation, 200 µl of culture medium (5 % HS + 1 % P/S in αMEM) was added on top of each sample. However, the culture medium given to samples containing fibrin hydrogels contained 50 µg/ml of aprotinin (abcam, United Kingdom) because without aprotinin, the fibrin gels shrunk or degraded in two days. In addition, inhibitory tests were made separately by supplementing culture medium with either 0.223 pg/ml (0.0497 nM) Collagenase Inhibitor I (Sigma-Aldrich, United States of America), 50 µg/ml aprotinin, or with 1:1 mixture of them (MIX). The medium was exchanged every day during the 10-day experiment.

4.1.2 Hydrogel size change in different hydrogels on well plate

The size change of the hydrogels in well plate samples were studied by imaging the whole well every day with Leica DMI8 widefield fluorescent microscope (Leica Microsystems, Germany). Whole well was imaged by taking multiple images which were merged to form a single tile scan image by using Leica's own software, LAS X. The area of the sample was measured from the tile scan images by using Fiji/ImageJ [136,137]. In addition, the thickness of the sample was measured by using Leica DMI8 widefield microscope. The thickness was studied by using z-stack and light with 488 (475) nm wavelength. First, the microscope was focused on the bottom of the well where the lowest fluorescent microbeads were in focus and that point was marked as "begin". Then the microscope was focused on top of the sample where the highest microbeads were in focus, which was then marked as "end". After that, LAS X, gave a difference between these two z-coordinates which equals the thickness of the sample. The measurement was done once per sample including the highest and lowest point of the whole sample. From these values, the volumes of the samples were calculated as area times thickness, and from that the size change of the samples were analyzed. The data was collected, processed, and analyzed with Microsoft Excel (Microsoft Corporation, United States of America). All data in size change graphs is presented as average \pm standard deviation.

4.1.3 Live/Dead staining

Live/Dead staining was done to see the viability of the cells in samples on day 2. The staining was done to separate well plate samples including two samples per material and condition, and one control sample without cells. Live/Dead staining solution was made by mixing DPBS, Calcein-AM (dissolved in dimethyl sulfoxide (DMSO), Life Technologies, United States of America), and Ethidium homodimer (EthD-1, Life Technologies, United States of America) so that Calcein-AM concentration in final solution was 0.2 μ M and EthD-1 concentration was 1.0 μ M. The medium was then removed and replaced by adding 200 μ l Live/Dead solution to each sample. The samples were incubated for at least 1 h in room temperature (RT) placed on a rocking plate (gyro-rocker SSL3 StuartTM, Sigma-Aldrich, United States of America) protected from light. Finally, the samples were imaged with Olympus IX51 Fluorescence microscope (Olympus Corporation, Japan) by using 488 nm light wavelength for living cells and 568 nm for dead ones. Images were processed with Fiji/ImageJ and FigureJ [138].

4.1.4 Cytochemical staining

Cytochemical staining was done to well plate samples after 10 days cultivation period. DAPI (4',6-diamidino-2-phenylindole) was used to detect nuclei of the cells while phalloidin was used to detect actin filaments of the cell. There were one control sample without cells and three parallel samples per each material and condition stained. After 10 days of cell culture, the samples were washed once with DPBS with 5 minutes incubation at RT and then fixed with 4 v/v-% paraformaldehyde (PFA; Electron Microscopy Sciences, United States of America) in DPBS with 30 minutes incubation at RT inside fume hood, after which the samples were washed three times with DPBS with 5 minutes incubation at RT. The samples were then stained with phalloidin (ad643-81, ATTO 649, 1:500, ATTO-TEC, Germany) in 1 v/v-% bovine serum albumin (BSA, Sigma-Aldrich, United States of America) in DPBS for overnight at + 4 °C and the samples were then again washed three times with DPBS with 5 minutes and two times with 1 h incubation at RT. After that the samples were stained with 0.5 µg/ml DAPI (D9542, 1 mg/ml, 1:2000, Sigma-Aldrich, United States of America) in DPBS for 45 minutes at RT after which the samples were washed again three times with DPBS with 5 min incubation at RT. Finally, the samples were imaged with Leica DMI8 widefield microscope by using 390 nm light wavelength for DAPI, and 643 (635) nm for phalloidin. Images were processed with Fiji/ImageJ and FigureJ.

4.2 3D cell culturing in a hydrogel on-a-chip

The chip used in this study is AIM Biotech's idenTx 3 Chip (Singapore). It is easy-to-use microfluidic chip allowing the creation of 3D model. There are three identical compartments which all include 3D gel channel in the middle and two medium channels, one in both sides of the gel channel. Between these channels, there is line of posts. [139,140] Figure 11 shows more detailed image of the chip design and scale.

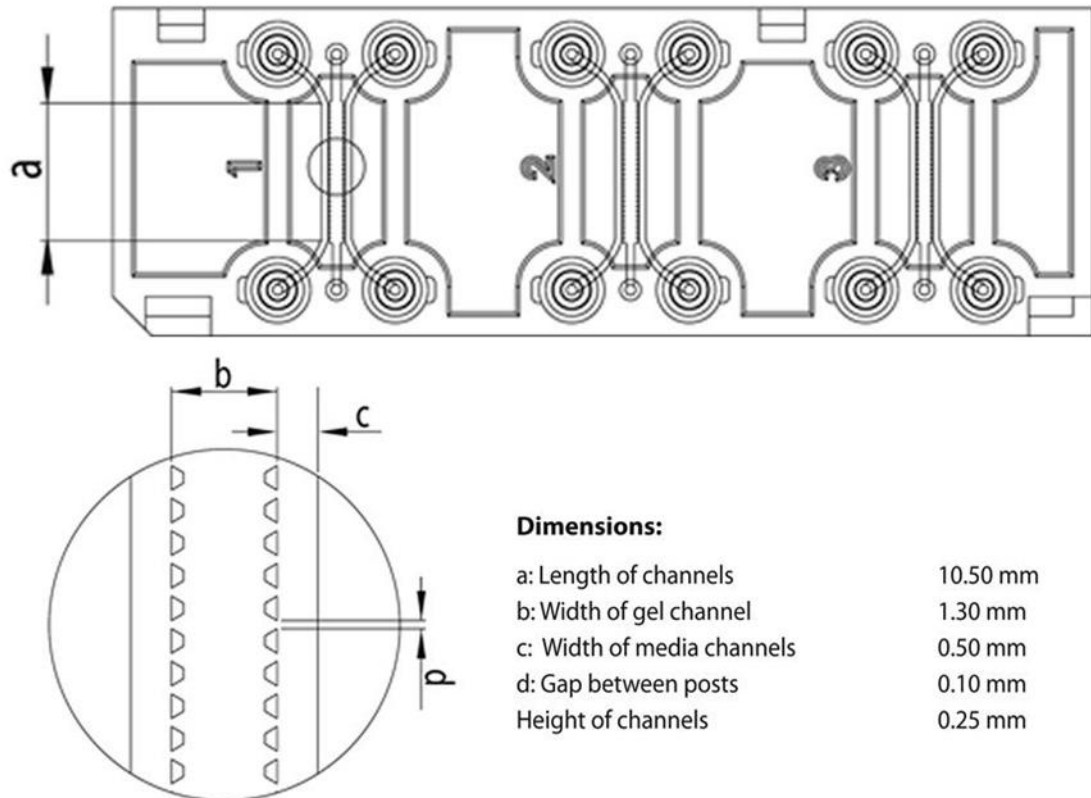


Figure 11. Descriptive image of AIM Biotech's idenTx 3 Chip. Modified from [139]

The chip has gas permeable laminate which allows effective gas exchange. In addition, it is optically clear which enables the use of different imaging methods. Furthermore, it is compatible with all polymerizable hydrogels including collagen, fibrinogen and Matrigel. The chip can be used in monotypic or organotypic co-culture models. Interstitial flow and chemical gradients across the 3D gel region can also be controlled. Medium exchange has also been made easy because the vacuum aspiration can be used in removing the medium without the risk of over-aspiration. Lastly, the chip is sterile and ready-to-use product which is also easy-to-use. [139,140]

4.2.1 Establishment of 3D vascular network in microfluidic chip using different hydrogels

Human BMSCs (6/20) obtained with the donor's written informed consent and processed under ethical approval of the Ethics Committee of the Expert Responsibility area of Tampere University Hospital, Tampere, Finland (TAYS, R15174), are used in this study. They are cultured in α MEM supplemented with 5 v/v-% HS, 1 v/v-% P/S and 5 ng/ml FGF. The cells passages used in this study were between 5 and 7.

Commercial HUVECs (1.29715, Cellworks, India) tagged with green fluorescent protein (GFP) are also used in this study. They are cultured in EGM-2 (Endothelial Cell Growth Medium-2 BulletKit, Lonza, Clonetics™, Switzerland) which consists of Endothelial Cell Growth Basal Medium-2 (EBM-2) and Endothelial Cell Growth Medium-2 Supplements (Appendix, Table A). However, the 2 v/v-% HS was used instead of fetal bovine serum which was supplied with the Kit. The cells passages used in these experiments were between 6 and 7.

Three parallel samples per material and each condition was made. In addition, two parallel samples per material without cells were made as controls. The used materials and conditions were chosen based on well plate experiments and they are listed in Table 4. TeloCol® was not used in chip experiments but VitroGel® Hydrogel Matrix (The Well Bioscience, United States of America) was used instead.

Materials were prepared as done before (4.1.1). The cells were collected, divided into aliquots containing 5 M cells/ml HUVECs and 1 M cells/ml BMSCs (cell ratio 5:1), and centrifuged at 200 G for 5 minutes. The formed cell pellet was then mixed with the material. In case of fibrin, the cell pellet was resuspended in thrombin and the solution was then mixed with fibrinogen. Similarly in case of gelaGG, cell pellet was resuspended into GGox, and the solution was then mixed with gelaCDH. For collagen I samples, both rat tail and human (VitroCol®), the cell pellet was resuspended into the final material solution. For VitroGel® samples, the cell pellet was resuspended into culture medium, and the cell suspension was mixed with VitroGel® Hydrogel Matrix solution with 1:2 v/v ratio.

When the cell-material mixtures were ready, 10 µl or 15 µl of the mixture were injected into AIM Biotech Chip's gel channel. The chips were flipped upside down for 30 seconds after which the chips were turned right side up, placed inside a humidified chamber and observed under microscope. The flipping was done to improve cell division evenly in the chip. The chips were left to gelate upside down at + 37 °C for 30 minutes. The flipping of the chips was done to every other material except for VitroGel® because its protocol guides not to disrupt the gelation process by tilting or shaking the culture platform [141]. After gelation 15 µl of EGM-2 culture medium was injected inside each medium channels. Next, 90 µl of EGM-2 was added into left side medium chambers and 50 µl into right side ones as shown in Figure 12 (A). Chips were placed inside the incubator at + 37 °C. The culture medium was changed every day with volumes shown in Figure 12 (A).

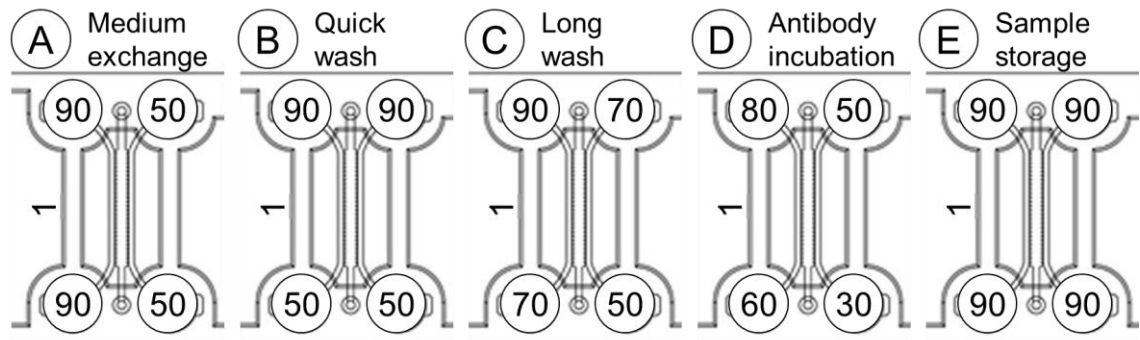


Figure 12. Different volumes (μl) used in medium exchange and immunocytochemical staining. Modified from [139]

The vascular network formation was followed by imaging the GFP-signal of HUVECs. The chips were imaged live during culturing period with Leica DMI8 widefield microscope at days 3, 7 and 10 with phase contrast view and GFP filter (475 nm wavelength). Images were processed with Fiji/ImageJ and FigureJ.

4.2.2 Immunocytochemistry

Chips were stained after 10 days cultivation period with DAPI, alpha-smooth muscle actin (αSMA), and phalloidin. DAPI allows the detection of nuclei of the cells, αSMA is a perivascular cell marker allowing the detection of vSMC, and phalloidin allows the detection of actin filaments of the cells. The αSMA and phalloidin stain almost the same structures so both stains were not necessary. The HUVECs were already tagged with GFP so no staining was needed to detect these structures.

After 10 days of culturing, the chips were washed two times with DPBS with 3 minutes incubation by using volumes (B) and (C) in Figure 12. After that, the chips were fixed with 4 v/v-% PFA in DPBS by using volumes (C) and incubating for 30 minutes at RT inside fume hood. Then the chips were washed three times with DPBS with 3 minutes incubation by using volumes (B) once and two times volumes (C). The chip samples could have been left in the third DPBS at + 4 °C to wait the staining or the staining could have been started right away after washing.

First, the chips were permeabilized with 0.1 v/v-% Triton-X-100 (Sigma-Aldrich, United States of America) in DPBS for 10 minutes at RT by using volumes (C) in Figure 12. Then the samples were blocked with 0.1 v/v-% Triton-X-100, 1 v/v-% BSA in DPBS for 2 hours at RT by using volumes (C). Finally, the primary antibodies were introduced to the chips with 0.1 v/v-% Triton-X-100, 1 v/v-% BSA in DPBS. The used antibody was αSMA ([1A4], ab7817, mouse, 1 mg/ml, 1:300, abcam, United Kingdom). The primary antibody solution was centrifuged for 3 minutes at 1 300 rpm to homogenize the solution

and then it was applied with volumes (D) to the chips which were then incubated for 2 days at + 4 °C. After the incubation, the chips were washed four times with 1 v/v-% BSA in DPBS by using volumes (B) once without incubation, volumes (C) two times with 2-3 hours incubation and lastly volumes (C) once with overnight incubation at + 4 °C.

Next day, the secondary antibodies were introduced to the chip samples with 0.1 v/v-% Triton-X-100, 1 v/v-% BSA in DPBS. Into that secondary antibody solution, phalloidin (1:500) and DAPI (1 mg/ml, 1:1500) was added in addition to the secondary antibody Alexa Fluor goat anti-mouse IgG (A11031, 2 mg/ml, 1:400, Life Technologies Corporation, Thermo Fisher Scientific, United States of America). The secondary antibody solution was also centrifuged for 3 minutes at 1 300 rpm to homogenize the solution. After that the solution were added by using volumes (D), and the chips were incubated for two days at + 4 °C. After the incubation, the chips were washed three times with DPBS by using volumes (B) once without incubation, volumes (C) once with 1-2 hours incubation and lastly volumes (C) once with overnight incubation at + 4 °C. After incubation, fresh DPBS was added with volumes (C) before visualization.

Finally, the chips were imaged with Leica DMI8 widefield microscope by using 390 nm light wavelength for DAPI, 488 (475) nm for GFP, 568 (560) nm for α SMA and 643 (635) nm for phalloidin. Images were processed with Fiji/ImageJ and FigureJ.

4.2.3 Vascular image analysis and statistical analysis

AngioTool [142] (United Kingdom) was used to analyze vessels' morphological and spatial parameters, including vessel area (%), and total vessel length (mm). All data in graphs is presented as average \pm standard deviation. Normality of the data obtained from AngioTool was studied with Shapiro-Wilk test. Difference between fibrin with aprotinin compared to other conditions and difference between materials \pm inhibitors were tested with nonparametric Mann–Whitney U test. The difference is considered to be statistically significant with a p value ≤ 0.05 . The statistical analysis was done with IBM SPSS Statistics (Version 29.0.1.0, Revision 6, SPSS Inc., United States of America) software.

5. RESULTS

5.1 3D cell culturing in a hydrogel in static condition on a well plate

5.1.1 Hydrogel size change in different hydrogels on well plate

Tile scan images of each well plate sample were taken every day during 10-day cultivation period. The best examples of these tile scan images are shown in the Figure A in Appendix. The thicknesses of the samples were measured every day during 10-day cultivation by using microscope and fluorescent beads. These results are shown in Figure 13. In addition, the areas of the samples were measured from tile scan images and the results are shown in Figure 14. Furthermore, the volumes of cylindrically shaped samples were calculated according to the data obtained from the results of thickness and area. These results are presented in Figure 15. TeloCol[®] was dropped out from the inhibitory test due to the poor cell results obtained from the first experiments without inhibitors. Therefore, thicknesses, areas, and volumes of TeloCol[®] have been collected into Figure 16 and no inhibitor experiments were done.

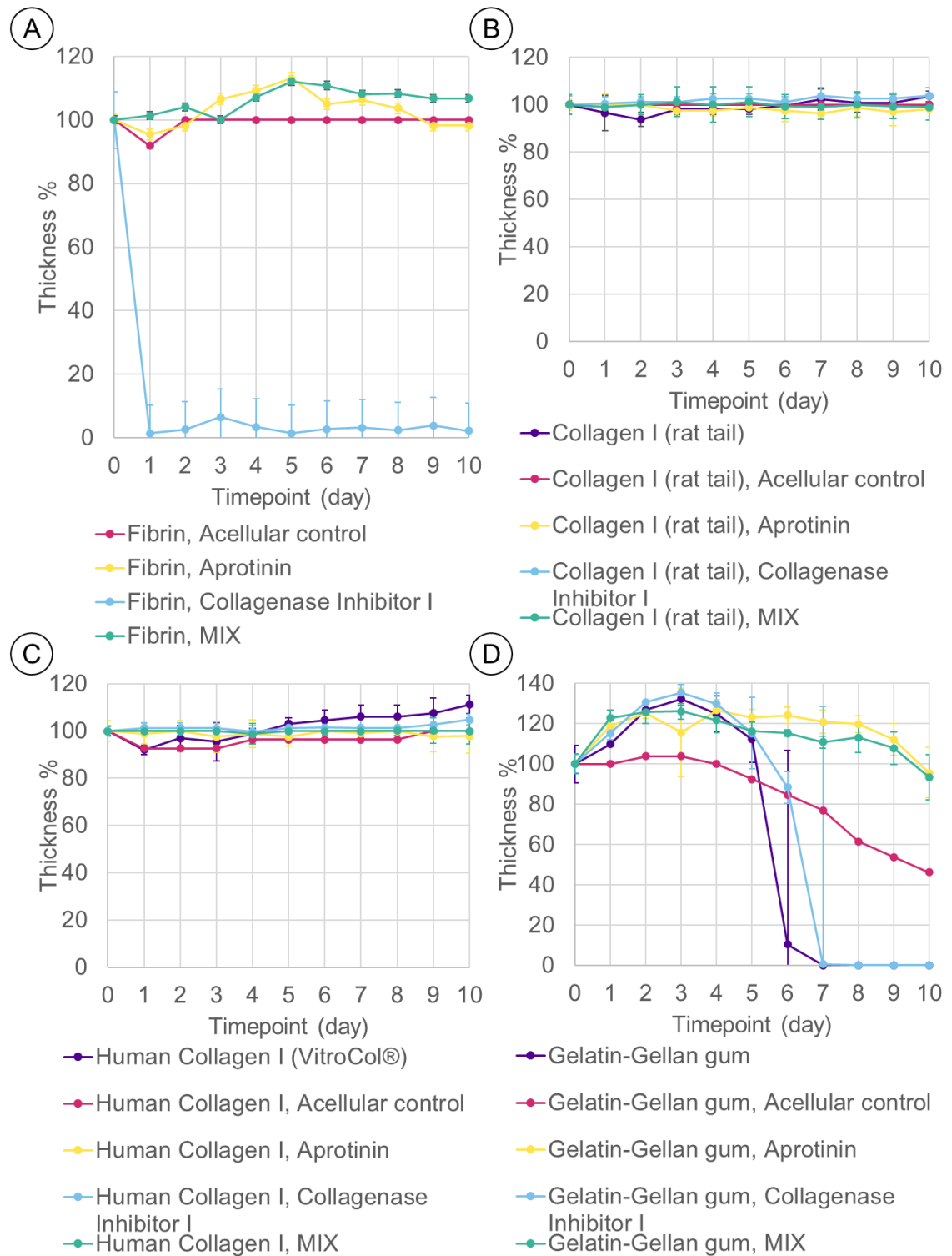


Figure 13. Thicknesses of the samples measured every day during cultivation. (A): Fibrin, (B): Collagen type I (rat tail), (C): human Collagen type I (VitroCol®), (D): Gelatin-gellan gum, Average \pm standard deviation, N=3 per material and condition (Acellular control N=1)

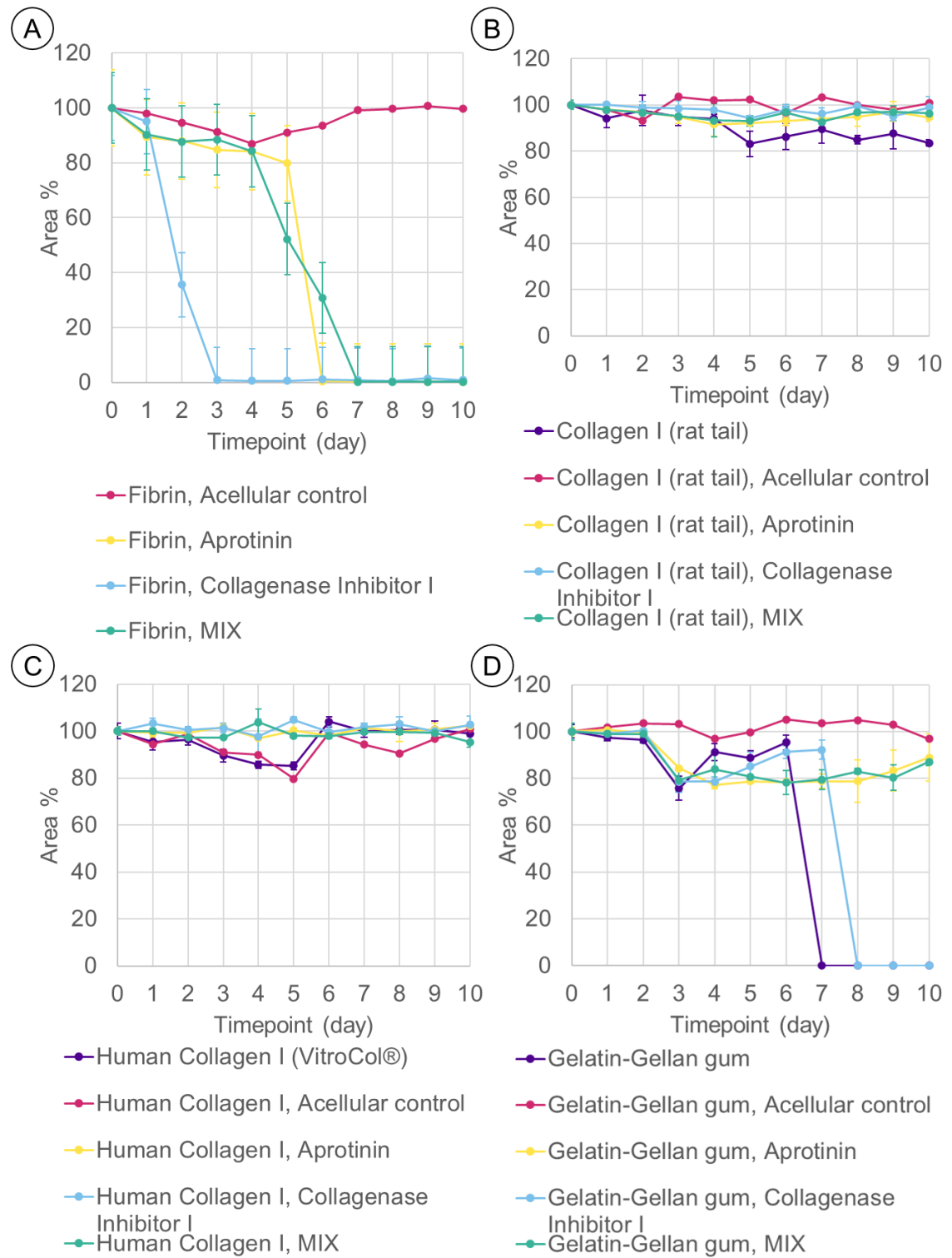


Figure 14. Areas of the samples measured from tile scan images which were taken every day during cultivation. (A): Fibrin, (B): Collagen type I (rat tail), (C): human Collagen type I (VitroCol®), (D): Gelatin-gellan gum, Average \pm standard deviation, N=3 per material and condition (Acellular control N=1)

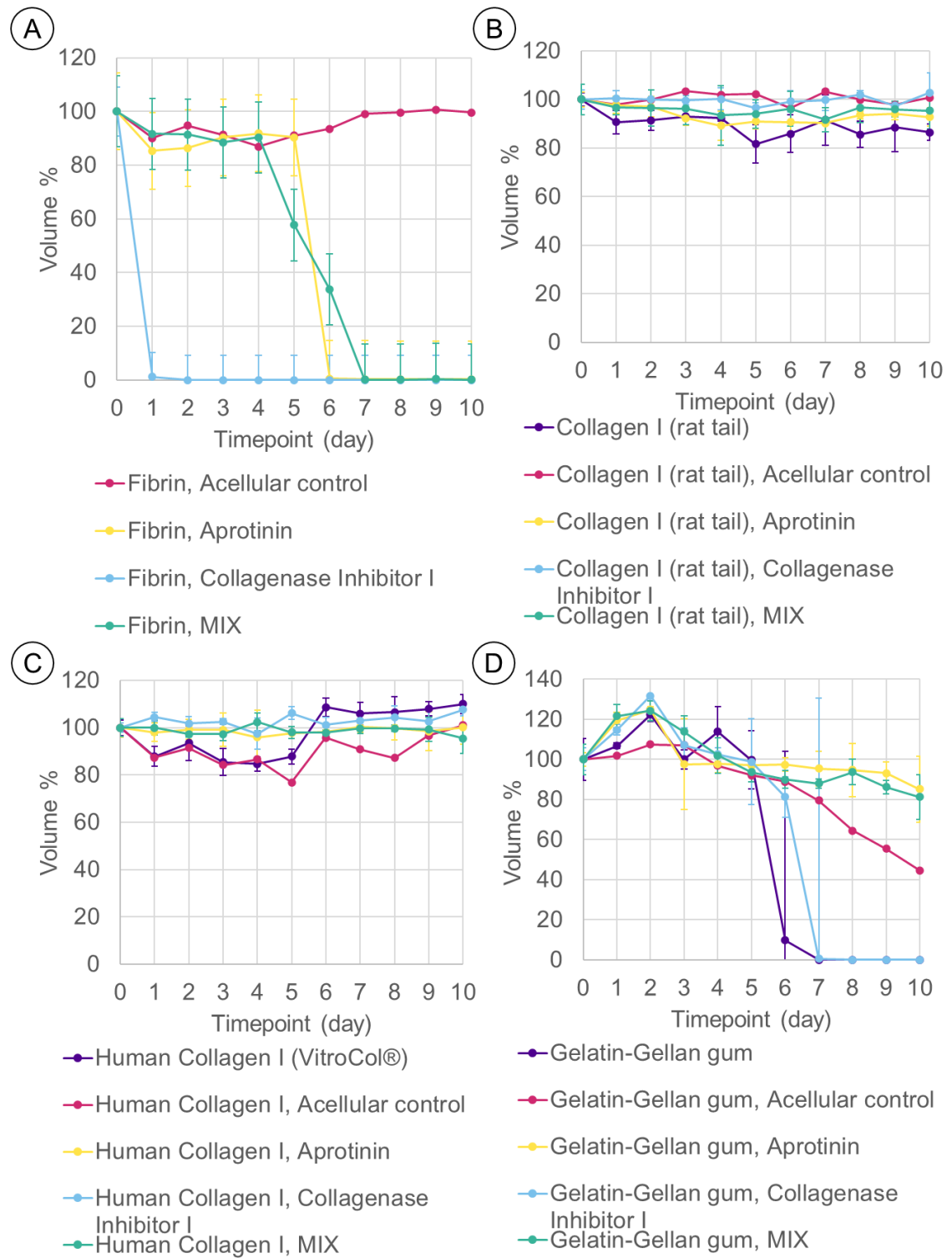


Figure 15. Volumes of the samples calculated from the thicknesses and areas measured every day during cultivation. (A): Fibrin, (B): Collagen type I (rat tail), (C): human Collagen type I (VitroCol®), (D): Gelatin-gellan gum, Average \pm standard deviation, $N=3$ per material and condition (Acellular control $N=1$)

According to the curves in Figure 13, Figure 14, and Figure 15 the collagen I (rat tail) and VitroCol® kept their thicknesses, areas and volumes the best, especially, when Collagenase Inhibitor I was used. The values of areas (Figure 14) acellular control and cellular control without inhibitors have variability and they differ from other values during the cultivation. Values of areas of collagen I (rat tail) samples in Figure 14 (B) have more variability in the end compared to the VitroCol®'s values. All collagen I samples with some inhibitor kept their area well.

VitroCol® samples kept their volumes a bit better compared to collagen I (rat tail) samples (Figure 15). In Figure 13 and Figure 15, the thickness and volume of VitroCol® samples increased in the end of cultivation. The volumes of VitroCol® samples where inhibitor was not used, or the used inhibitor was Collagenase Inhibitor I showed to increase most in the end. Values of acellular sample's volumes vary quite a lot during cultivation.

Even though volumes of collagen I (rat tail) samples stay quite stable, there is bigger variation between conditions. Volumes of cellular control without inhibitors seem to decrease most while the samples where Collagenase Inhibitor I was used, seemed to be most stable and their volumes stayed close the volumes of acellular control. Values of two other conditions, samples with aprotinin alone or in mixture with Collagenase Inhibitor I, stayed between acellular and cellular controls. The sample where only Collagenase Inhibitor I was used showed to prevent the degradation or decrease in volume the most.

The thickness and volumes curve (Figure 13 and Figure 15) of gelaGG differs from the other curves a lot. The values increase in the beginning, and then decrease in the end. The biggest difference is that the thickness and volume of the acellular control sample also decrease. There are quite dramatic drops in the areas in cellular control samples without inhibitors and samples with use of Collagenase Inhibitor I. Only acellular control kept its area while the area decreased in all other samples. However, the gelaGG samples with use of aprotinin alone or with Collagenase Inhibitor I kept the area quite well and the area decreased only a little. GelaGG's cellular control sample without inhibitors and sample with Collagenase Inhibitor I degraded completely while samples with aprotinin alone or together with Collagenase Inhibitor I stood better against the degradation or volume change. Volumes of acellular control sample stayed between these two groups. In addition, the samples where aprotinin was used, either alone or together with Collagenase Inhibitor I, kept their volume better than acellular control.

The thicknesses of fibrin samples with Collagenase Inhibitor I decreased immediately while samples where aprotinin was used, alone or in a mixture with Collagenase Inhibitor I, kept their thicknesses much better. All the cellular fibrin samples lost their area's during cultivation. Fibrin samples with only use of Collagenase Inhibitor I lost their areas fastest while samples with use of aprotinin alone or in mixture with Collagenase Inhibitor I, kept their areas better but the areas still degraded almost completely in the end of culturing period. Volume values of fibrin samples varied a lot. All fibrin samples containing cells degraded almost completely in the end of the cultivation. As said before, fibrin samples without aprotinin degrade immediately while samples, where aprotinin was used either alone or in mixture with Collagenase Inhibitor I, stood against the degradation or decrease in volume longer, but they also degraded in the end. Only acellular control sample kept its thickness, area, and volume for the total culturing period. There were no cellular fibrin samples without the use of inhibitors (N/A: not applicable) due to degradation and shrinking problems.

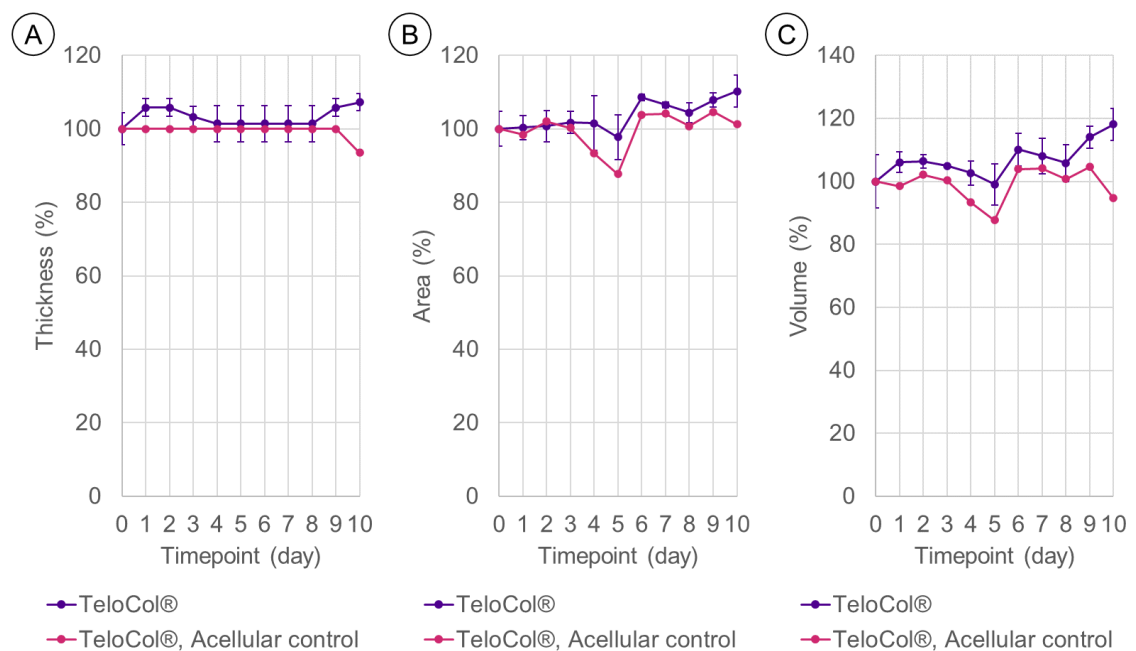


Figure 16. (A): Thicknesses, (B): Areas, and (C): Volumes of the TeloCol® (bovine Telocollagen I) samples measured and calculated every day during cultivation, Average \pm standard deviation, N=3 cellular samples (Acellular control N=1)

Even though, TeloCol® was also part of the experiments in the beginning, it was dropped out from the inhibitory tests and further experiments because the cells did not elongate in the gel (Figure 17 and Figure 18). The cells stayed as dots in the gel, and it looked like the cells did not like to have it as their living environment. In addition, according to Figure 16, the thicknesses, areas, and volumes of the samples did not change that much during the cultivation. However, their values increased in the end.

5.1.2 Viability of cells in static condition on well plate

Live/Dead staining was done to well plate samples with fibroblasts at day 2 to observe the viability of the cells. The results are shown in Figure 17. In Appendix in Figure B, Figure C, Figure D, Figure E, and Figure F, these Live/Dead images are presented with separate channels.

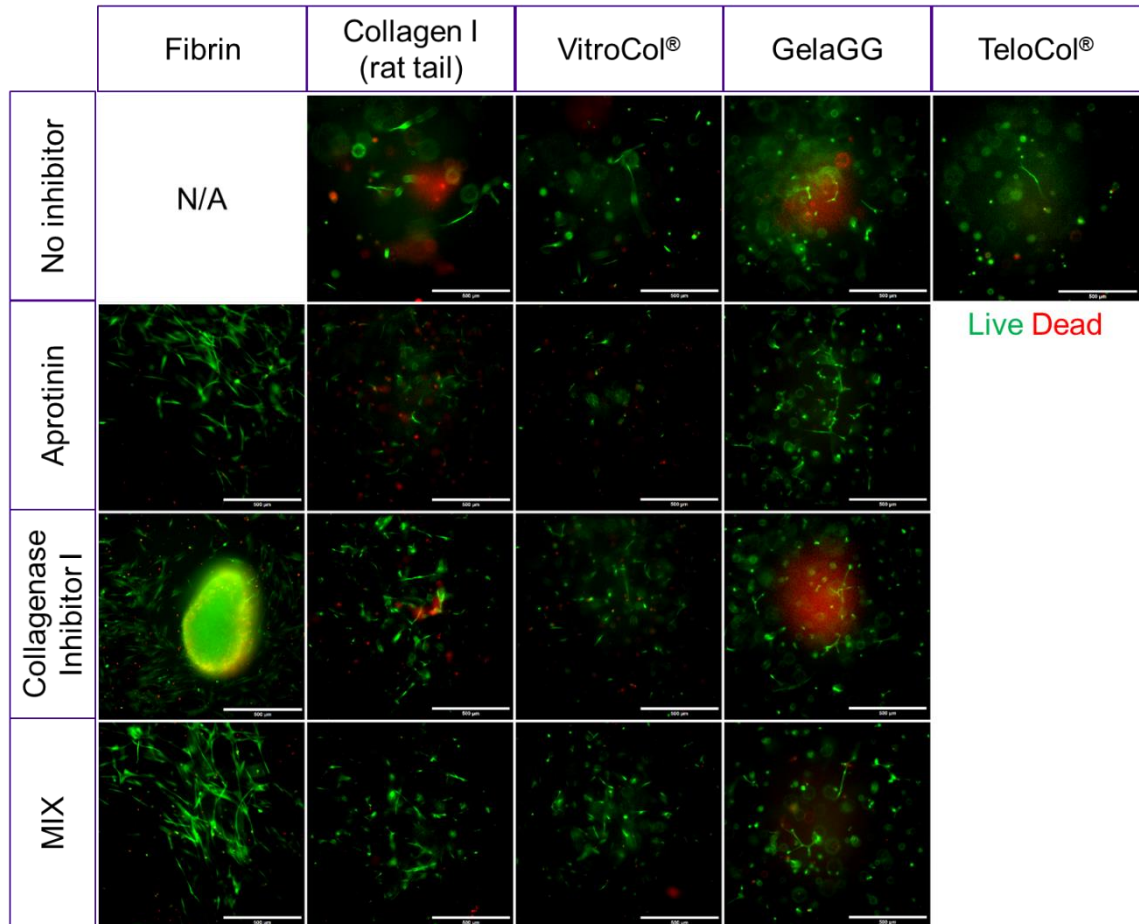


Figure 17. Live/Dead images of well plate samples taken on day 2. N/A: not applicable: fibrin was not used without inhibitors. TeloCol® was not used in further inhibitory experiments because poor results in first experiment without inhibitors. Green: live, Red: dead, 10x, Scale bar: 500µm, MIX: mixture of inhibitors aprotinin and Collagenase Inhibitor I (1:1), N=2 per material and condition

In Live/Dead images taken at day 2 (Figure 17), only fibrin samples where Collagenase Inhibitor I was used alone were degraded or shrunken into a small dot. The dot was quite thick as can be seen in the Figure 17. Otherwise, fibrin samples looked good, the cells were alive and elongated nicely. There were no cellular fibrin samples without the use of inhibitors (N/A) due to degradation and shrinking problems.

In Live/Dead images (Figure 17), cells in collagen I (rat tail) and VitroCol® looked good except the control samples without inhibitors. In those samples, there were less cells and only few of them were elongated. Cells were most elongated in samples where only

Collagenase Inhibitor I was used but there were also more dead cells showed as red dots.

GelaGG had that red background in samples without inhibitors or with only Collagenase Inhibitor I. Samples where aprotinin was used alone or in a mixture with Collagenase Inhibitor I, looked the best because the cells were alive and elongated. In TeloCol[®] samples, most of the cells were alive but only couple of them were elongated. Therefore, TeloCol[®] was not used in the further experiments.

All in all, the viability was high in all tested materials and conditions. Only few dead cells were observed in fibrin sample with Collagenase Inhibitor I, collagen I samples both rat tail and human (VitroCol[®]) in every condition, gelaGG samples in every condition and TeloCol[®]. Fibrin with mixture of inhibitors, collagen I both rat tail and human (VitroCol[®]) with Collagenase Inhibitor I and gelaGG with aprotinin or mixture of the inhibitors seem to have more alive and elongated cells compared to other samples. Live/Dead assessment is based on visual inspection, so no quantitative analysis methods were used.

5.1.3 Cellular morphology and alignment in static condition on well plate

Well plate samples with fibroblasts were cytochemically stained after 10-day cultivation period. Cytochemical staining was done to study and observe the cell morphology, orientation, and density. The results of these staining are shown in Figure 18. In the figures, DAPI showing the nuclei are shown with blue color and phalloidin showing filamentous actin is shown with red color. In Appendix in Figure G, Figure H, Figure I, Figure J, and Figure K, these cytochemical images are presented with separate channels.

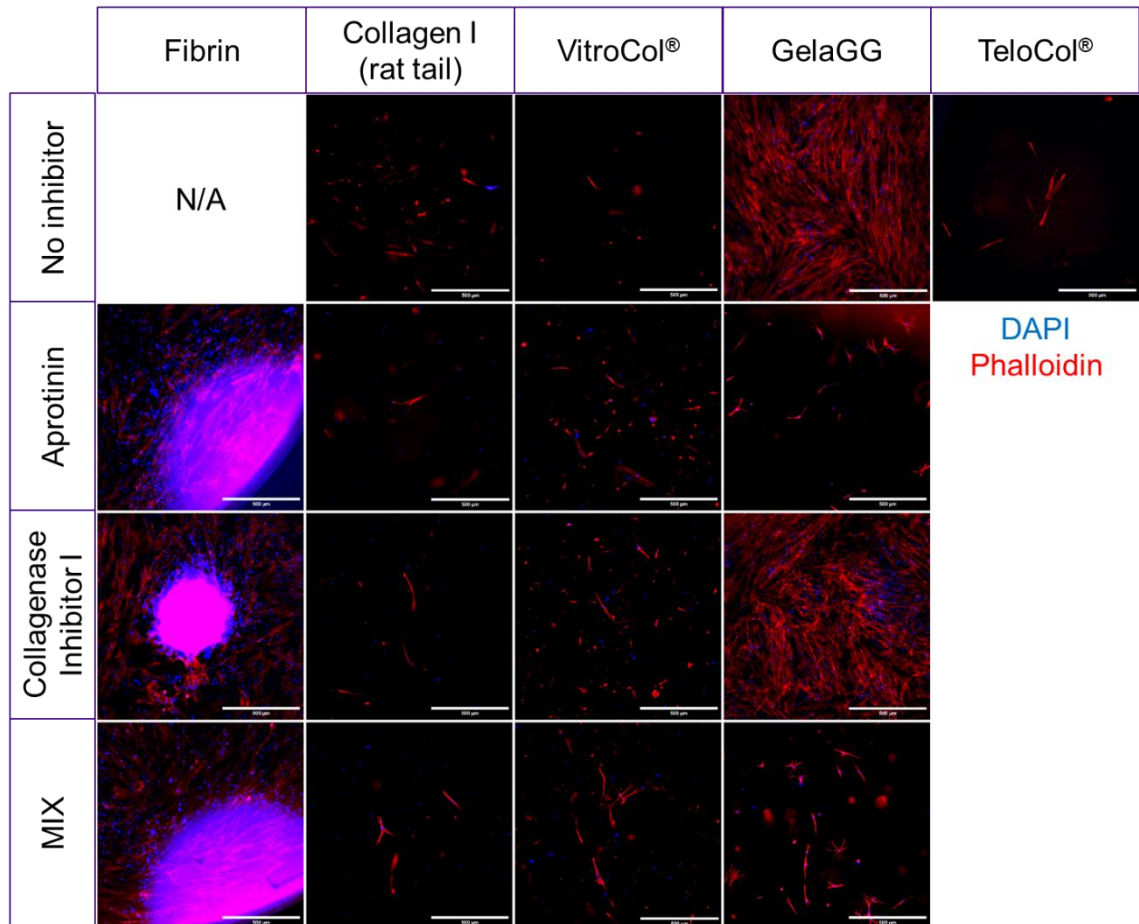


Figure 18. Cytochemical staining of well plate samples taken after 10 days of cultivation. N/A: not applicable: fibrin was not used without inhibitors. TeloCol® was not used in further inhibitory experiments because poor results in first experiment without inhibitors. Blue: DAPI, Red: phalloidin, 10x, Scale bar: 500µm, MIX: mixture of inhibitors aprotinin and Collagenase Inhibitor I (1:1), N=3 per material and condition

As said before, all fibrin samples containing cells degraded during the 10-day cultivation period. The cells in fibrin samples, in Figure 18, are on the bottom of the well because there was no gel left. The brighter and thicker dots are the fibrin gel or what is left from it. Cells were nicely elongated, and they occupied the bottom of the well after the gel had degraded or shrunken away. As a result, the cells on the bottom of the well were in 2D. However, there seem to be cells also in the gel dots, but the dots were so thick that the cells could not be imaged or observed properly. There were no cellular fibrin samples without the use of inhibitors (N/A) due to degradation and shrinking problems.

In collagen I (rat tail) samples, there were only a few cells from which some were elongated but some were not. VitroCol® samples, on the other hand, had more cells except in the control samples without inhibitors. Cells in samples where Collagenase Inhibitor I was used looked the best. There were only a few cells in TeloCol® samples

and only few of them were elongated. Therefore, TeloCol[®] hydrogel was not used in further experiments.

In gelaGG samples where inhibitors were not used at all or where the only used inhibitor was Collagenase Inhibitor I, the hydrogel was degraded during cultivation period. Therefore, there is no gel left and the cells are cultured on the bottom of the well in 2D. The cells in 2D were nicely extended and occupied the bottom of the well. The samples where aprotinin was used either alone or as a mixture with Collagenase Inhibitor I looked good, the cells were really elongated, also in multiple directions in 3D.

All in all, all the tested materials and conditions supported partial elongation. In all fibrin samples and gelaGG samples without inhibitors and with Collagenase Inhibitor I, the hydrogel degraded during cultivation, so the cells were cultured on the bottom of the well in 2D as seen in the Figure 18. The cells in collagen I both rat tail and human (VibroCol[®]) with Collagenase Inhibitor I and gelaGG with mixture of inhibitors seem to be most elongated and proliferated compared to other conditions. This assessment is based on visual inspection, so no quantitative analysis methods were used.

5.2 3D vascular network formation in dynamic condition on-chip

Differences between different hydrogels' ability to support vascularization were observed. Some of the gels were able to support cell organization. In some hydrogels, the cells stayed rounded and did not elongate while in others they formed unified vascular networks.

The HUVECs used in the study had green fluorescent protein (GFP) tag in them so their growth and spread could be followed with fluorescent microscope during cultivation in microfluidic chip. Tile scans of the chips taken at day 3, 7, and 10 are shown in Figure 19.

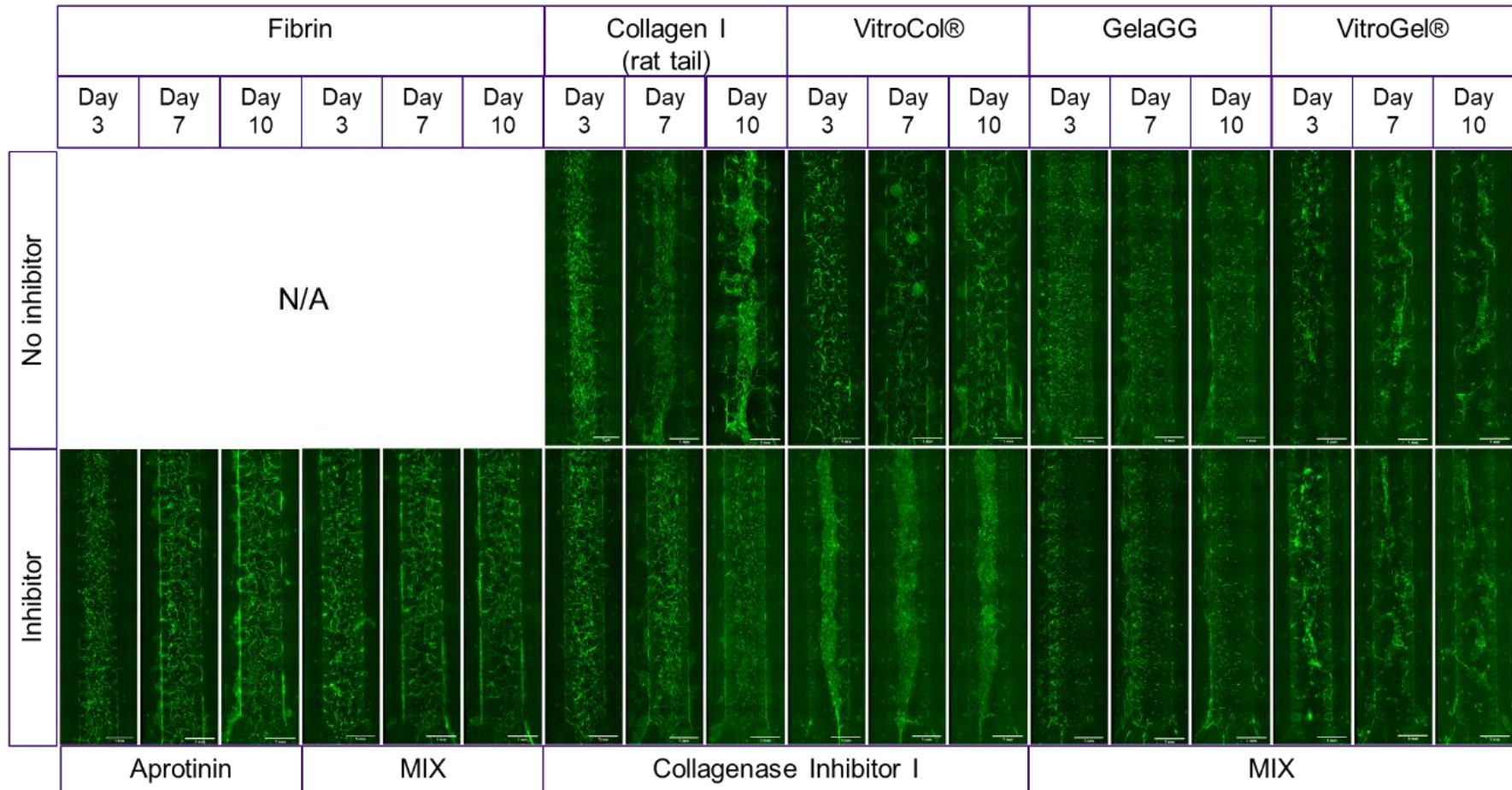


Figure 19. Green fluorescent protein (GFP) tagged human umbilical vein endothelial cells (HUVEC) in Vascularization-on-Chip. Tile scan images taken at days 3, 7, and 10 during cultivation. Top row includes the samples without inhibitors. N/A: not applicable: fibrin was not used without inhibitors. Bottom row includes the samples where chosen inhibitors (shown under the image) were used. Medium flow from left to right. Scale bar: 1 mm, MIX: mixture of inhibitors aprotinin and Collagenase Inhibitor I (1:1), gelaGG: gelatin-gellan gum, N=3 per material and condition

From the Figure 19, the vascular formation in different hydrogels can be observed. The chips in the images are orientated so that the flow moves from the left side to the right side of the chip. The vascular networks formed in the samples in Figure 19, are visually detected.

Vascular network formed in fibrin hydrogel seem to be most mature compared to other tested hydrogels. Fibrin gel included vascular structures that were connected into intact network throughout the chip. Importantly, in fibrin, connected vascular network was formed in the presence of aprotinin as well as with mixture of aprotinin and Collagenase Inhibitor I. Differences in morphology of the formed vessels was observed with larger vessels in chips where both inhibitors were used. There were no cellular fibrin samples without the use of inhibitors (N/A) due to degradation and shrinking problems.

Vascular network formed in collagen (rat tail) hydrogel with Collagenase Inhibitor I is promising. Vascular structures were formed throughout the chip, however the vessel-like structures started to degrade already at day 10. Collagen I (rat tail) hydrogel samples without inhibitors started to degrade or decrease in size already at day 7 and the vascular network was not as mature as seen in samples with inhibitor.

Vascular network formed in VitroCol[®] hydrogel without inhibitors is promising. The endothelial cells form vessel-like structures. Samples where Collagenase Inhibitor I was used, the endothelial cells did not form vessel-like structures. The gel collapsed already when medium was added into the medium channels when establishing the samples.

Vascularization in gelaGG hydrogel with or without inhibitors is not as good as in other materials. Some of the endothelial cells formed vessel-like structures but they did not form connected network. Samples with mixture of inhibitors seem to have less cells compared to the samples without inhibitors. Most of the cells escaped to the medium channels.

Vascularization in VitroGel[®] is poor. The hydrogel could not stand the addition of culture medium so there is not much gel left. Few vessel-like structures can be found but they do not form connected network.

5.2.1 Vessel parameters

AngioTool was used to analyze vessel parameters. Results from this analysis are shown in Figure 20.

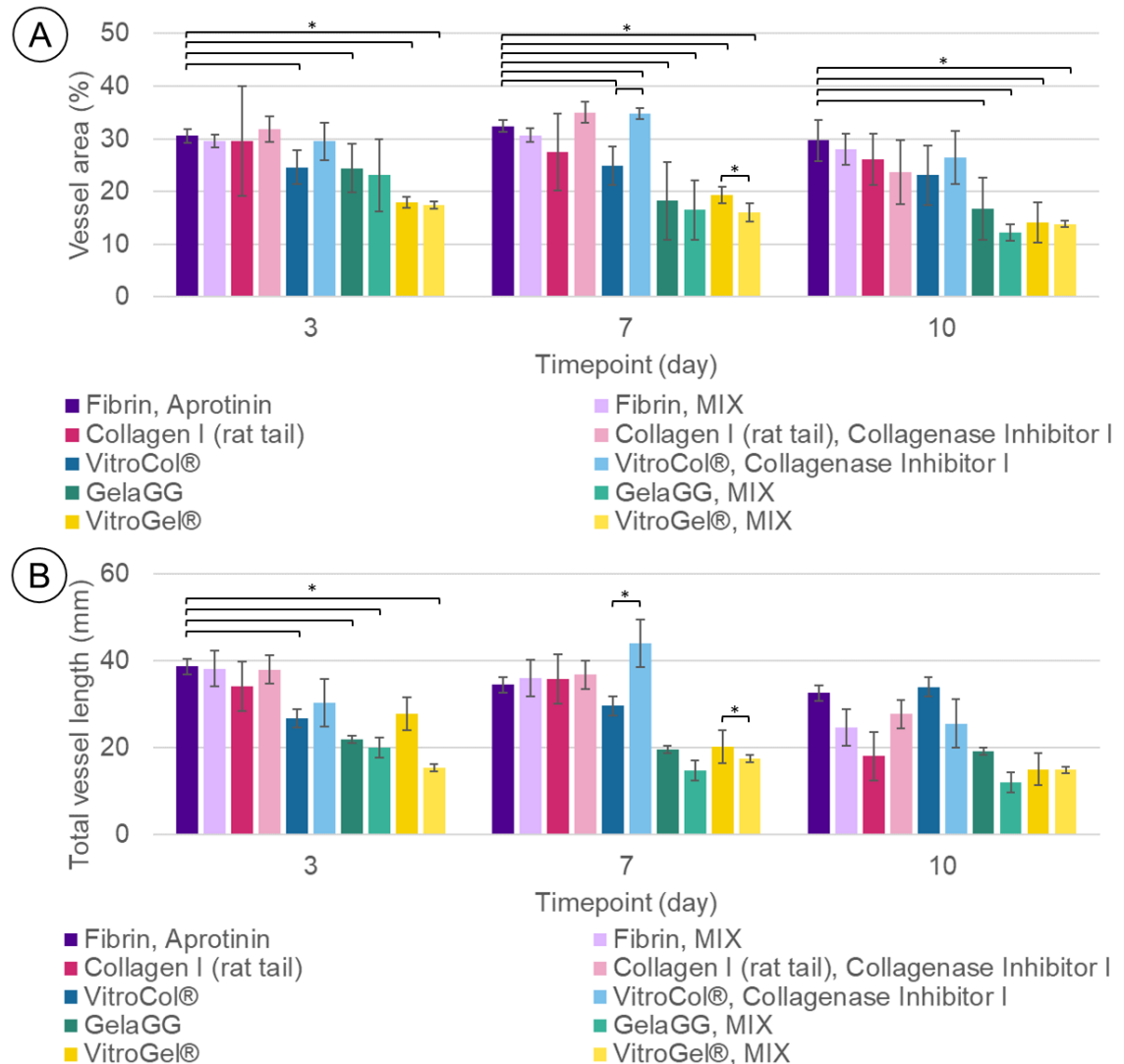


Figure 20. Vessel parameters studied with AngioTool. (A) Vessel area (%), (B): Total vessel length (mm). Fibrin with aprotinin was used as control to which other samples were compared. MIX: mixture of inhibitors aprotinin and Collagenase Inhibitor I (1:1), Average \pm standard deviation, *= significant difference between tested hydrogel samples and conditions $p \leq 0.05$, $N=3$ per material and condition

According to Figure 20, largest vessel area is obtained with collagen I (rat tail) with Collagenase Inhibitor I at day 7 and smallest with gelaGG with mixture of inhibitors at day 10. Longest vessel is obtained with VitroCol® at day 7 and shortest with gelaGG with mixture of inhibitors at day 10.

All samples' difference with golden standard, fibrin with aprotinin, was analyzed with statistical analysis (Mann–Whitney U test). The differences that are considered statistically significant (p value ≤ 0.05) are marked into the figure. In vessel area,

VitroCol[®], gelaGG, and VitroGel[®] without inhibitors and VitroGel[®] with mixture of inhibitors have statistically significant differences to golden standard, fibrin with aprotinin, at day 3. At day 7, VitroCol[®], gelaGG, and VitroGel[®] with or without inhibitors, and at day 10, gelaGG, and VitroGel[®] with or without inhibitors, have statistical differences to the golden standard. In total vessel length, VitroCol[®], and gelaGG without inhibitors and gelaGG and VitroGel[®] with mixture of inhibitors have statistically significant differences to golden standard, fibrin with aprotinin, at day 3. At day 7 and 10, there were no statistical differences to golden standard in any conditions.

5.2.2 Vascular network structure in dynamic environment on-chip

Figure 21 shows the results of immunocytochemical staining done to the chips after 10 days of culturing. In the figures, α SMA is colored as red showing α smooth muscle actin of vSMCs, GFP as green showing the HUVECs, and DAPI as blue showing the nuclei of the cells. In Appendix in Figure L, these immunocytochemical images are presented with separate channels.

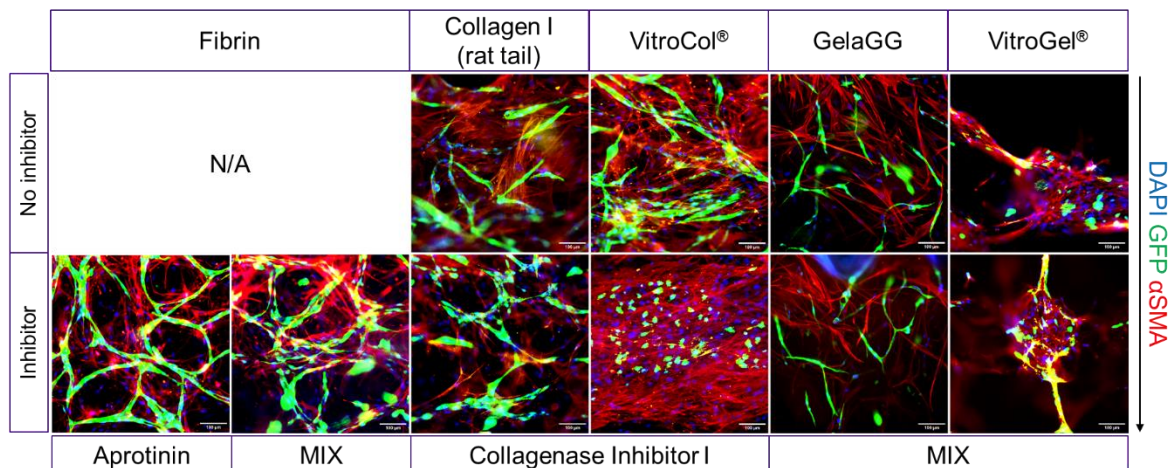


Figure 21. Immunocytochemical staining of vascularization model on a chip taken after 10 days of cultivation. Top row includes the samples without inhibitors. N/A: not applicable: fibrin was not used without inhibitors. Bottom row includes the samples where chosen inhibitors (showed under the image) were used. Medium flow from top to down. Blue: DAPI, Green: GFP-HUVEC, Red: α SMA, 20x, Scale bar: 100 μ m, MIX: mixture of inhibitors aprotinin and Collagenase Inhibitor I (1:1), gelaGG: gelatin-gellan gum, N=3 per material condition

Vascular network formed in fibrin hydrogel was visually detected as the most mature one (Figure 21). Fibrin gel included vascular structures that were connected into intact network throughout the chip and α SMA positive pericytes aligning the formed vascular structures. Importantly, in fibrin, connected vascular network was formed in the presence of aprotinin as well as with mixture of aprotinin and Collagenase Inhibitor I. Differences

in morphology of the formed vessels was observed with larger vessels in chips where both inhibitors were used. There were no cellular fibrin samples without the use of inhibitors (N/A) due to degradation and shrinking problems.

Vascular network formed in collagen I (rat tail) hydrogel with Collagenase Inhibitor I was more promising compared to the sample without the inhibitor. This can be seen in endothelial cells which form better vascular structures that are connected to each other and in pericytes which are aligned better around the endothelial cells and are not filling the whole hydrogel.

Vascularization in VitroCol[®] hydrogel without inhibitor looked promising because endothelial cells formed vessel-like structures but the pericytes did not align around them that well. Samples where Collagenase Inhibitor I was used did not form vascular networks. The endothelial cells did not elongate or form vessel-like structures. The pericytes, on the other hand, elongated nicely and filled the whole hydrogel.

Vascularization in gelaGG hydrogel was not as good as in other tested hydrogels. Endothelial cells tried to form vessel-like structures but there were not so many cells left since most of them escaped to the medium channels and the remaining cells were also located next to the pillars, close to the medium channels. The pericytes were also elongated but did not seem to align the formed vessel-like structures.

Vascularization in VitroGel[®] hydrogel is poor. There were not so many vessel-like structures and the pericytes were not aligned next to these structures. In addition, only little pieces of hydrogel were left in the samples.

6. DISCUSSION

6.1 3D Cell culturing in a hydrogel in static condition on well plate

6.1.1 Hydrogel size change in different hydrogels on well plate

According to the thickness, area and volume curves, the collagen I (rat tail) and VitroCol® kept their thicknesses, areas, and volumes the best. This would indicate that the possible degradation of the hydrogels did not happen significantly in the elevation nor latitude directions. The area values of cellular control sample of collagen I (rat tail) without inhibitors decreased the most and because the acellular control kept its area quite stable, the decrease in the area is most probably due to the actions of the cells embedded in the gel. All collagen I samples with some inhibitor kept their area well, meaning that all tested inhibitors have some preventing effect on the degradation of the gel. Same thing was seen in volumes of collagen I (rat tail) samples. Samples with aprotinin alone or in mixture with Collagenase Inhibitor I, stayed between acellular and cellular controls without inhibitors meaning that they have an effect on preventing the degradation of the hydrogel. However, the sample where only Collagenase Inhibitor I was used showed to prevent the degradation or decrease in volume the most making it promising tool for the future *in vitro* cell culturing applications. This result can also be explained by the literature because collagen is naturally degraded via metalloproteases such as collagenases and serine proteases [3,20] which indicates that both aprotinin and Collagenase Inhibitor I should effect on the degradation of the hydrogel.

VitroCol® did not degrade significantly during 10-day cultivation which makes it promising option for the future cell culturing applications. In addition, an interesting thing is that the thicknesses and volumes of VitroCol® increased in the end of the cultivation period. Usually, hydrogels' size can increase when they absorb more water but that commonly happens in the beginning as can be seen in case of gelaGG samples which values first increases a lot before decreasing drastically. However, there is another difference between the increase of thicknesses and volumes of these two materials since in case of gelaGG, also the values of acellular control sample increases which indicates that the hydrogel is absorbing more water while in case of VitroCol®, the values of acellular control do not increase. This could mean that the cells embedded in VitroCol® start producing their own ECM which would increase the amount of ECM. However, this theory cannot be verified because the composition of ECM matrix after cultivation was

not studied. Therefore, the ECM composition after cultivation should be studied in the future experiments.

In addition to the increase of values of the gelaGG samples in the beginning, all values decreased drastically after increasing. This happened to both cellular and acellular samples meaning that the increase in values was due to absorption of water and decrease in the values is not only caused by the cells but also due to hydrolytic degradation or hydrolysis. Hydrolysis is a degradation mechanism where water molecules break polymer chains resulting smaller chains [143]. Furthermore, the thicknesses and volumes of gelaGG without any inhibitor and with Collagenase Inhibitor I decreased even faster compared to acellular control indicating that also the cells affect the degradation of the hydrogel. The decrease in thicknesses and volumes were slower in samples where aprotinin was used alone or in mixture with Collagenase Inhibitor I compared to other samples. This means that the aprotinin has positive effect when preventing the degradation of the ECM and that aprotinin would also prevent on the hydrolytic degradation which is not caused by the cells. This could be due to the possibility of aprotinin binding to the GGox part of the hydrogel making it more stable compared to gelaGG mixture. GGox forms hydrazone crosslinks with gelaCDH in which hydrazide group of gelaCDH form crosslinks with aldehyde group of GGox [39,40]. Aldehyde group can, for example, form crosslinks with alcohol, amine, and hydrazide groups [144]. Aprotinin has free amine group and alcohol group in its structure, so it should be possible to form crosslinks between GGox and aprotinin. Therefore, there could be parts in the gel where there is only GGox and only gelaCDH when these two parts have not completely reacted with each other. In addition, ions from culture medium have shown to promoting the crosslinking of GG and therefore enhancing the mechanical properties of the gel [145]. This theory is based on that the GG is more stable [41] than gelatin so when gelaCDH degrades the GGox might have stayed and therefore the sample could have been more stable.

The thicknesses, areas, and volumes of fibrin samples with Collagenase Inhibitor I decreased immediately while samples with aprotinin, alone or in mixture with Collagenase Inhibitor I, kept their values much better, but the areas and volumes still degraded almost completely in the end of culturing period. Acellular control of fibrin stayed stable during the 10-day cultivation period indicating that the decrease in thicknesses, areas, and volumes have been due to the actions of cells embedded in the gel. In addition, the curves indicate that aprotinin is the key player when preventing the degradation of the fibrin gel. Aprotinin is commonly used in cell culturing applications

with fibrin hydrogel to prevent the degradation of the gel [22]. This study also shows that the aprotinin prevents the degradation of the fibrin hydrogel.

Fibrin is naturally degraded by proteases, such as plasmin and MMPs [23]. Therefore, there could be chance that Collagenase Inhibitor I could also prevent the degradation of the fibrin gel. Samples where Collagenase Inhibitor I was used together with aprotinin showed that the degradation was slower compared to the samples where only aprotinin was used. Even though the mixture of these two inhibitors slowed the degradation, it did not prevent it totally. This could be due to so small concentration of used Collagenase Inhibitor I.

The concentration of used Collagenase Inhibitor I was 2.23×10^{-11} g/ml \approx 0.0497 nM even though literature [146] generally proposed to use 5-10x IC_{50} value which in this case would have been 5-10 μ M. The IC_{50} value is a concentration value which is needed to produce 50 % inhibition. According to literature, 5-10 times higher concentration compared to IC_{50} value should be used to maximally inhibit the enzyme activity. [146] The amount used in this study was about 0.00005 times IC_{50} value which is super small concentration compared to the recommended value. The used concentration was obtained due to calculation error and therefore in the future when this inhibitor is used, the proper concentration generally proposed by literature should be tested and used.

TeloCol[®] was also part of the experiments in the beginning, it was dropped out from the inhibitory tests and further experiments because the cells were not active in the gel. This can be seen in microscope images where the cells did not elongate but stayed as dots, as well as in size measurements since thicknesses, areas, and volumes of the samples did not change that much during the cultivation. Therefore, the gel would not need any inhibitors and further experiments were not done. However, the values of thickness, area and volume increased in the end which could indicate that the cells could have produced their own ECM. The increase in size is most probably due to the cells producing ECM because the values of acellular control did not increase. In addition, the increase in size happened in the end of cultivation which was also seen in case of VitroCol[®]. Nonetheless, the TeloCol[®] hydrogel have shown promising results in other studies [147] and therefore, in the future, some other protein concentration could be tested.

The size changes of the samples were studied but the reason for size change is still unclear. In cases where inhibitors prevented the decrease in size, the size change was most probably due to degradation caused by cells secreting proteases. However, the size change can also be due to changes in crosslinks and 3D network instead of

degradation where polymer chains break. Therefore, more studies are needed in the future to find out the cause of size changes and whether the size change is due to degradation (breaking polymer chains) or shrinking/swelling (changes in crosslinks and 3D network).

Even though variation and human error was present in this new method to measure the size changes of the samples during cultivation, the results might be closer to the real situation compared to the other methods used to study size change of the hydrogels. Traditional way to measure size changes of the hydrogel samples is to remove the sample from the mold, remove excess liquid from its surfaces, weigh it, and measure its diameter and thickness, for example, with vernier caliper [47]. This measuring method has also few problems. Firstly, the sample can be damaged when demolding and handling it and therefore the same sample may not be used in multiple timepoints which may cause variation between the results when the same sample is not used. In addition, the measurements are also done manually which may cause variation and error to the results. Compared to this traditional method, the new method created in this study is better because it allows to measure the same samples in multiple timepoints without damaging the samples. In addition, even though both methods have error in them, the error is probably smaller in this new method, since the measurements are done with microscope and computer software where the values are more exact compared, for example, to vernier caliper. Furthermore, when the measurements with microscope and Fiji/ImageJ are done always in the same way by same person, and when percentage values are used, the human error in the values should not be that severe.

Other methods to study the degradation of the hydrogels have also been developed. Boucard et al. (2022) measured the degradation of fibrin based hydrogel cultured with fibroblast by measuring white light diffusion through the sample [46]. The setup needed LED light source and a digital microscope. The results were presented as percentages and they used freshly casted and crosslinked hydrogel without cells to mark 0 % degradation and pure culture medium to mark 100 % degradation. [46] This method would give more exact values concerning the degradation of the hydrogels, but it does not give any values or estimations of size changes of the samples. In addition, the measurement setup would need the LED light source and detector for the transmitted light. In the future, this kind of method would be good to add to the measurements to be able to study not only the size change but also the degradation of the hydrogels.

6.1.2 Cellular viability, morphology, and alignment in static condition on well plate

Fibroblasts' morphology in this study is similar to the morphology obtained in previous study [148]. In that study, the cultivation time was shorter and the degradation of the fibrin hydrogel was observed after 24 h and the degradation was greater with higher cell concentration [148]. The degradation affected also to the cells' alignment which can also be seen in this study. When the hydrogel degrades, the cells lose their supporting 3D scaffolds which lead to 2D cell culturing conditions on the bottom of the well.

It has been reported that proliferation and grow rate of fibroblasts in collagen hydrogel are slower compared to fibroblasts seeded on plastic. This was most probably due to cells arresting in G0/1 phase of cell cycle. [73] This difference in proliferation rate of fibroblasts between collagen and fibrin hydrogels can be seen in this study. Fibroblasts embedded in fibrin are more elongated and proliferated compared to collagen samples.

Collagen I (rat tail) samples had only a few elongated cells which indicates that the cells have not proliferated as they have done, for example, in fibrin hydrogel. These observations suggest that the cells have not been so active in the cultivation and therefore they may not have liked the environment. This can be due to wrong pH or protein concentration of the hydrogel. However, some of the cells in VitroCol® samples were elongated nicely which indicates that the cells have been active. Furthermore, according to the results, the use of inhibitors in samples containing either one of the collagens (rat tail or VitroCol®), influenced the elongation of the cells because the cells in these samples looked better and the cells were more extended compared to the control samples without inhibitors. Especially, samples where Collagenase Inhibitor I was used, the cells showed the best outcome.

The viability, morphology and alignment of the fibroblasts in gelaGG is similar compared to previous study [39] done with the same materials and cells but with different culture medium. However, the cells in gelaGG samples where aprotinin was used alone or in mixture with Collagenase Inhibitor I are more elongated which indicates that aprotinin supports the cell activity.

The difference in cell morphology between the different hydrogels may be due to gels being either relaxed or mechanically loaded. Relaxed hydrogels are free to contract while mechanically loaded hydrogels are anchored and thus tension is formed when they try to contract. It has been reported that the cells in different conditions have different morphology. In relaxed hydrogels, the fibroblasts are nonproliferative and have dendritic

morphology while in loaded hydrogels, the cells are proliferative and form bipolar extension. [73] Due to this and according to the results, the different collagen I gels (rat tail, VitroCol[®], TeloCol[®]) would probably be relaxed hydrogels whereas fibrin seem to be more mechanically loaded and GelaGG is somewhere between. This grouping is based on the cells' morphology and proliferation state.

According to the results seen in chapter 5.1, the best inhibitor hydrogel combinations were observed. Fibrin would be most suitable to be used with aprotinin but also the mixture containing both aprotinin and Collagenase Inhibitor I is worth to test further. Both collagen I (rat tail) and VitroCol[®] samples seem to have best outcome when they are used together with Collagenase Inhibitor I. GelaGG samples looked the best when they were used with aprotinin but because the results were similar when the mixture of aprotinin and Collagenase Inhibitor I was used, the mixture is used in the further experiments of this thesis. In addition, the mixture was chosen for further applications because the hydrogel contains gelatin which is a form of collagen so the Collagenase Inhibitor I could also have an effect on the prevention of the degradation of the hydrogel. As said before, TeloCol[®] did not show any good outcomes so it will not be used in further experiments of this thesis.

6.2 3D vascular network formation in dynamic condition on-chip

Vascular network formed into fibrin hydrogel looked the most mature with interconnected vascular structures and supporting stromal cells that aligned the formed vessels. They formed vessel network in both conditions when aprotinin was used alone or when it was used together with Collagenase Inhibitor I. However, the morphology of the formed vessels differs between these two conditions. The formed vessels are larger in chips where both inhibitors were used compared to the golden standard chip created in our research group [28]. This could mean that by using different inhibitors the morphology of the vessels could be adjusted but more studies are needed to confirm that. However, the idea is to form microvessels or capillaries so when the vessels are thicker or larger, it should be confirmed whether the vascular diameter is comparable to *in vivo* capillaries (8-10 μm) or do they mimic bigger vessels.

The fibrin has shown to be the golden standard in these vascularization models maybe due to its native location in the human body being in the vascular network. Aprotinin have shown to prevent the degradation of fibrin hydrogels and it have become norm to be used with fibrin in cell culture applications. The idea of mixing the two inhibitors was to

test if Collagenase Inhibitor I would also have some kind of effect on the degradation of fibrin hydrogel. As a result, the gel did not degrade visually but also the formed vessels were a bit larger compared to the vessels formed in the samples where only aprotinin was used. The concentration of used Collagenase Inhibitor I were so small that it may not have had any effect on those morphological changes. On the other hand, it could be possible that the Collagenase Inhibitor I disturbed the cells' natural ability to modify the surrounding matrix and therefore the tip cells may not had been able to extend and form the new vessels as they are used to. More studies are needed to confirm the potential of using both inhibitors with fibrin hydrogel.

The vessel formation in collagen I (rat tail) samples looked promising in the beginning, but gel detached from the edges of the chip and the cells lost their 3D support. This can be seen in the samples without the use of inhibitors since the cells are no longer spread around the whole chip at day 7 like they were at day 3. Instead the cells are located in the middle of the channel and more closely to each other. In addition, they have lost the vessel-like structures and these structures have degraded into cell aggregates. However, when the Collagenase Inhibitor I was used, the gel stayed more intact which allowed the formation of the vessel-like structures. In addition, the samples with the inhibitor looked better, the vascularization was improved, and the gel did not degrade visually during the experiment. Therefore, it could be said that the use of inhibitor improved the vascular formation while also prevented the degradation of the hydrogel. However, the vessels' morphology does not look the same as in the golden standard, fibrin, but it looks still promising compared to other hydrogel conditions tested in this study. The vascular network looked the best at day 7 after which the vessel-like structures started to degrade in those collagen I (rat tail) hydrogels where Collagenase Inhibitor I was used.

VitroCol® (human collagen I) samples looked promising in supporting vessel formation when the inhibitor was not used. Even though the vessels' morphology was not comparable to the vessels formed in fibrin hydrogel, they still formed some kind of vessel-like structures. In those samples, the vessel formation was still ongoing at day 10 so maybe with longer cultivation period the vessels could have improved more mature-like structures. However, in VitroCol® samples where Collagenase Inhibitor I was used, the gel could not endure dynamic condition with fluidic flow, that is addition of the culture medium to the medium channels. The hydrogel leaking or collapsing was detected immediately after adding the medium. This can also be seen later in the cultivation since cells were located in the middle part of the chip, close to each other. Since the hydrogel

could not stand the force caused by adding the medium, the gel could not provide the 3D support for the cells so no vessel-like structures can be found. In the experiment where the inhibitor was used, vascularization did not happen but pericytes were spread nicely meaning that the support provided by the hydrogel was enough for pericytes to elongate but not enough for endothelial cells to form vessel-like structures.

Even though, the VitroCol[®] hydrogel in inhibitor experiments did not fill the whole gel channel at day 3, it can be seen from the images that the size of the gel increases during cultivation which could be due to cells producing more ECM. The same increase in size was also seen in VitroCol[®] curves in static well plate experiments.

In the experiment where inhibitors were used, the gelation time of VitroCol[®] could have been longer to prevent the gel from leaking or collapsing when adding the medium but cannot be sure why the gel could not stand the adding medium in all tested experiments. Maybe the pH of the gel was different between the two experiments. The pH was measured with both phenol red pH indicator and pH indicator paper but still there could have been some difference which could have affected the gelation. All in all, more studies need to be done to see the full potential of VitroCol[®] hydrogel.

GelaGG composed of gelaCDH and GGox was the only in-house made hydrogel in the study. The vascular formation in gelaGG was poor. Only a few vessel-like structures could be found but they did not form any kind of network. In addition, some of the cells escaped from the gel channel to the medium channel so only a few cells remained in gel channel embedded in the gelaGG hydrogel. Even though the gelaGG did not support the vessel formation, it was possible to inject the hydrogel into the chip without gel leaking to the medium channels and therefore not blocking them. This was a huge achievement since the in-house made gelaGG have not been used on a microfluidic chip successfully before.

Commercial VitroGel[®] hydrogel with unknown composition could not endure in dynamic condition and adding the medium to the medium channels, so it leaked or collapsed immediately after adding the medium. Therefore, there is not much gel left even at day 3 so the cells did not have proper 3D environment and support from the gel. Without the support provided by the hydrogel, the cells could not form any vessel-like structures. VitroGel[®] could not stand the pressure of the medium flow and there were only little pieces of the gel left after 10 days. There was not visible difference between the samples with and without the use of inhibitors probably due to the hydrogel got broken already in

the beginning when the medium was added meaning that the cells did not have 3D support almost at all.

This commercial hydrogel, VitroGel[®], has not been used in a microfluidic chip before, but it had shown promising results in stable cultures on 3D [141] so therefore it was chosen to be tested on a microfluidic chip. The gelation method of the hydrogel was not clear since the gel was just mixed with medium and cells and left in the laminar for 15 minutes. Therefore, the gelation could not be based on temperature or chemical components. After that time, the gel had not been gelatinized properly based on visual observations, so the chips were transferred into the incubator (+ 37°C) to ensure the gelation, but it did not help either. Overall, it was possible to inject the VitroGel[®] into the chip but before adding the medium, the gelation should be somehow ensured in the future experiments.

VitroGel[®] has been used in multiple studies and few of them included vascularization [149–151]. In these studies, the VitroGel[®] induced the cell proliferation, differentiation, and self-assembly [149,150]. However, in these vascularization studies [149–151] the VitroGel[®] was not used alone but in mixture with other hydrogels like collagen I. Therefore, the VitroGel[®] could and should be used together with other hydrogels such as collagen I in the future studies. However, mixing this material with other hydrogels may not eliminate the problems faced with dynamic culture conditions but it should be tested.

The perfusability of the vessels were not detected but it could be a good parameter to test in the further studies. However, vessel area (%) and total vessel length (mm) were analyzed from cropped tile scan images by using AngioTool. According to these results, the most extensive vascular network is obtained at day 7. Vascular network starts to degrade already at day 10 since both vessel area and total vessel length values are decreasing.

When comparing fibrin samples' values of vessel area and total vessel length when only aprotinin or both aprotinin and Collagenase Inhibitor I was used, the values do not differ that much. Fibrin samples with aprotinin seem to have higher values in both analyzed parameters (vessel area, and total vessel length) most of the time and both values stayed quite stable through the 10-day cultivation period. However, when both inhibitors were used, the total vessel length seem to drop quite drastically in the end. This could mean that the vessel structures, formed in samples where both inhibitors are used, were not as stable as the vessels formed in fibrin samples where only aprotinin was used. The instability could be due to the use of both inhibitors which may have inhibited the ECM

degradation too much so that the cells could not have functioned normally. However, the used Collagenase Inhibitor I concentration was so small that it is unlikely that the degradation could have been inhibited too much.

The use of Collagenase Inhibitor I seems to influence the vascularization in both collagen I (rat tail and VitroCol®) samples. This is because the samples with Collagenase Inhibitor I has higher values in vessel area and total vessel length than the control sample without inhibitors in almost every timepoint. At day 7 the difference between VitroCol® samples with or without inhibitor in both analyzed parameters is even considered significant based on statistical analysis. However, the statistical analysis is not so reliable since the sample size was only three samples. In addition, the AngioTool recognized cells close to each other as vessels even though no vessel-like structures could be visually found VitroCol® samples with Collagenase Inhibitor I.

The golden standard fibrin seems to have significantly different vessel area compared to almost every other sample and every time point. However, in total vessel length it has significantly different values only at day 3, after which the difference is no longer significant with other materials and conditions. This may be due to the software's analysis not being so exact and because it considers cells close to each other as vessels even though vessel-like structures are not seen in the images. Nevertheless, the golden standard has most stable vessel network regardless of the way to analyze the morphology of the vessels.

Both gelaGG and VitroGel® have distinctly lower values in every timepoint and in both parameters compared to other samples. This supports the observations done before meaning that these materials are not suitable for this kind of application.

Gering et al. (2022) studied vascularization in gelaGG on static well plate [40]. They used ASCs instead of BMSC, the used gelaGG concentration was 40-40 mg/ml while in this study it was 60-40 mg/ml and lastly, they used static culturing conditions while in this study the conditions were dynamic. Despite all these differences, they obtained quite similar vascular network compared to this study but the pericytes were aligned more nicely forming denser network. Their results of HUVEC coverage are comparable with results of vessel area studied in this study. They obtained smaller values of coverage compared to this study. [40] This difference could be due to different culturing conditions, static vs. dynamic, or use of different pericytes.

Andrée et al. (2019) formed 3D vascular network on small intestinal submucosa by using HUVECs and ASCs in either human collagen I or in Matrigel-collagen I (rat tail) mixture

[152]. With human collagen I samples, they used serum free medium. The vascular network formed in their human collagen I samples is much denser and more mature compared to the vascularization formed in VitroCol[®] samples of this study. The vascularization formed in the Matrigel-collagen I (rat tail) samples is also much denser and more mature compared to vascular network formed in collagen I (rat tail) samples, with or without the Collagenase Inhibitor I, of this study. The HUVECs formed intact vascular network with perfusable vessels in both of their samples. [152] The differences between their results and results of this study may be due to use of different pericytes, medium or culture conditions since they used fixed small intestinal submucosa as culture platform while perfused microfluidic chip was used in this study. They also used smaller cell concentrations and protein concentrations of the hydrogel compared to this study which could also have affected to the results.

Mykuliak and Yrjänäinen et al. (2022) used similar experiment setups than used in this study's control, fibrin, but they did not use aprotinin [28]. When comparing the results between these two studies, the vascular network obtained in their study was denser and they seem to have more cells in their samples compared to samples of this study. In addition, the vasculature area (%) of their samples were also higher compared to the values obtained in this study. The morphology of the vessels formed in their study seem to be somewhere between the vasculature formed in fibrin samples where aprotinin was used alone or in a mixture with Collagenase Inhibitor I in this study. The vessels in their study seem to be larger compared to this study's fibrin samples where aprotinin was used, but still smaller compared to fibrin samples with mixture of inhibitors. The vessels formed in the samples of this study, where aprotinin was used, appear similar than their vasculature formed in samples where ASCs were used instead of BMSCs. In addition, the values of vessel or vasculature area and length obtained in this study are similar to the ones obtained in their study in samples where ASCs were used. [28] This difference in vessel morphology could be due to the use of inhibitors, but different cell lines and timing could also affect to the results.

Isosaari et al. (2023) also used similar experiment setups in their neurovascular and vascular studies but the used hydrogel was fibrin-collagen I [43]. When comparing the results of their vascular cocultures to the results of this study, the BMSC-HUVEC coculture seem to be similar with the collagen I (rat tail) samples with Collagenase Inhibitor I of this study. In addition, the vascular network in their neurovascular multiculture, looks like the fibrin sample, of this study where aprotinin was used. Furthermore, the vascular coculture where ASCs were used look similar to VitroCol[®]

samples of this study, where inhibitors were not used. [43] The similarity between these samples could be because mixture of these materials was used in their study. They also reported that the neurons supported the vascularization [43]. The morphological differences between the vessels formed in different hydrogels and inhibitor conditions are probably due to the differences in their environments. An interesting thing is that the vascular network formed in golden standard, fibrin, used in this study is similar to the vascularization formed in fibrin-collagen I hydrogel with the support of neurons. This could indicate that the support given by neurons is similar to the influence lost when the environment is composed of both fibrin and collagen I, compared to vascularization in only fibrin hydrogel.

The difference between vascular network formed in fibrin or collagen I hydrogel is noticeable. However, both these materials are naturally located in close to the vascular network which could indicate that they would equally support the vascularization. However, these materials are located a bit differently, fibrin is located inside the bloodstream in sites of injuries while collagen I is found from the vessel structure and outside of the vessels. This difference in location could be the reason for different supporting ability of these hydrogels.

Inhibitors' effects on vascular formation should be studied more in the future. Here, widely used aprotinin and novel Collagenase Inhibitor I were used in Vascularization-on-a-Chip models. Previous study done by Shang et al. (2022) proved that either one of these inhibitors used in this study should not disrupt the vascular formation [56]. However, they used different concentration of aprotinin and different inhibitor and inhibitor concentration for MMP-1 compared to the concentrations used in this study. Furthermore, they used HUVEC monoculture and human lung fibroblasts together with HUVECs with 1:7 cell ratio embedded in fibrin hydrogel meaning that also the culturing parameters differed. The most of the inhibitory tests were done with HUVEC monocultures. [56] When comparing the results between this study and the study done by Shang et al. (2022), the HUVECs in their microfluidic device with monoculture of HUVECs, where aprotinin were used, were more branched and formed denser network [56]. Texas Red Dextran was used in that study to analyze the permeability of the formed vessels. Based on that, the perfused areas were large in their samples which could indicate that also the vessels were large and thick. The MMP-1 inhibition also resulted large perfusable vessels but the HUVECs were not so branched and proliferated compared to samples where aprotinin was used. [56] That could also be seen in this study where mixture of the inhibitors was used. The endothelial cells formed thicker

vessels and the network were not so dense compared to the control sample where only aprotinin was used with fibrin. In addition, the perfusability was not studied in this study, but in the future experiments, it should be included.

In this study, the used aprotinin concentration was 50 $\mu\text{m}/\text{ml}$ based on the protocols used in our research group. However, the concentration used in other studies was usually smaller. For example, Jockenhoevel et al. (2001) and Ahmed et al. (2007) used 20 $\mu\text{g}/\text{ml}$ aprotinin concentrations in their studies [27,153]. Isosaari et al. (2023) used 40 $\mu\text{g}/\text{ml}$ aprotinin concentration in their neurovascular and vascular studies with fibrin-collagen I hydrogel [43]. Furthermore, Boucard et al. (2022) used both 20 $\mu\text{g}/\text{ml}$ and 40 $\mu\text{g}/\text{ml}$ in their study to test the dose-effect of aprotinin on fibrin degradation [46]. The concentration of the used aprotinin may affect the vascularization or its morphology. This is due to inhibitors inhibiting the enzymes that modify the environment surrounding the cultured cells. Therefore, when the enzymes activity is inhibited, they cannot modify the environment of the cells which may disturb the cells natural functions. It has also been studied that a few MMPs have significant role in angiogenesis [11,12,52], especially the inhibition of MMP-2, disrupts the vascular formation [56]. Therefore, the amount of inhibition may have a significant effect on the functions of the cells. This means that the balance between preventing the degradation of the supporting hydrogel and disrupting the cell functionality must be found to be able to form better cell models. As a result, more studies related to the use of inhibitors are highly needed.

6.3 General sources of error

The values of thickness, area and volume are indicative and not absolute because the measurements are done manually. The values of thickness have been obtained by focusing manually to the bottom and top of the samples, and the values of area have been measured from tile scan images by using Fiji/ImageJ and by drawing the area manually. Therefore, there might be a lot of variation between the results. Despite all this, these results give approximation how the hydrogels behave during the culturing period, and they show that the gels' sizes change and decrease during cultivation in the presence of cells. In addition, the size of acellular control of gelaGG changed and decreased without the presence of cells. In the future experiments, the method how to measure the size changes should be improved.

Areas of gelaGG were hard to measure due to the loss of the thickness, and thus it was difficult to see whether there was gel left or not. Therefore, there is quite dramatic drops in the areas in cellular control samples without inhibitors and samples with use of

Collagenase Inhibitor I. This could have also added error to the results because the area measurements were done manually so when the edge of the sample was not clear, the measurements could have differed a lot from the real values.

The values of hydrogel size changes have variation which could be due to the measurement error or the fact that samples without inhibitors were cultivated at different time compared to samples with inhibitors. In addition, the area values of collagen I (rat tail), VitroCol[®] (human collagen I) and TeloCol[®] without inhibitors on day 5 differ a lot from others because there were problems with the microscope and forming tile scans so the well was not round in those images which could have affected the measured values.

Images used in the results (Figure 17, Figure 18, Figure 19, Figure 20, and Figure 21) are presenting the best parts of the samples. Therefore, they are not representative images of the whole samples but rather showing the difference between best parts of the samples. Some of the samples were poor, had really few cells, or the cells were not proliferated or elongated. Therefore, the used images show the best parts of the samples where some of the cells and their behavior can be detected. For example, the TeloCol[®] samples had only a couple elongated cells and overall, all of the samples seemed to have quite few cells. However, in Figure 17 and Figure 18, the TeloCol[®] sample do not differ so much from the others but the real situation was poorer.

The difference between samples with or without use of inhibitors may be due to being cultured at different times so there might have been differences between the conditions. In addition, there might have been difference in pH between sample conditions since the gels were made separately and the pH of both collagen I (rat tail and VitroCol[®]) hydrogels was measured only with phenol red indicator in well plate experiments which is not the most accurate method. Furthermore, the gels are natural so there might also be some variation between the dissolved hydrogels. In addition, the number of cells in samples are not exact and the cells behavior in samples are not constant meaning that there are multiple reasons why the samples can act differently at different times. This is a common problem with biological samples.

In AngioTool results, the number of samples could affect the reliability of the graph which is presented as average \pm standard deviation. There were only 3 parallel samples so the average \pm standard deviation can differ a lot from the actual deviation of the results. In addition, because of the small sample size, the statistical analysis may not be so reliable. Furthermore, AngioTool software recognized cells close to each other as vessels even though vessel-like structures could not be observed visually. Therefore, the results of

AngioTool may not be so reliable and parameters, used in the analysis, should be adjusted more deeply in the future experiments.

6.4 Future perspectives

As mentioned before, more studies are needed to reveal the full potential of tissue engineering in this area. According to this study, things that could be considered in the future are:

- Adding more analysis like reverse transcription-quantitative polymerase chain reaction (RT-qPCR) to study cellular functions and composition of ECM matrix after cultivation.
- Adjusting AngioTool parameters more deeply so that it would recognize vessel-like structures better.
- Analyzing the MMPs that each used cell type express and screening specific inhibitors for each.
- Finding suitable concentrations for inhibitors.
- Improve the method to measure size of the samples. Including methods and analyses to study the reason for size change: degradation, swelling, shrinking, or something else.
- Improve the staining protocol of 3D well plate samples. DAPI could be added together with secondary antibodies and phalloidin with overnight incubation as done in chip staining protocol. With this current protocol, the incubation time of DAPI is quite short which is shown as weaker signal.
- Test VitroCol[®] again with inhibitors. Also, longer cultivation period could be tried to see whether the formed vascular network would mature later.
- Try different hydrogel concentrations and mixtures like fibrin-collagen I mixture.
- Try mixing VitroGel[®] with some other hydrogel like fibrin and using the mixture in chip experiments.

7. CONCLUSIONS

This thesis consists of two experiment series: cell culture in 3D on well plate with static condition and chip experiment with dynamic cell culture environment. In well plate experiment, a method to analyze hydrogel shrinking or size change by using fluorescent beads and imaging was successfully created. Therefore, the size change of the hydrogel can be measured. In addition, hydrogels showed varying characteristics in both sample size changes and elongation and spreading of the cells. Suitable inhibitor cocktails to prevent the degradation of the tested hydrogels were found. Furthermore, all tested hydrogels and inhibitor conditions supported cell viability and partial elongation of cells according to Live/Dead and cytochemical staining.

In chip experiments, the used inhibitors did not prevent the vascularization. The vascularization in fibrin, with aprotinin, appeared to be more mature compared to other hydrogels. However, the use of aprotinin together with Collagenase Inhibitor I in fibrin samples looked promising but more studies need to be done to unlock the whole potential of the use of these inhibitors. Overall, no better hydrogel option for vascularization model were found.

From other materials tested in this study, VitroCol[®] looked promising in well plate experiments and in the first chip experiment, but more research is needed to find out its true potential to be used on a chip with Collagenase Inhibitor I. Collagen I (rat tail) looked second best in both well plate and chip experiments especially when Collagenase Inhibitor I was used. However, the concentration of used Collagenase Inhibitor I was so small that further studies are needed to reveal its full potential.

GelaGG (gelatin-gellan gum), TeloCol[®] and VitroGel[®] were also used in this study. From those materials, the gelaGG looked most promising but its potential did not reach the collagen I (rat tail), VitroCol[®] or fibrin's potential. TeloCol[®] did not support cellular organization in this study even though promising studies are done with different cell types. Therefore, maybe some other concentration could have been more suitable for the fibroblasts used in this study. VitroGel[®] cannot be used with microfluidic chip before improved formulation or gelation. The gelation of the gel was not strong enough to

endure the forces caused by adding the medium. Therefore, some improvements are needed before it can be used in such applications.

Overall, the size change of the well plate samples can be measured during cultivation period and the change can be influenced by using protease inhibitors. Better material options for Vascularization-on-a-Chip model were not found but collagen I, both rat tail and human (VitroCol®), has potential to be used in that kind of application. Maybe by mixing collagen I with fibrin and by using both inhibitors, aprotinin and Collagenase Inhibitor I, better Vascularization-on-a-Chip model could be created but further studies are needed to confirm that. In addition, further studies concerning the use of inhibitors are needed to be able to reveal their full potential and therefore to be able to develop better models for *in vivo*-like studies.

REFERENCES

1. Langer R, Vacanti JP. Tissue Engineering. *Sci Am Assoc Adv Sci*. 1993;260(5110):920–6.
2. Ghasemi-Mobarakeh L, Kolahreez D, Ramakrishna S, Williams D. Key terminology in biomaterials and biocompatibility. *Curr Opin Biomed Eng*. 2019 Jun 1;10:45–50.
3. Drury JL, Mooney DJ. Hydrogels for tissue engineering: scaffold design variables and applications. *Biomaterials*. 2003 Nov 1;24(24):4337–51.
4. Shamloo A, Heilshorn SC. Matrix density mediates polarization and lumen formation of endothelial sprouts in VEGF gradients. *Lab Chip*. 2010;10(22):3061–8.
5. Hafner J, Grijalva D, Ludwig-Husemann A, Bertels S, Bensinger L, Raic A, et al. Monitoring matrix remodeling in the cellular microenvironment using microrheology for complex cellular systems. *Acta Biomater*. 2020;111:254–66.
6. Li K, Tay FR, Yiu CKY. The past, present and future perspectives of matrix metalloproteinase inhibitors. *Pharmacol Ther Oxf*. 2020;207:107465–107465.
7. Gaffney J, Solomonov I, Zehorai E, Sagi I. Multilevel regulation of matrix metalloproteinases in tissue homeostasis indicates their molecular specificity in vivo. *Matrix Biol*. 2015 May 1;44–46:191–9.
8. Djuric T. Overview of MMP Biology and Gene Associations in Human Diseases. In *IntechOpen*; 2017.
9. Henderson AR, Choi H, Lee E. Blood and Lymphatic Vasculatures On-Chip Platforms and Their Applications for Organ-Specific In Vitro Modeling. *Micromachines Basel*. 2020;11(2):147-.
10. Talman V, Kivelä R. Cardiomyocyte-Endothelial Cell Interactions in Cardiac Remodeling and Regeneration. *Front Cardiovasc Med*. 2018;5:101-.
11. Raffetto JD, Khalil RA. Matrix Metalloproteinases and their Inhibitors in Vascular Remodeling and Vascular Disease. *Biochem Pharmacol*. 2008 Jan 15;75(2):346–59.
12. Wang X, Khalil RA. Matrix Metalloproteinases, Vascular Remodeling, and Vascular Disease. *Adv Pharmacol San Diego Calif*. 2018;81:241–330.
13. Kim S, Kim W, Lim S, Jeon JS. Vasculature-On-A-Chip for In Vitro Disease Models. *Bioengineering*. 2017 Jan 24;4(1):8.
14. Osaki T, Sivathanu V, Kamm RD. Vascularized microfluidic organ-chips for drug screening, disease models and tissue engineering. *Curr Opin Biotechnol*. 2018 Aug;52:116–23.
15. Bhatt A, Dhiman N, Giri PS, Kasinathan GN, Pati F, Rath SN. Biocompatibility-on-a-chip: Characterization and evaluation of decellularized tendon extracellular matrix (tdECM) hydrogel for 3D stem cell culture in a microfluidic device. *Int J Biol Macromol*. 2022 Jul 31;213:768–79.
16. Figure 1. Structure of hydrogel at molecular level. [Internet]. ResearchGate. [cited 2024 Mar 14]. Available from: https://www.researchgate.net/figure/Structure-of-hydrogel-at-molecular-level_fig1_340479680
17. Sung JH, Shuler ML. A micro cell culture analog (microCCA) with 3-D hydrogel culture of multiple cell lines to assess metabolism-dependent cytotoxicity of anti-cancer drugs. *Lab Chip*. 2009;9(10):1385–94.

18. Haase K, Kamm RD. Advances in on-chip vascularization. *Regen Med.* 2017 Apr;12(3):285–302.
19. Adamiak K, Sionkowska A. Current methods of collagen cross-linking: Review. *Int J Biol Macromol.* 2020 Oct 15;161:550–60.
20. Parry DA, Squire JM. *Fibrous Proteins: Structures and Mechanisms.* 1st ed. 2017. Cham: Springer International Publishing; 2017. viii+629. (Subcellular Biochemistry, 82).
21. Ahmed TAE, Dare EV, Hincke M. Fibrin: A Versatile Scaffold for Tissue Engineering Applications. *Tissue Eng Part B Rev.* 2008 Jun;14(2):199–215.
22. Lorentz KM, Kontos S, Frey P, Hubbell JA. Engineered aprotinin for improved stability of fibrin biomaterials. *Biomaterials.* 2011;32(2):430–8.
23. Lee F, Kurisawa M. Formation and stability of interpenetrating polymer network hydrogels consisting of fibrin and hyaluronic acid for tissue engineering. *Acta Biomater.* 2013;9(2):5143–52.
24. Liu H, Kitano S, Irie S, Levato R, Matsusaki M. Collagen Microfibers Induce Blood Capillary Orientation and Open Vascular Lumen. *Adv Biosyst.* 2020;4(5):2000038.
25. Syedain ZH, Bjork J, Sando L, Tranquillo RT. Controlled compaction with ruthenium-catalyzed photochemical cross-linking of fibrin-based engineered connective tissue. *Biomaterials.* 2009;30(35):6695–701.
26. Rowe SL, Stegemann JP. Interpenetrating Collagen-Fibrin Composite Matrices with Varying Protein Contents and Ratios. *Biomacromolecules.* 2006;7(11):2942–8.
27. Ahmed TAE, Griffith M, Hincke M. Characterization and Inhibition of Fibrin Hydrogel-Degrading Enzymes During Development of Tissue Engineering Scaffolds. *Tissue Eng.* 2007 Jul;13(7):1469–77.
28. Mykuliak A, Yrjänäinen A, Mäki AJ, Gebraad A, Lampela E, Kääriäinen M, et al. Vasculogenic Potency of Bone Marrow- and Adipose Tissue-Derived Mesenchymal Stem/Stromal Cells Results in Differing Vascular Network Phenotypes in a Microfluidic Chip. *Front Bioeng Biotechnol.* 2022;
29. Ramshaw JAM. Biomedical applications of collagens. *J Biomed Mater Res B Appl Biomater.* How to cite this article: Ramshaw JAM. 2016. Biomedical applications of collagens. *J Biomed Mater Res Part B* 2016;104B:665-675. 2016;104(4):665–75.
30. Ricard-Blum S. The Collagen Family. *Cold Spring Harb Perspect Biol.* 2011 Jan;3(1):a004978.
31. Gordon MK, Hahn RA. Collagens. *Cell Tissue Res.* 2010 Jan 1;339(1):247–57.
32. Shoulders MD, Raines RT. Collagen structure and stability. *Annu Rev Biochem.* 2009;78(1):929–58.
33. Sobczak-Kupiec A, Drabczyk A, Florkiewicz W, Głąb M, Kudłacik-Kramarczyk S, Słota D, et al. Review of the Applications of Biomedical Compositions Containing Hydroxyapatite and Collagen Modified by Bioactive Components. *Materials.* 2021 Jan;14(9):2096.
34. Yang C, Hillas PJ, Báez JA, Nokelainen M, Balan J, Tang J, et al. The application of recombinant human collagen in tissue engineering. *BioDrugs Clin Immunother Biopharm Gene Ther.* 2004;18(2):103–19.
35. Advanced BioMatrix - VitroCol® Solution, 3 mg/ml (human) #5007 [Internet]. [cited 2024 Feb 13]. Available from: <https://advancedbiomatrix.com/vitrocol.html>

36. Advanced BioMatrix - TeloCol®-6 Solution, 6 mg/ml (bovine) #5225 [Internet]. [cited 2024 Feb 13]. Available from: <https://advancedbiomatrix.com/telocol6.html>
37. Maher MK, White JF, Glattauer V, Yue Z, Hughes TC, Ramshaw JAM, et al. Variation in Hydrogel Formation and Network Structure for Telo-, Atelo- and Methacrylated Collagens. *Polymers*. 2022 Apr 27;14(9):1775.
38. Advanced BioMatrix - Telo vs Atelo Collagen [Internet]. [cited 2024 Feb 13]. Available from: <https://advancedbiomatrix.com/telo-vs-atelo-collagen.html>
39. Koivisto JT, Gering C, Karvinen J, Maria Cherian R, Belay B, Hyttinen J, et al. Mechanically Biomimetic Gelatin–Gellan Gum Hydrogels for 3D Culture of Beating Human Cardiomyocytes. *ACS Appl Mater Interfaces*. 2019 Jun 12;11(23):20589–602.
40. Gering C, Parraga Meneses J, Vuorenää H, Botero L, Miettinen S, Kellomäki M. Bioactivated gellan gum hydrogels affect cellular rearrangement and cell response in vascular co-culture and subcutaneous implant models. *Biomater Adv* [Internet]. 2022 Nov 8 [cited 2023 Jul 13]; Available from: <https://trepo.tuni.fi/handle/10024/143757>
41. Gering C. Design Strategies for Polysaccharide Hydrogels Used in Soft Tissue Engineering : Modification, Testing and Applications of Gellan Gum [Internet]. Tampere University; 2023 [cited 2023 Jul 13]. Available from: <https://trepo.tuni.fi/handle/10024/147595>
42. Isoaari L. Optimizing hydrogels for neuro-vascular co-culture studies in microfluidic devices. 2021.
43. Isoaari L, Vuorenää H, Yrjänäinen A, Kapucu FE, Kelloniemi M, Pakarinen TK, et al. Simultaneous induction of vasculature and neuronal network formation on a chip reveals a dynamic interrelationship between cell types. *Cell Commun Signal CCS*. 2023 Jun 14;21(1):132.
44. Wang M, Li W, Tang G, Garciamendez-Mijares CE, Zhang YS. Engineering (Bio)Materials through Shrinkage and Expansion. *Adv Healthc Mater*. 2021;10(14):2100380-n/a.
45. Li S, Wang W, Li W, Xie M, Deng C, Sun X, et al. Fabrication of Thermoresponsive Hydrogel Scaffolds with Engineered Microscale Vasculatures. *Adv Funct Mater*. 2021;31(27):2102685-n/a.
46. Boucard E, Vidal L, Coulon F, Mota C, Hascoët JY, Halary F. The degradation of gelatin/alginate/fibrin hydrogels is cell type dependent and can be modulated by targeting fibrinolysis. *Front Bioeng Biotechnol*. 2022;10:920929–920929.
47. Luo X, Liu Y, Pang J, Bi S, Zhou Z, Lu Z, et al. Thermo/photo dual-crosslinking chitosan-gelatin methacrylate hydrogel with controlled shrinking property for contraction fabrication. *Carbohydr Polym*. 2020 May 15;236:116067.
48. Chung T, Han IK, Han J, Ahn K, Kim YS. Fast and Large Shrinking of Thermoresponsive Hydrogels with Phase-Separated Structures. *Gels*. 2021 Feb 16;7(1):18.
49. Nakamura K, Nobutani K, Shimada N, Tabata Y. Gelatin Hydrogel-Fragmented Fibers Suppress Shrinkage of Cell Sheet. *Tissue Eng Part C Methods*. 2020;26(4):216–24.
50. Shotorbani BB, André H, Barzegar A, Zarghami N, Salehi R, Alizadeh E. Cell sheet biofabrication by co-administration of mesenchymal stem cells secretome and vitamin C on thermoresponsive polymer. *J Mater Sci Mater Med*. 2018;29(11):170–17.
51. Takagi S, Ohno M, Ohashi K, Utoh R, Tatsumi K, Okano T. Cell Shape Regulation Based on Hepatocyte Sheet Engineering Technologies. *Cell Transplant*. 2012;21(2–3):411–20.

52. Liu J, Khalil RA. Matrix Metalloproteinase Inhibitors as Investigational and Therapeutic Tools in Unrestrained Tissue Remodeling and Pathological Disorders. *Prog Mol Biol Transl Sci.* 2017;148:355–420.
53. Cruz-Munoz W, Khokha R. The Role of Tissue Inhibitors of Metalloproteinases in Tumorigenesis and Metastasis. *Crit Rev Clin Lab Sci.* 2008 Jun;45(3):291–338.
54. la Rosa CCD, Garza-Veloz I, Cardenas-Vargas E. Biological Activity and Implications of the Metalloproteinases in Diabetic Foot Ulcers. In *IntechOpen*; 2017.
55. Quiding-Järbrink M, Smith DA, Bancroft GJ. Production of Matrix Metalloproteinases in Response to Mycobacterial Infection. *Infect Immun.* 2001 Sep;69(9):5661–70.
56. Zhang S, Wan Z, Pavlou G, Zhong AX, Xu L, Kamm RD. Interstitial Flow Promotes the Formation of Functional Microvascular Networks In Vitro through Upregulation of Matrix Metalloproteinase-2. *Adv Funct Mater.* 2022;32(43):2206767.
57. Lee E, Vaughan DE, Parikh SH, Grodzinsky AJ, Libby P, Lark MW, et al. Regulation of Matrix Metalloproteinases and Plasminogen Activator Inhibitor-1 Synthesis by Plasminogen in Cultured Human Vascular Smooth Muscle Cells. *Circ Res.* 1996 Jan;78(1):44–9.
58. Trivedi A, Noble-Haeusslein LJ, Levine JM, Santucci AD, Reeves TM, Phillips LL. Matrix metalloproteinase signals following neurotrauma are right on cue. *Cell Mol Life Sci.* 2019 Aug;76(16):3141–56.
59. Kalluri R. Basement membranes: structure, assembly and role in tumour angiogenesis. *Nat Rev Cancer.* 2003 Jun;3(6):422–33.
60. WEGNER J. Biochemistry of serine protease inhibitors and their mechanisms of action: A review. *J Extra Corpor Technol.* 2003;35(4):326–38.
61. Alston TA. Aprotinin. *Int Anesthesiol Clin.* 2004;42(4):81–91.
62. Otake S, Okayama T, Obata M, Morikawa T, Hattori S, Hori H, et al. Vertebrate collagenase inhibitor. I. Tripeptidyl hydroxamic acids. *Chem Pharm Bull (Tokyo).* 1990;38(4):1007–11.
63. Bottomley KM, Johnson WH, Walter DS. Matrix Metalloproteinase Inhibitors in Arthritis. *J Enzym Inhib.* 1998;13(2):79–101.
64. Sorsa T, Tjäderhane L, Kontinen YT, Lauhio A, Salo T, Lee H, et al. Matrix metalloproteinases: Contribution to pathogenesis, diagnosis and treatment of periodontal inflammation. *Ann Med.* 2006 Jan 1;38(5):306–21.
65. Park H jin, Zhang Y, Georgescu SP, Johnson KL, Kong D, Galper JB. Human umbilical vein endothelial cells and human dermal microvascular endothelial cells offer new insights into the relationship between lipid metabolism and angiogenesis. *Stem Cell Rev.* 2006 Jun;2(2):93–102.
66. Kocherova I, Bryja A, Mozdziak P, Angelova Volponi A, Dyszkiewicz-Konwińska M, Piotrowska-Kempisty H, et al. Human Umbilical Vein Endothelial Cells (HUVECs) Co-Culture with Osteogenic Cells: From Molecular Communication to Engineering Prevascularised Bone Grafts. *J Clin Med.* 2019 Oct 3;8(10):1602.
67. Dai X, Cai S, Ye Q, Jiang J, Yan X, Xiong X, et al. A novel in vitro angiogenesis model based on a microfluidic device. *Chin Sci Bull.* 2011;56(31):3301–9.
68. Jin K, Ji X, Zhuge Q. Bone marrow stem cell therapy for stroke. 1st ed. 2017. Singapore: Springer Singapore; 2017. xv+332.

69. Li G, Zhang XA, Wang H, Wang X, Meng CL, Chan CY, et al. Erratum to: Comparative Proteomic Analysis of Mesenchymal Stem Cells Derived from Human Bone Marrow, Umbilical Cord and Placenta: Implication in the Migration. In: *Advances in Experimental Medicine and Biology*. New York, NY: Springer New York; 2012. p. E1–E1. (*Advances in Experimental Medicine and Biology*; vol. 720).
70. Fu X, Liu G, Halim A, Ju Y, Luo Q, Song G. Mesenchymal Stem Cell Migration and Tissue Repair. *Cells*. 2019 Jul 28;8(8):784.
71. Abercrombie M. Fibroblasts. *J Clin Pathol Suppl (R Coll Pathol)*. 1978;12:1–6.
72. Sorrell JM, Caplan AI. Chapter 4 Fibroblasts—A Diverse Population at the Center of It All. In: *International Review of Cell and Molecular Biology* [Internet]. Academic Press; 2009 [cited 2024 Feb 19]. p. 161–214. (*International Review of Cell and Molecular Biology*; vol. 276). Available from: <https://www.sciencedirect.com/science/article/pii/S1937644809760046>
73. Woodley JP, Lambert DW, Asencio IO. Understanding Fibroblast Behavior in 3D Biomaterials. *Tissue Eng Part B Rev*. 2022 Jun;28(3):569–78.
74. Buckley CD. Fibroblast cells reveal their ancestry. *Nature*. 2021 May;593(7860):511–2.
75. Healy L, Ruban L. Mouse and Human Fibroblasts. In: Healy L, Ruban L, editors. *Atlas of Human Pluripotent Stem Cells in Culture* [Internet]. Boston, MA: Springer US; 2015 [cited 2024 Feb 19]. p. 3–18. Available from: https://doi.org/10.1007/978-1-4899-7507-2_2
76. Frank Bertoncelej M, Lakota K, editors. *Fibroblasts - Advances in Inflammation, Autoimmunity and Cancer* [Internet]. IntechOpen; 2021 [cited 2024 Feb 20]. (*Biochemistry*; vol. 25). Available from: <https://www.intechopen.com/books/9659>
77. Darby IA, Hewitson TD. Fibroblast Differentiation in Wound Healing and Fibrosis. In: *International Review of Cytology* [Internet]. Academic Press; 2007 [cited 2024 Feb 20]. p. 143–79. Available from: <https://www.sciencedirect.com/science/article/pii/S007476960757004X>
78. WI-38 - CCL-75 | ATCC [Internet]. [cited 2024 Feb 20]. Available from: <https://www.atcc.org/products/ccl-75>
79. Gorvett Z. The controversial cells that saved 10 million lives [Internet]. [cited 2024 Feb 20]. Available from: <https://www.bbc.com/future/article/20201103-the-controversial-cells-that-saved-10-million-lives>
80. Goddard LM, Iruela-Arispe ML. Cellular and molecular regulation of vascular permeability. *Thromb Haemost*. 2013;109(3):407–15.
81. Yang G, Mahadik B, Choi JY, Fisher JP. Vascularization in tissue engineering: fundamentals and state-of-art. *Prog Biomed Eng Bristol Engl*. 2020 Jan;2(1):012002.
82. Ager A. High Endothelial Venules and Other Blood Vessels: Critical Regulators of Lymphoid Organ Development and Function. *Front Immunol*. 2017;8:45–45.
83. Lust ST, Shanahan CM, Shipley RJ, Lamata P, Gentleman E. Design considerations for engineering 3D models to study vascular pathologies in vitro. *Acta Biomater*. 2021 Sep 15;132:114–28.
84. Fig. 1.2 New blood vessel formation occurs via vasculogenesis and... [Internet]. ResearchGate. [cited 2024 Jan 8]. Available from: https://www.researchgate.net/figure/New-blood-vessel-formation-occurs-via-vasculogenesis-and-angiogenesis-Vasculogenesis-is_fig1_298084071

85. Carmeliet P, Jain RK. Angiogenesis in cancer and other diseases. *Nat Lond.* 2000;407(6801):249–57.
86. Song JW, Munn LL. Fluid forces control endothelial sprouting. *Proc Natl Acad Sci - PNAS.* 2011;108(37):15342–7.
87. Farahat WA, Wood LB, Zervantonakis IK, Schor A, Ong S, Neal D, et al. Ensemble analysis of angiogenic growth in three-dimensional microfluidic cell cultures. *PLoS One.* 2012;7(5):e37333–e37333.
88. Nguyen DHT, Stapleton SC, Yang MT, Cha SS, Choi CK, Galie PA, et al. Biomimetic model to reconstitute angiogenic sprouting morphogenesis in vitro. *Proc Natl Acad Sci - PNAS.* 2013;110(17):6712–7.
89. Vickerman V, Kamm RD. Mechanism of a flow-gated angiogenesis switch: early signaling events at cell-matrix and cell-cell junctions. *Integr Biol Camb.* 2012;4(8):863–74.
90. Shamloo A, Ma N, Poo MM, Sohn LL, Heilshorn SC. Endothelial cell polarization and chemotaxis in a microfluidic device. *Lab Chip.* 2008;8(8):1292–9.
91. Camasão DB, Li L, Drouin B, Lau C, Reinhardt DP, Mantovani D. Physiologically relevant platform for an advanced in vitro model of the vascular wall: focus on in situ fabrication and mechanical maturation. *Vitro Models.* 2022;1(2):179–95.
92. Chung S, Sudo R, Mack PJ, Wan CR, Vickerman V, Kamm RD. Cell migration into scaffolds under co-culture conditions in a microfluidic platform. *Lab Chip.* 2009;9(2):269–75.
93. Chen MB, Whisler JA, Jeon JS, Kamm RD. Mechanisms of tumor cell extravasation in an in vitro microvascular network platform. *Integr Biol Camb.* 2013;5(10):1262–71.
94. Jeon JS, Bersini S, Whisler JA, Chen MB, Dubini G, Charest JL, et al. Generation of 3D functional microvascular networks with human mesenchymal stem cells in microfluidic systems. *Integr Biol Camb.* 2014;6(5):555–63.
95. Jusoh N, Oh S, Kim S, Kim J, Jeon NL. Microfluidic vascularized bone tissue model with hydroxyapatite-incorporated extracellular matrix. *Lab Chip.* 2015;15(20):3984–8.
96. Li Y, Hu C, Wang P, Liu Y, Wang L, Pi Q, et al. Indoor nanoscale particulate matter-induced coagulation abnormality based on a human 3D microvascular model on a microfluidic chip. *J Nanobiotechnology.* 2019;17(1):20–20.
97. Guo Z, Yang CT, Maritz MF, Wu H, Wilson P, Warkiani ME, et al. Validation of a Vasculogenesis Microfluidic Model for Radiobiological Studies of the Human Microvasculature. *Adv Mater Technol.* 2019;4(4):1800726-n/a.
98. Sharma D, Ross D, Wang G, Jia W, Kirkpatrick SJ, Zhao F. Upgrading prevascularization in tissue engineering: A review of strategies for promoting highly organized microvascular network formation. *Acta Biomater.* 2019;95:112–30.
99. Wang Y, Huang X, Shen Y, Hang R, Zhang X, Wang Y, et al. Direct writing alginate bioink inside pre-polymers of hydrogels to create patterned vascular networks. *J Mater Sci.* 2019;54(10):7883–92.
100. Bhatia SN, Ingber DE. Microfluidic organs-on-chips. *Nat Biotechnol.* 2014 Aug;32(8):760–72.
101. Ho CT, Lin RZ, Chen RJ, Chin CK, Gong SE, Chang HY, et al. Liver-cell patterning lab chip: mimicking the morphology of liver lobule tissue. *Lab Chip.* 2013;13(18):3578–87.

102. Wang L, Liu W, Wang Y, Wang J chun, Tu Q, Liu R, et al. Construction of oxygen and chemical concentration gradients in a single microfluidic device for studying tumor cell-drug interactions in a dynamic hypoxia microenvironment. *Lab Chip*. 2013;13(4):695–705.
103. Galie PA, Nguyen DHT, Choi CK, Cohen DM, Janmey PA, Chen CS. Fluid shear stress threshold regulates angiogenic sprouting. *Proc Natl Acad Sci - PNAS*. 2014;111(22):7968–73.
104. Booth R, Kim H. Characterization of a microfluidic in vitro model of the blood-brain barrier (μ BBB). *Lab Chip*. 2012;12(1):1784–92.
105. Shuchat S, Yossifon G, Huleihel M. Perfusion in Organ-on-Chip Models and Its Applicability to the Replication of Spermatogenesis In Vitro. *Int J Mol Sci*. 2022 May 12;23(10):5402.
106. Wu Q, Liu J, Wang X, Feng L, Wu J, Zhu X, et al. Organ-on-a-chip: recent breakthroughs and future prospects. *Biomed Eng Online*. 2020;19(1):9–9.
107. Ahmed I, Akram Z, Bule MH, Iqbal HMN. Advancements and Potential Applications of Microfluidic Approaches—A Review. *Chemosensors*. 2018 Dec;6(4):46.
108. Halldorsson S, Lucumi E, Gómez-Sjöberg R, Fleming RM. Advantages and challenges of microfluidic cell culture in polydimethylsiloxane devices. *Biosens Bioelectron*. 2015;63:218–31.
109. Whitesides GM. The origins and the future of microfluidics. *Nat Lond*. 2006;442(7101):368–73.
110. FIGEYS D, PINTO D. Lab-on-a-Chip: A Revolution in Biological and Medical Sciences. *Anal Chem Wash*. 2000;72(9):330 A-335 A.
111. Haeberle S, Zengerle R. Microfluidic platforms for lab-on-a-chip applications. *Lab Chip*. 2007 Aug 22;7(9):1094–110.
112. Kwon JS, Oh JH. Microfluidic Technology for Cell Manipulation. *Appl Sci*. 2018 Jun;8(6):992.
113. Huh D, Hamilton GA, Ingber DE. From Three-Dimensional Cell Culture to Organs-on-Chips. *Trends Cell Biol*. 2011 Dec;21(12):745–54.
114. Kuncova-Kallio J, Kallio PJ. PDMS and its Suitability for Analytical Microfluidic Devices. In: 2006 International Conference of the IEEE Engineering in Medicine and Biology Society [Internet]. 2006 [cited 2024 Apr 11]. p. 2486–9. Available from: <https://ieeexplore.ieee.org/abstract/document/4462299>
115. Kreutzer J, Ylä-Outinen L, Kärnä P, Kaarela T, Mikkonen J, Skottman H, et al. Structured PDMS chambers for enhanced human neuronal cell activity on MEA platforms. 2012;
116. Xia Y, Whitesides GM. Soft Lithography. *Angew Chem Int Ed*. 1998;37(5):550–75.
117. Mehling M, Tay S. Microfluidic cell culture. *Curr Opin Biotechnol*. 2014;25:95–102.
118. Koh WG, Itle LJ, Pishko MV. Molding of Hydrogel Microstructures to Create Multiphenotype Cell Microarrays. *Anal Chem Wash*. 2003;75(21):5783–9.
119. Bircsak KM, DeBiasio R, Miedel M, Alsehabi A, Reddinger R, Saleh A, et al. A 3D microfluidic liver model for high throughput compound toxicity screening in the OrganoPlate®. *Toxicology*. 2021 Feb 28;450:152667.

120. Vickerman V, Blundo J, Chung S, Kamm R. Design, fabrication and implementation of a novel multi-parameter control microfluidic platform for three-dimensional cell culture and real-time imaging. *Lab Chip*. 2008;8(9):1468–77.
121. Zheng Y, Chen J, Craven M, Choi NW, Totorica S, Diaz-Santana A, et al. In vitro microvessels for the study of angiogenesis and thrombosis. *Proc Natl Acad Sci U S A*. 2012 Jun 12;109(24):9342–7.
122. Kim S, Lee H, Chung M, Jeon NL. Engineering of functional, perfusable 3D microvascular networks on a chip. *Lab Chip*. 2013 Mar 19;13(8):1489–500.
123. Kim C, Kasuya J, Jeon J, Chung S, Kamm RD. A quantitative microfluidic angiogenesis screen for studying anti-angiogenic therapeutic drugs. *Lab Chip*. 2015;15(1):301–10.
124. Zhang B, Montgomery M, Chamberlain MD, Ogawa S, Korolj A, Pahnke A, et al. Biodegradable scaffold with built-in vasculature for organ-on-a-chip engineering and direct surgical anastomosis. *Nat Mater*. 2016 Jun;15(6):669–78.
125. Zhang B, Lai BFL, Xie R, Davenport Huyer L, Montgomery M, Radisic M. Microfabrication of AngioChip, a biodegradable polymer scaffold with microfluidic vasculature. *Nat Protoc*. 2018;13(8):1793–813.
126. Kolesky DB, Homan KA, Skylar-Scott MA, Lewis JA. Three-dimensional bioprinting of thick vascularized tissues. *Proc Natl Acad Sci*. 2016 Mar 22;113(12):3179–84.
127. Nashimoto Y, Hayashi T, Kunita I, Nakamasu A, Torisawa YS, Nakayama M, et al. Integrating perfusable vascular networks with a three-dimensional tissue in a microfluidic device. *Integr Biol Camb*. 2017;9(6):506–18.
128. Lee S, Chung M, Lee SR, Jeon NL. 3D brain angiogenesis model to reconstitute functional human blood–brain barrier in vitro. *Biotechnol Bioeng*. 2020;117(3):748–62.
129. Jones C, Stefania Di Cio, Connelly J, Gautrot J. Design of an Integrated Microvascularised Human Skin-on-a-Chip Tissue Equivalent Model. *bioRxiv*. Cold Spring Harbor: Laboratory Press; 2022.
130. Wan Z, Floryan MA, Coughlin MF, Zhang S, Zhong AX, Shelton SE, et al. New Strategy for Promoting Vascularization in Tumor Spheroids in a Microfluidic Assay. *Adv Healthc Mater*. 2023 Jun;12(14):e2201784.
131. Chesnais F, Joel J, Hue J, Shakib S, Di Silvio L, Grigoriadis AE, et al. Continuously perfusable, customisable, and matrix-free vasculature on a chip platform. *Lab Chip*. 2023;23(4):761–72.
132. Ponce ML. Tube Formation: an In Vitro Matrigel Angiogenesis Assay. In: Murray C, Martin S, editors. *Angiogenesis Protocols: Second Edition* [Internet]. Totowa, NJ: Humana Press; 2009 [cited 2024 Mar 18]. p. 183–8. Available from: https://doi.org/10.1007/978-1-59745-241-0_10
133. ISO 10993-5:2009 Biological evaluation of medical devices. Part 5: Tests for in vitro cytotoxicity. 2009.
134. Hauser S, Jung F, Pietzsch J. Human Endothelial Cell Models in Biomaterial Research. *Trends Biotechnol*. 2017 Mar 1;35(3):265–77.
135. Hayflick L, Moorhead PS. The serial cultivation of human diploid cell strains. *Exp Cell Res*. 1961 Dec 1;25(3):585–621.
136. Schneider CA, Rasband WS, Eliceiri KW. NIH Image to ImageJ: 25 years of image analysis. *Nat Methods*. 2012 Jul;9(7):671–5.

137. Schindelin J, Arganda-Carreras I, Frise E, Kaynig V, Longair M, Pietzsch T, et al. Fiji: an open-source platform for biological-image analysis. *Nat Methods*. 2012 Jul;9(7):676–82.
138. Mutterer J, Zinck E. Quick-and-clean article figures with FigureJ. *J Microsc*. 2013;252(1):89–91.
139. idenTx 3 Chip 25 Chips per Box - AIM Biotech [Internet]. [cited 2023 Nov 6]. Available from: <https://aimbiotech.com/product/identx-3-chip/>, <https://aimbiotech.com/product/identx-3-chip/>
140. idenTx 3 Chip - AIM Biotech [Internet]. 2021 [cited 2023 Nov 6]. Available from: <https://aimbiotech.com/identx-3-chip/>, <https://aimbiotech.com/identx-3-chip/>
141. VitroGel® Hydrogel Matrix - 3D Cell Culture | TheWell Bioscience [Internet]. [cited 2024 Feb 16]. Available from: <https://www.thewellbio.com/product/3d-cell-culture-vitro-gel-hydrogel-matrix/>
142. Zudaire E, Gambardella L, Kurcz C, Vermeren S. A Computational Tool for Quantitative Analysis of Vascular Networks. *PLOS ONE*. 2011 Nov 16;6(11):e27385.
143. Lyu S, Untereker D. Degradability of Polymers for Implantable Biomedical Devices. *Int J Mol Sci*. 2009 Sep 11;10(9):4033–65.
144. Zafar S, Hanif M, Azeem M, Mahmood K, Gondal SA. Role of crosslinkers for synthesizing biocompatible, biodegradable and mechanically strong hydrogels with desired release profile. *Polym Bull Berl Ger*. 2022;79(11):9199–219.
145. Vuornos K, Ojansivu M, Koivisto JT, Häkkänen H, Belay B, Montonen T, et al. Bioactive glass ions induce efficient osteogenic differentiation of human adipose stem cells encapsulated in gellan gum and collagen type I hydrogels. *Mater Sci Eng C*. 2019 Jun 1;99:905–18.
146. Mohan C, Long K, Mutneja M. *Introduction to Inhibitors*. 2014.
147. Koivisto JT, Oelschlaeger C, Menne D, Willenbacher N, Näreoja T. Microrheology study on matrix remodelling by osteoblasts in 3D hydrogel in vitro culture. *Bone Rep*. 2022;16:101388-.
148. Raz V, Natan S, Tchaicheeyan O, Kolel A, Zussman M, Lesman A. FITC-Dextran Release from Cell-Embedded Fibrin Hydrogels. *Biomolecules*. 2021 Feb 23;11:337.
149. Baltazar T, Jiang B, Moncayo A, Merola J, Albanna MZ, Saltzman WM, et al. 3D bioprinting of an implantable xeno-free vascularized human skin graft. *Bioeng Transl Med*. 2023;8(1):e10324.
150. Zeiringer S, Wiltschko L, Glader C, Reiser M, Absenger-Novak M, Fröhlich E, et al. Development and Characterization of an In Vitro Intestinal Model Including Extracellular Matrix and Macrovascular Endothelium. *Mol Pharm*. 2023 Oct 2;20(10):5173–84.
151. Lin YT, Tung YT, Wong JY, Wang GJ. Fabrication of perfusable microvessel networks by mimicking in vivo vasculogenesis using a novel scaffold-wrapping method. *Mater Des*. 2023 Mar 1;227:111707.
152. Andrée B, Ichanti H, Kalies S, Heisterkamp A, Strauß S, Vogt PM, et al. Formation of three-dimensional tubular endothelial cell networks under defined serum-free cell culture conditions in human collagen hydrogels. *Sci Rep*. 2019 Apr 1;9(1):5437.
153. Jockenhoevel S, Zund G, Hoerstrup SP, Chalabi K, Sachweh JS, Demircan L, et al. Fibrin gel – advantages of a new scaffold in cardiovascular tissue engineering. *Eur J Cardiothorac Surg*. 2001;19(4):424–30.

APPENDIX A: EGM-2 MEDIUM COMPOSITION

Table A. *Composition of EGM-2 Endothelial Cell Growth Medium-2.*

	EBM-2
2.0 volume/volume-% (v/v-%)	Human serum (sterile filtered)
0.1 v/v-%	GA-1000
0.1 v/v-%	R-IGF-1
0.1 v/v-%	VEGF
0.1 v/v-%	hEGF
0.04 v/v-%	Hydrocortisone
0.4 v/v-%	hFGF-B
0.1 v/v-%	Ascorbic acid
0.1 v/v-%	Heparin

EBM-2: endothelial cell growth basal medium, EGM-2: Endothelial Cell Growth Medium-2, GA-1000: Gentamicin sulfate-Amphotericin, hEGF: human epidermal growth factor, hFGF-B: human fibroblast growth factor-B, R-IGF-1: insulin-like growth factor 1, V/V-%: volume/volume-%, VEGF: vascular endothelial growth factor

APPENDIX B: FULL TILE SCAN IMAGES OF WELL PLATE

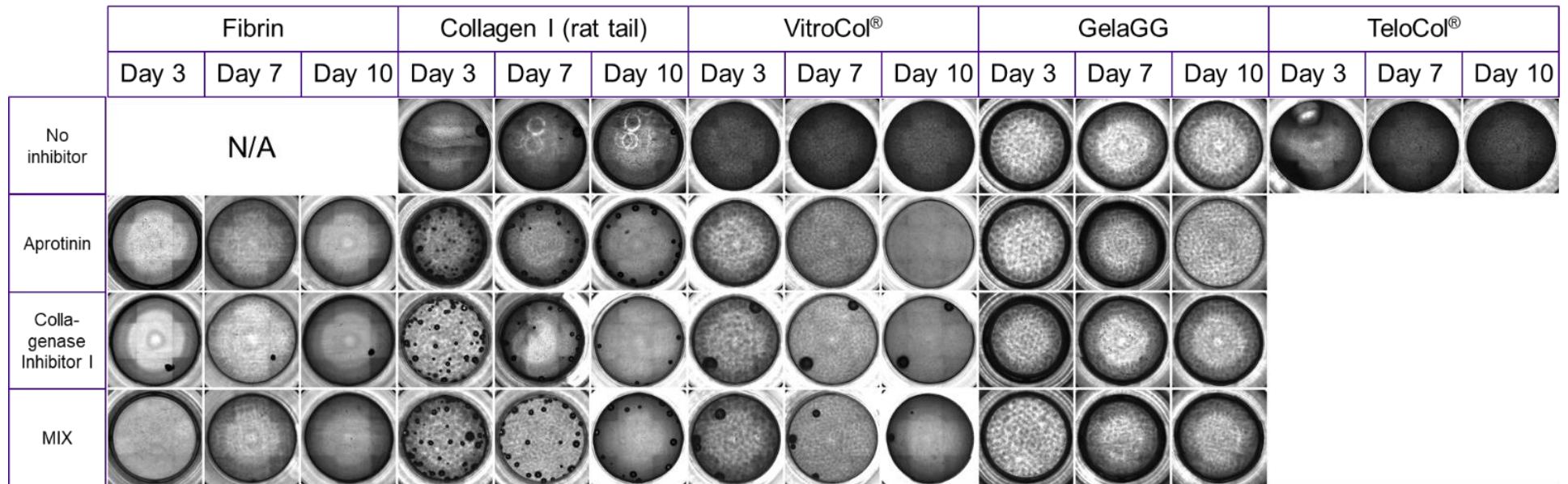


Figure A. Tile scan images of samples on 96-well plate taken at days 3, 7, and 10 with Leica DMI8 widefield microscope. N/A: not applicable, fibrin was not used without inhibitors. MIX: mixture of inhibitors aprotinin and Collagenase Inhibitor I (1:1), gelaGG: gelatin-gellan gum, N=3 per material and condition

APPENDIX C: LIVE/DEAD IMAGES OF WELL PLATE SAMPLES WITH SEPARATE CHANNELS

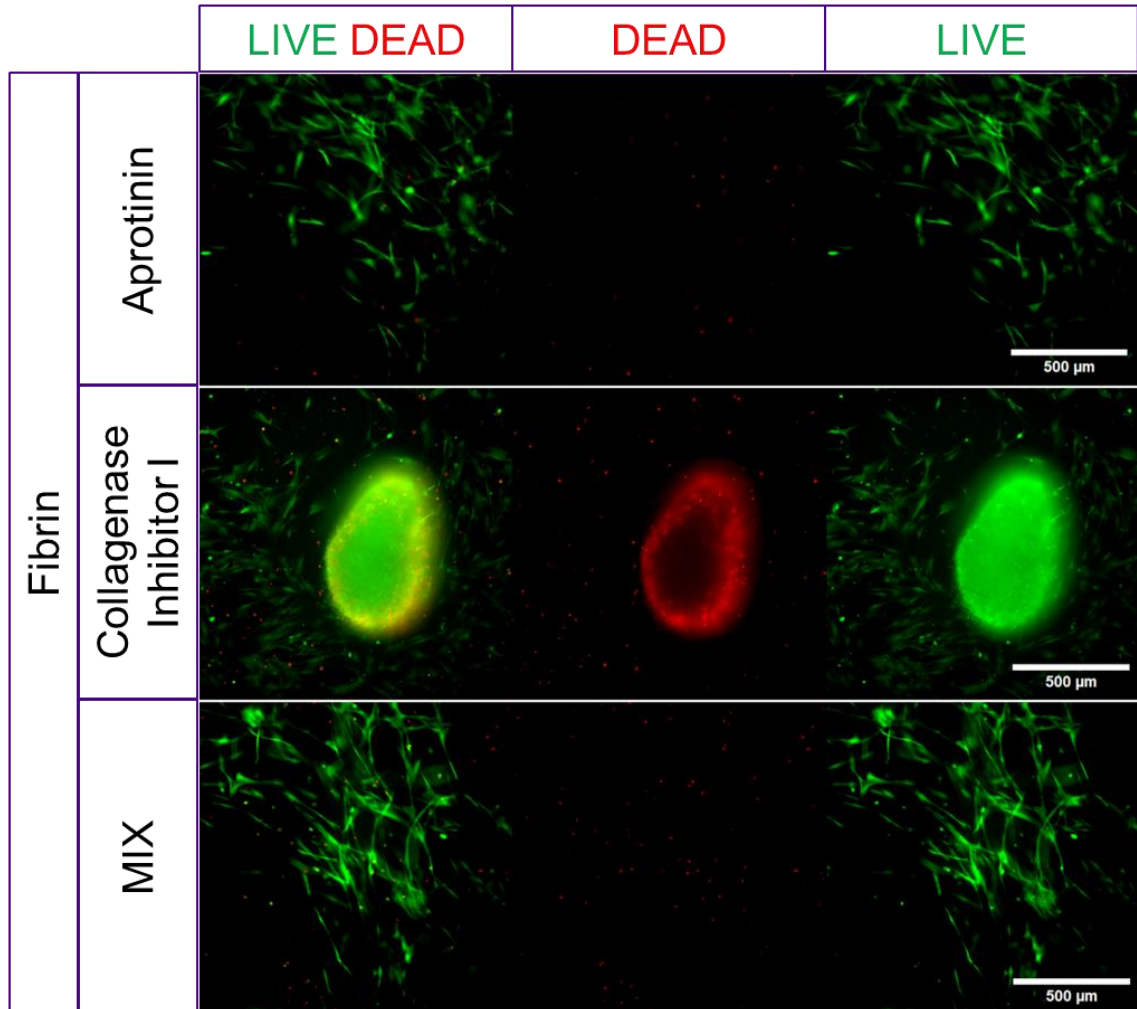


Figure B. *Live/Dead images of fibrin samples on well plate at day 2. Green: Live, Red: Dead, Scale Bar: 500 μ m, MIX: mixture of inhibitors aprotinin and Collagenase Inhibitor I (1:1), N=3 per material and condition*

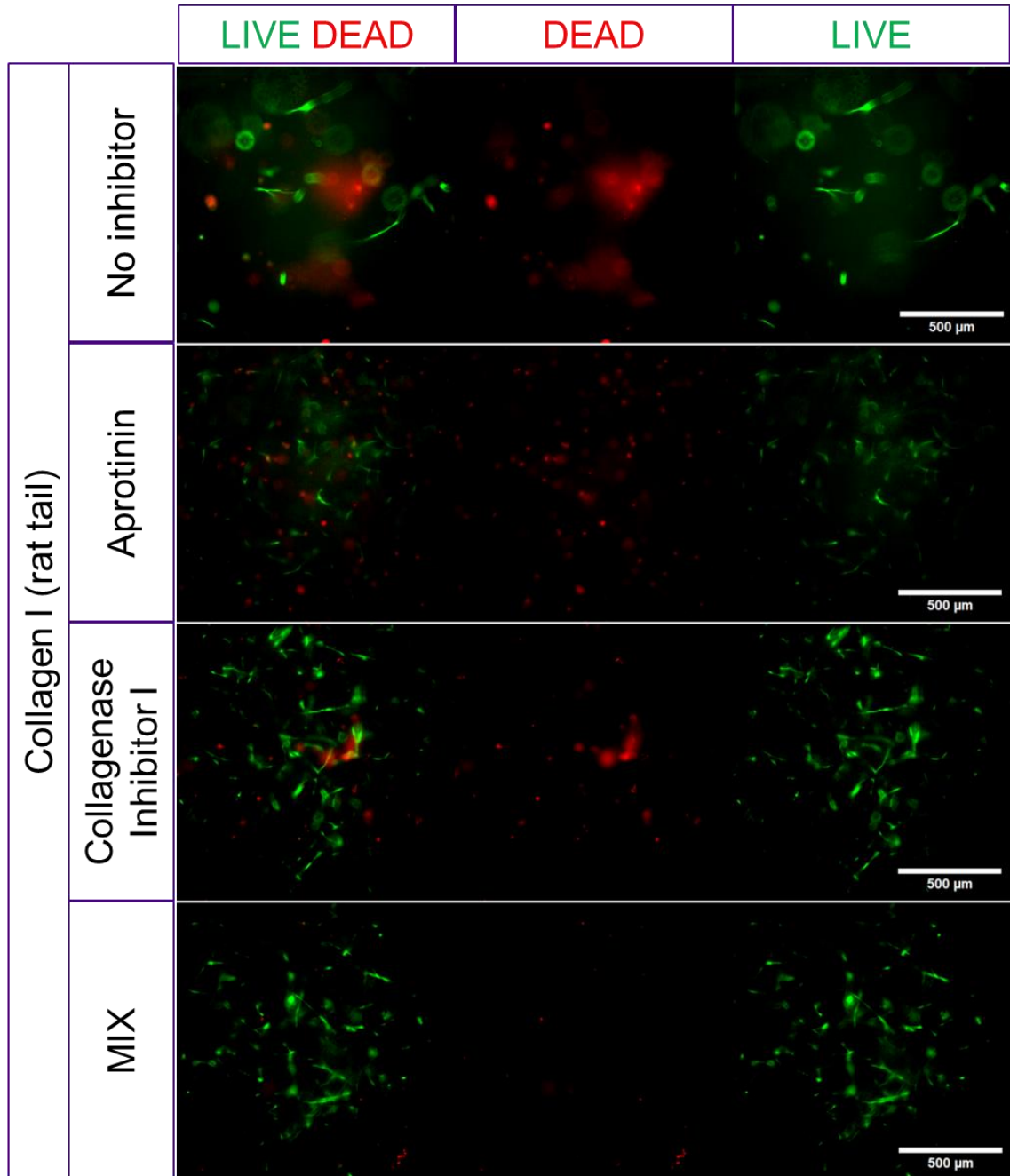


Figure C. *Live/Dead images of collagen I (rat tail) samples on well plate at day 2. Green: Live, Red: Dead, Scale Bar: 500 μ m, MIX: mixture of inhibitors aprotinin and Collagenase Inhibitor I (1:1), N=3 per material and condition*

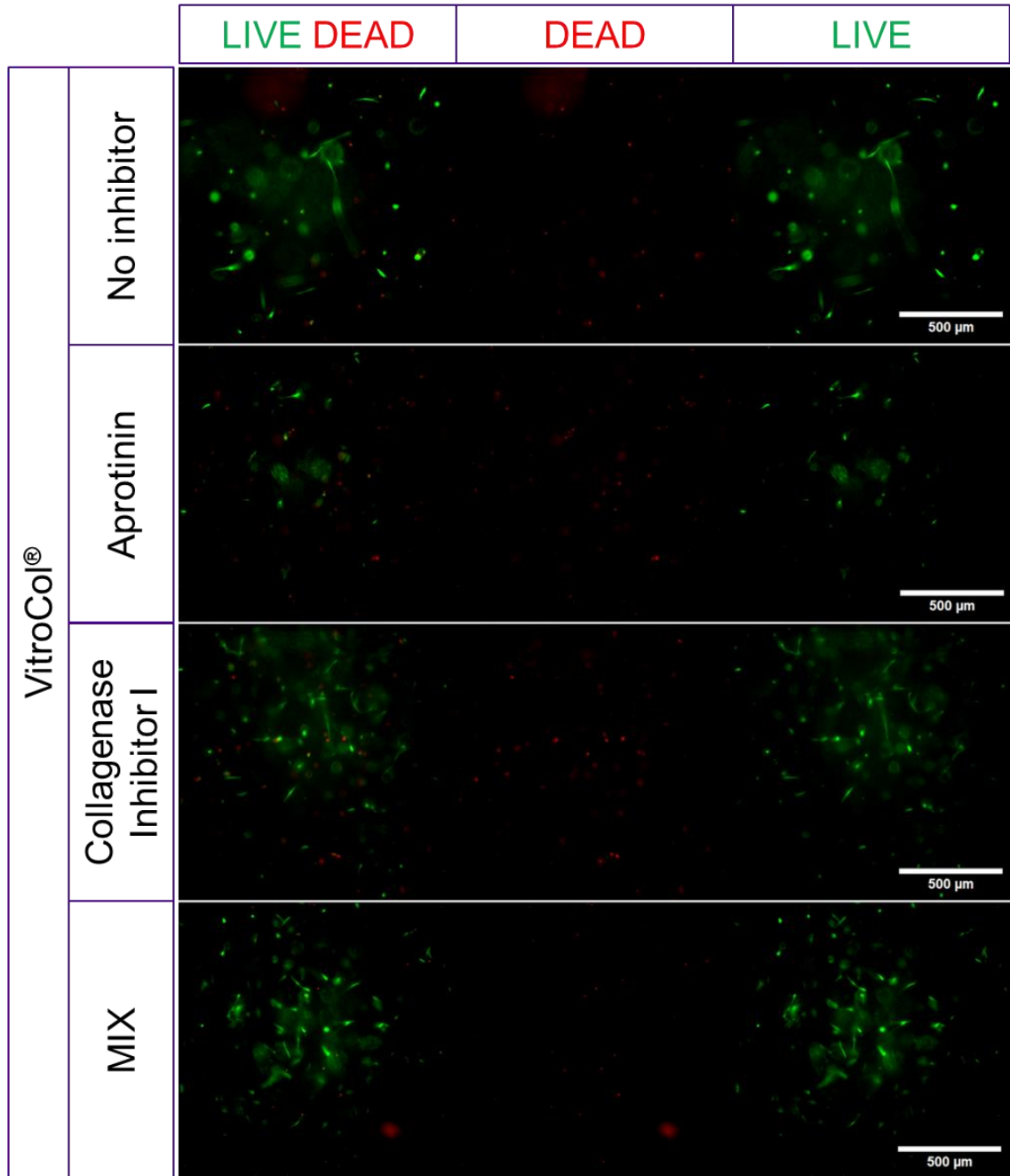


Figure D. *Live/Dead images of VitroCol® samples on well plate at day 2. Green: Live, Red: Dead, Scale Bar: 500 μm, MIX: mixture of inhibitors aprotinin and Collagenase Inhibitor I (1:1), N=3 per material and condition*

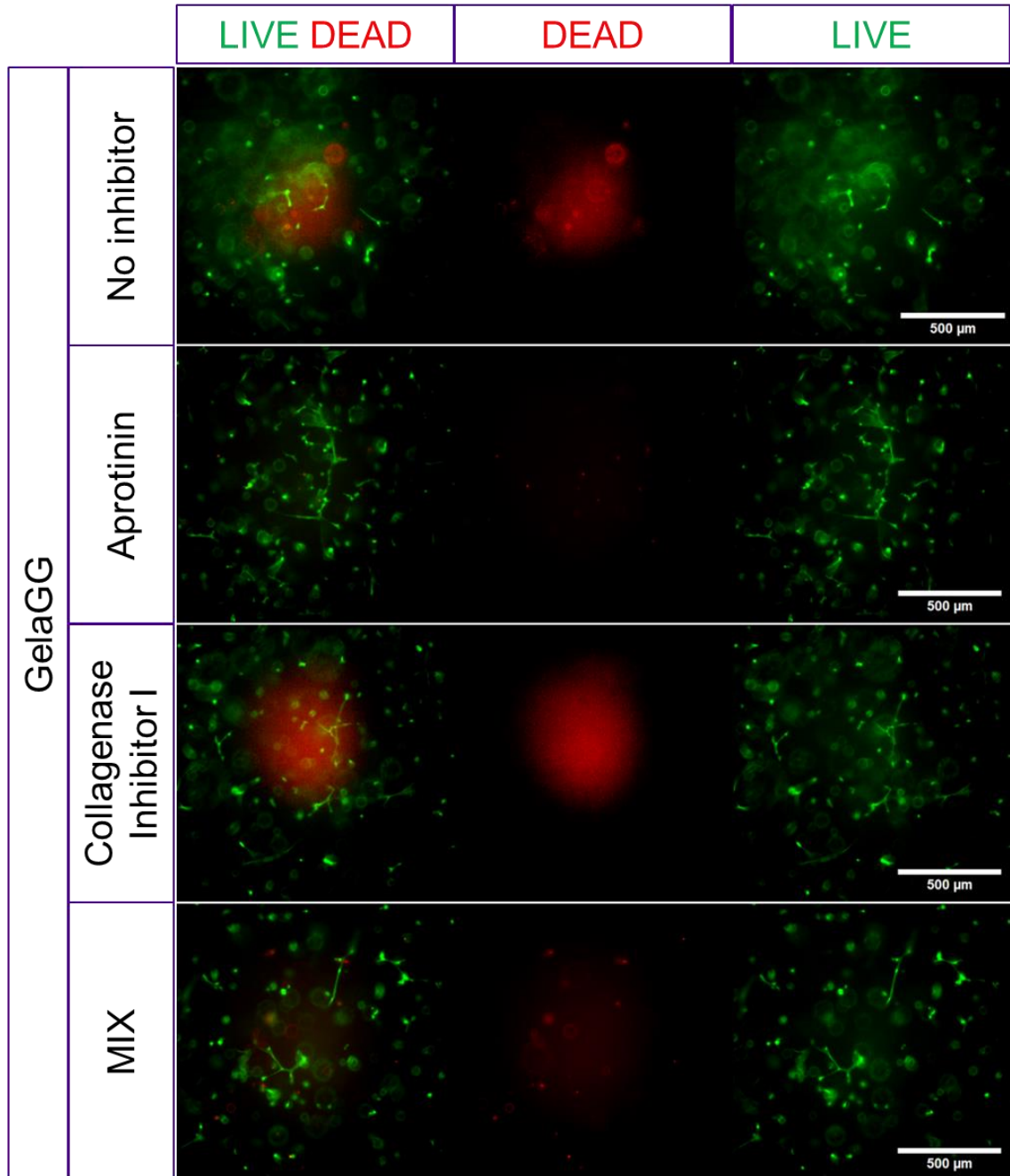


Figure E. *Live/Dead images of gelatin-gellan gum (gelaGG) samples on well plate at day 2. Green: Live, Red: Dead, Scale Bar: 500 μ m, MIX: mixture of inhibitors aprotinin and Collagenase Inhibitor I (1:1), N=3 per material and condition*

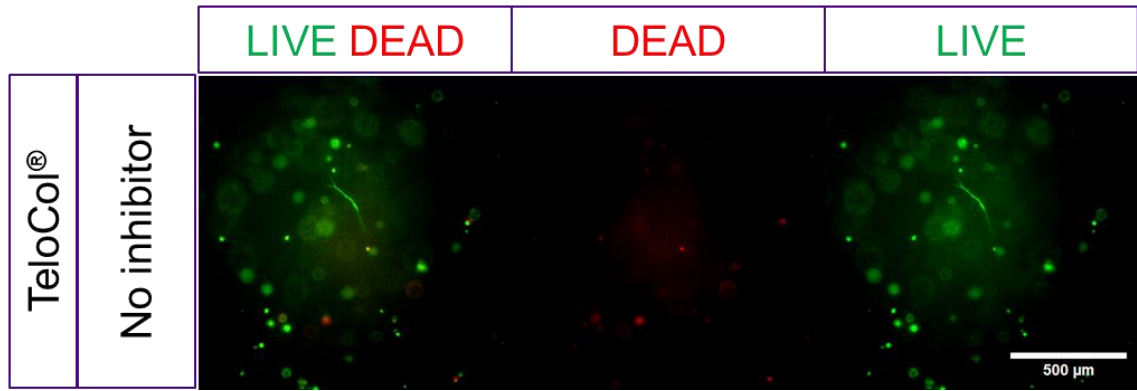


Figure F. *Live/Dead images of TeloCol® samples on well plate at day 2. Green: Live, Red: Dead, Scale Bar: 500 μ m, N=3 per material*

APPENDIX D: CYTOCHEMICALLY STAINED WELL PLATE SAMPLES WITH SEPARATE CHANNELS

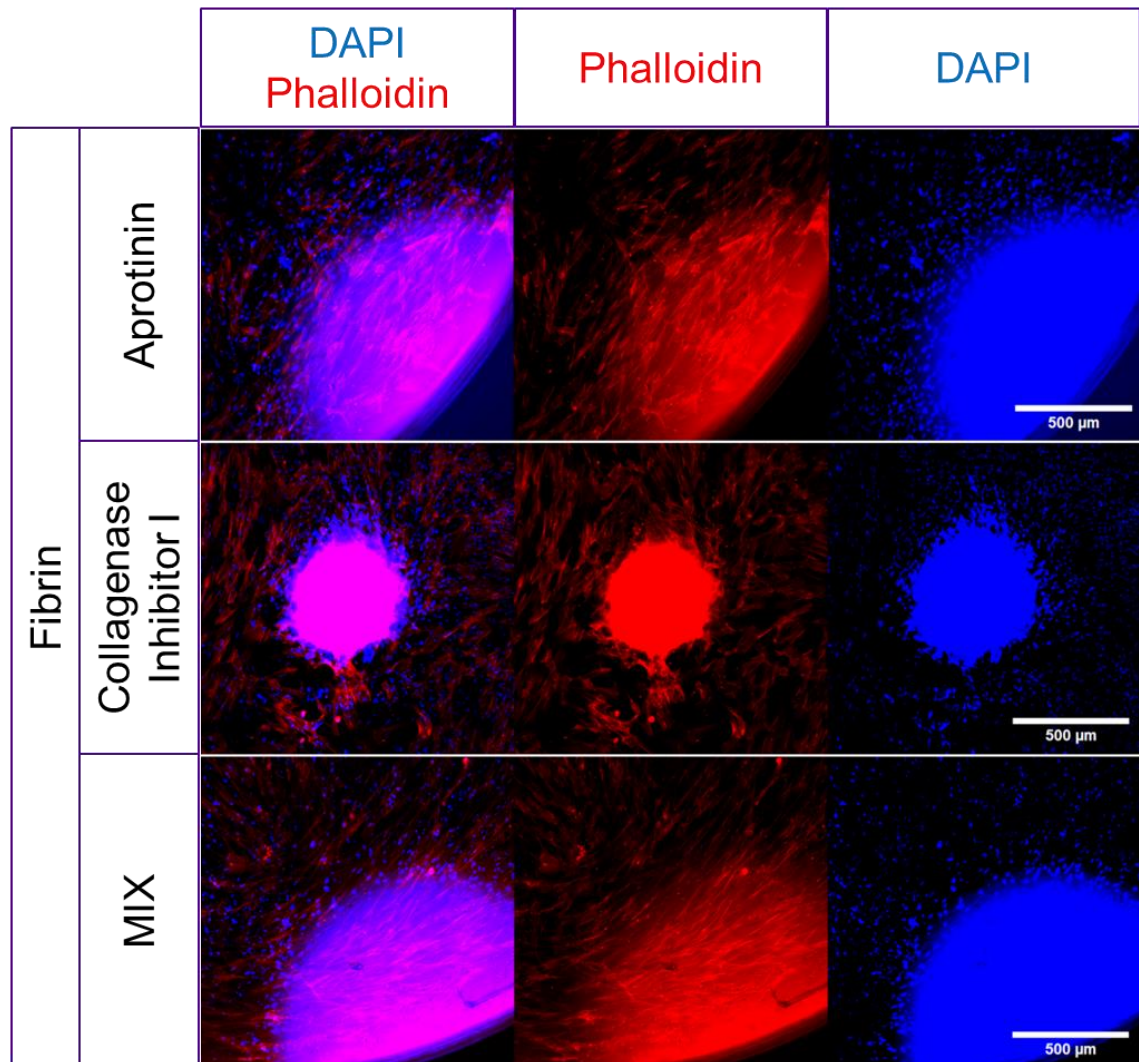


Figure G. Cytochemical staining images of fibrin samples on well plate at day 10. Blue: DAPI, Red: phalloidin, Scale Bar: 500 μm , MIX: mixture of inhibitors aprotinin and Collagenase Inhibitor I (1:1), N=3 per material and condition

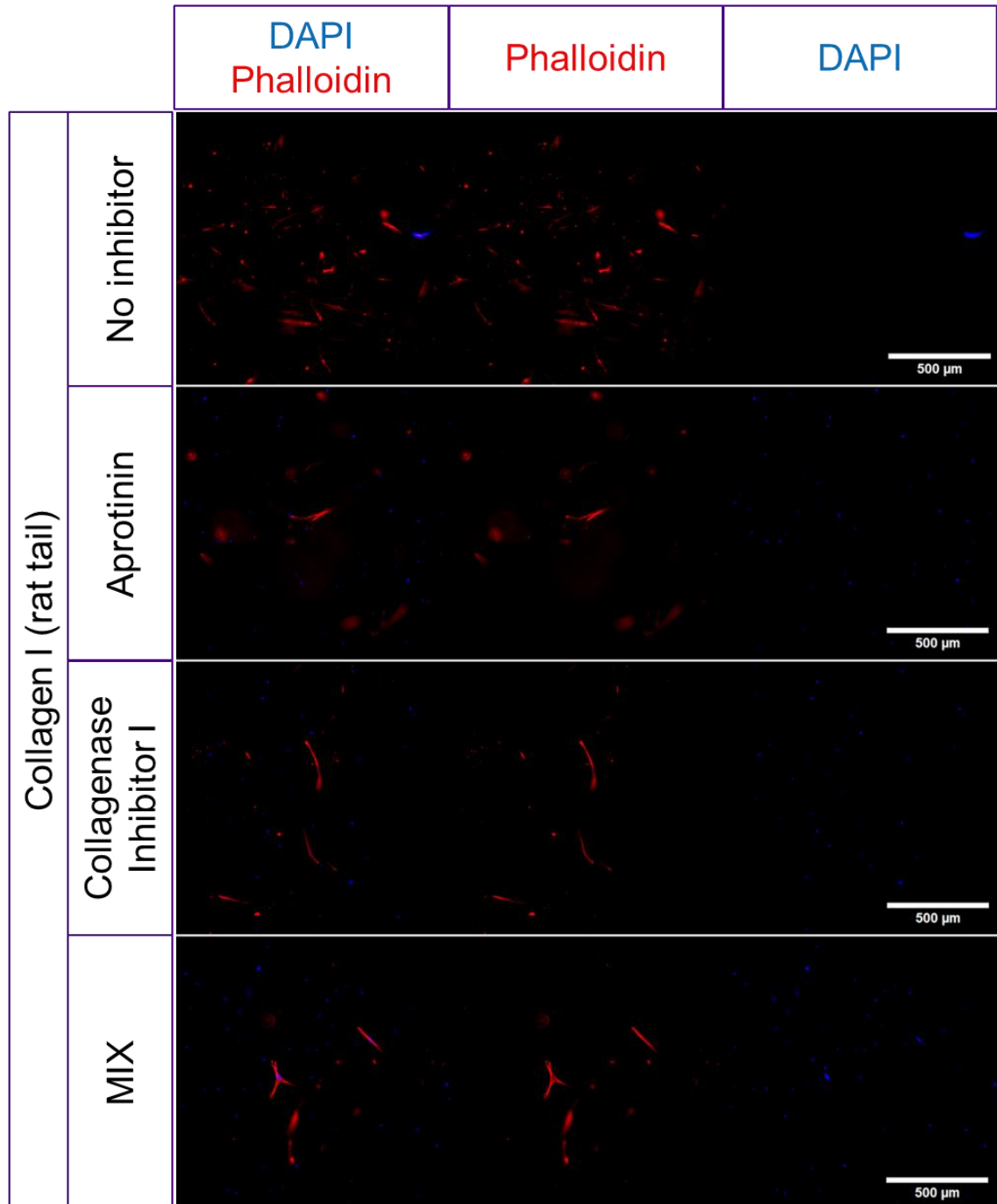


Figure H. *Cytochemical staining images of collagen I (rat tail) samples on well plate at day 10. Blue: DAPI, Red: phalloidin, Scale Bar: 500 μ m, MIX: mixture of inhibitors aprotinin and Collagenase Inhibitor I (1:1), N=3 per material and condition*

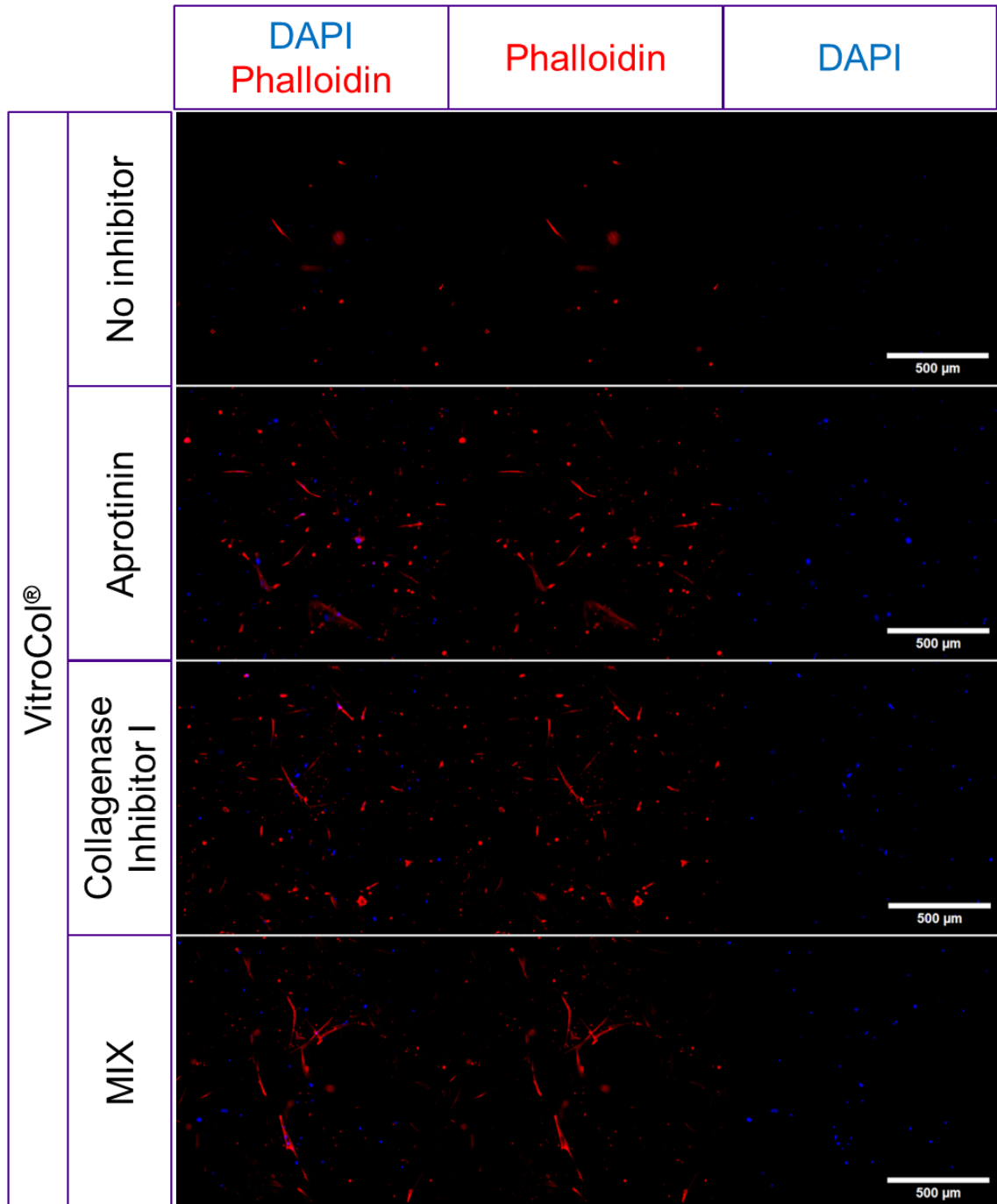


Figure 1. *Cytochemical staining images of VitroCol® samples on well plate at day 10. Blue: DAPI, Red: phalloidin, Scale Bar: 500 µm, MIX: mixture of inhibitors aprotinin and Collagenase Inhibitor I (1:1), N=3 per material and condition*

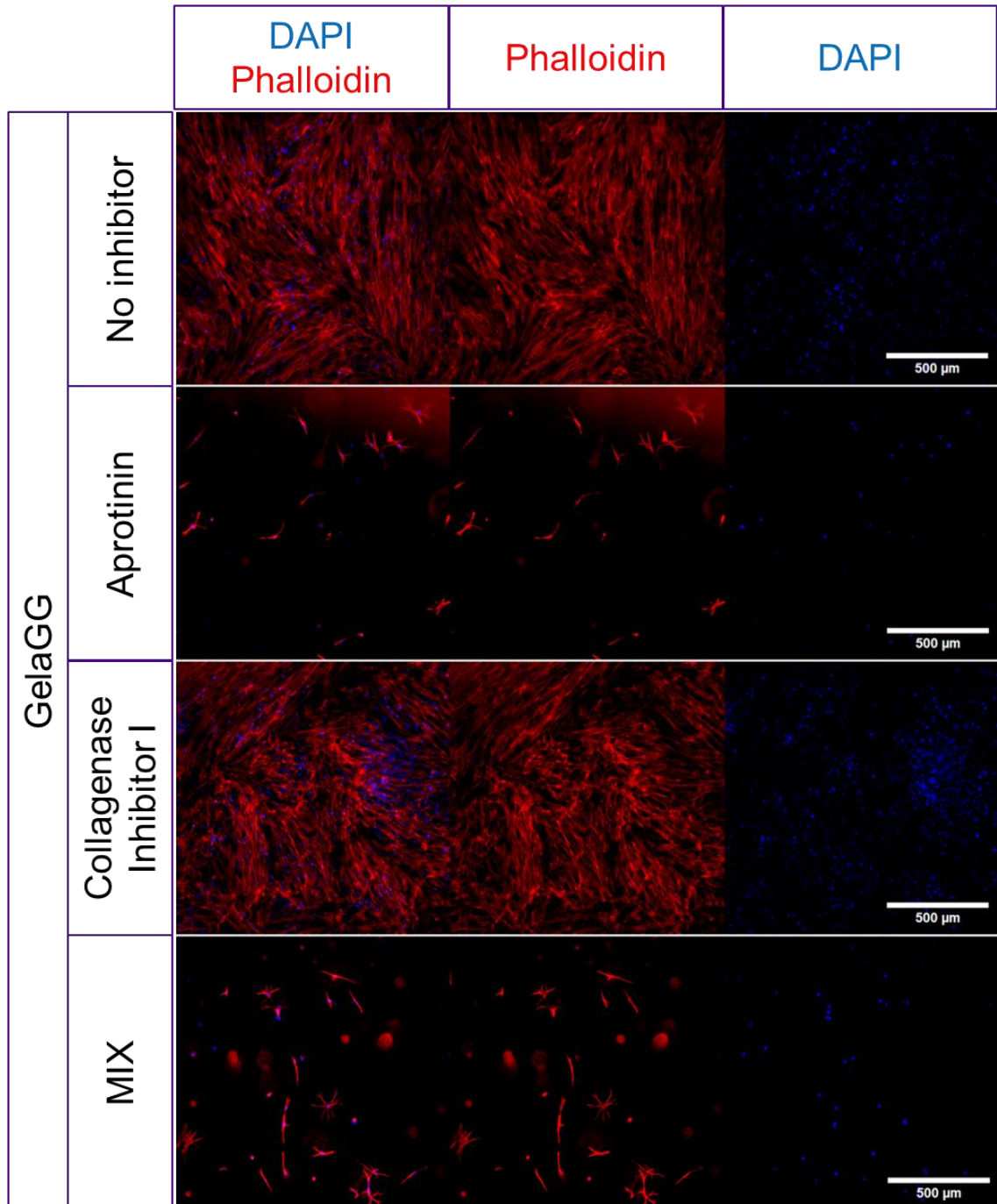


Figure J. *Cytochemical staining images of gelatin-gellan gum (gelaGG) samples on well plate at day 10. Blue: DAPI, Red: phalloidin, Scale Bar: 500 μm, MIX: mixture of inhibitors aprotinin and Collagenase Inhibitor I (1:1), N=3 per material and condition*

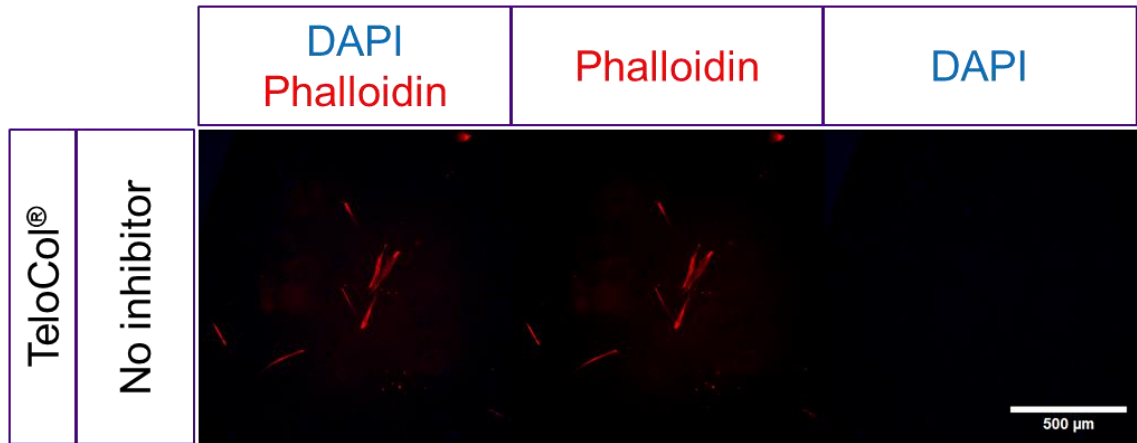


Figure K. Cytochemical staining images of TeloCol® samples on well plate at day 10. Blue: DAPI, Red: phalloidin, Scale Bar: 500 μm , N=3 per material

APPENDIX E: IMMUNOCYTOCHEMICALLY STAINED CHIP SAMPLES WITH SEPARATE CHANNELS

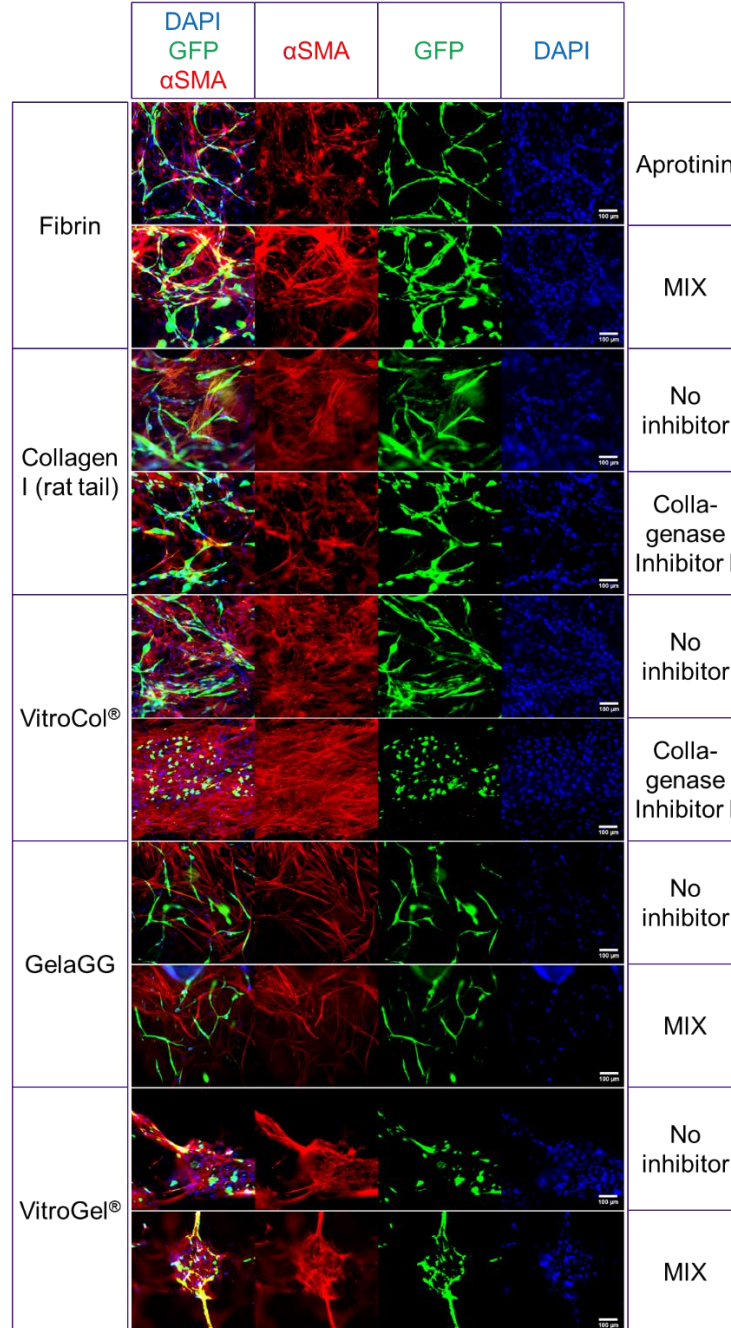


Figure L. Immunocytochemical staining images of Vascularization-on-a-Chip at day 10. Medium flow from top to bottom. Blue: DAPI, Green: green fluorescent protein tagged human umbilical vein endothelial cells (GFP-HUVEC), Red: α SMA, Scale Bar: 100 μ m, GelaGG: gelatin gellan gum, MIX: mixture of inhibitors aprotinin and Collagenase Inhibitor I (1:1), N=3 per material and condition